Supplementary Materials for

sNIR: A novel NIR dye for precision fluorescence-guided surgery

This pdf file includes:

1 Material and Methods

1.1 Synthesis

1.1.1 General Notes

Chemicals were purchased from Fluorochem (Amsterdam, Netherlands), Fisher Scientific (Schwerte, Germany), Novabiochem (Laufelfingen, Switzerland), TCI Chemicals (Zwijndrecht, Belgium), and VWR International (Darmstadt, Germany). IRDye800 was purchased from LI-COR (Lincoln, NE, USA). Commercially available starting materials were used directly without further purification. Moisture- and air-sensitive reactions were performed in oven-dried glassware under an argon atmosphere with anhydrous solvents. For oxygen-sensitive reactions, the solvent was degassed by passing an argon stream through the solution while sonicating. Reactions with light-sensitive substances were carried out in the dark as far as possible. Aqueous solutions used were prepared using demineralized water and were saturated unless otherwise specified.

UV/VIS-based reaction controls were conducted on a Nanodrop ND60 (Implen, Munich, Germany). The solvent was removed under reduced pressure with a Rotavapor (Büchi, Flawil, Switzerland) with a CVC 3000 vacuum pump (Vacuubrand, Wertheim, Germany). The aqueous solvent was removed by lyophilization with an Alpha 1-4 LDplus Freeze Dryer (Christ, Osterode am Harz, Germany) with an RZ6 vacuum pump (Vacuubrand, Wertheim, Germany). Sonication was performed using a Sonorex ultrasonic bath (Bandelin, Berlin, Germany).

Thin Layer Chromatography (TLC)

Thin-layer chromatography was performed using silica gel-coated glass plates 60 F254 with a fluorescence indicator (Merck Millipore, Burlington, USA). Visualization was performed using UV light (λ = 254 nm or 366 nm) and, if necessary, by treating the plate with a suitable stain (potassium permanganate, ceric ammonium molybdate, ninhydrin, and bromocresol green) and subsequent heating.

Flash Column Chromatography

Flash column chromatography was performed on a Reveleris system (Büchi) with integrated UV and evaporative light scattering detectors. Silica, amino-, C8- and C18- modified silica cartridges manufactured by Büchi, Axel Semrau (Stefansbecke, Germany), and Machery-Nagel (Düren, Germany) were used at recommended flow rates. The particle size was 40–63 µm irregular or 20–40 µm spherical. Used solvents and gradients are listed in the synthetic procedures.

Semi-Preparative High-performance Liquid Chromatography (HPLC)

Semi-preparative HPLC was performed on an UltiMate 30000 ultra-high performance liquid chromatography system with an integrated UV-detector (Thermo Fisher Scientific, Waltham, MA, USA). As stationary phase pentafluorophenyl-propyl (PFP) modified preparative HPLC column NUCLEODUR PFP (5 µm, 125x21 mm) was used with the corresponding precolumn (Machery-Nagel). Runs (**05-95_55 min**) employed a standard gradient, as listed in **Table 2**, at a flow rate of 3.0 mL/min and UC detection at 220 nm or 254 nm.

Table 1. Solvent gradient used for preparative HPLC.

Time [min]	Water + 0.1% FA [%]	MeCN + 0.1% FA [%]
0.00	95	5
45.00	5	95
55.00	5	95

NMR Spectroscopy

^{1}H and $^{13}C\{^{1}H\}$ NMR spectroscopic measurements were performed on an Ascend-400, Avance-400, Avance-500 and Avance-600 (Bruker, Billerica, USA) at 25 °C. Chemical shifts are reported relative to solvent signals ($CDCl_3$: δ_H = 7.26 ppm, δ_C = 77.16 ppm; DMSO-d_6: δ_H = 2.50 ppm, δ_C = 39.52 ppm; D_2O: δ_H = 4.79 ppm; CD_3OD: δ_H = 3.31 ppm). The chemical shift δ is given in parts per million (ppm) and the coupling constant *J* in Hz. For the multiplicities, the following abbreviations are used: singlet (s), doublet (d), triplet (t), quartet (q), quintet (quint.), broad singlet (bs), and multiplet (m). For a complete characterization, additional ^{1}H-^{1}H correlation spectra (COSY) and ^{1}H-^{13}C correlation spectra (HMBC, HSQC) were acquired. The numbering of the carbon atoms corresponds to an arbitrary determination and does not follow the IUPAC rules.

Infrared (IR) Spectroscopy

IR spectra were acquired on an IRAffinity-1S (Shimadzu, Kyōto, Japan).

High-Resolution Mass Spectrometry (HRMS)

HRMS measurements were performed using a Micromass LCT mass spectrometer with a lock-spray unit in combination with an Alliance 2695 system (Waters, Milford, USA). Alternatively, a Micromass Q-TOF Premier mass spectrometer connected to an Aquity ultra-performance liquid chromatography system was used (Waters). Ionization was carried out by electron spray ionization (ESI). The calculated (calc.) and detected masses are given.

Liquid Chromatography–Mass Spectrometry (LC-MS)

Analytical LC-MS measurements were performed using the following three systems:

LC-MS system (**1**) An Acquity UPLC H-class system utilizing a QDa quadrupole mass spectrometer, combined with a PDA eλ detector, and a UPLC BEH C18 column (50 x 2.1 mm, particle size: 1.7 µm) (Waters). Runs (**05-95_3.5 min**) employed a standard gradient, as listed in **Table 2**, at a flow rate of 0.8 mL/min. Electrospray ionization (ESI) was used, and the M/z range of 50-1250 was detected. MassLynx 4.1 (Waters) software was used for analysis.

Table 2. Solvent gradient used for the Waters Acquity UPLC H-Class System.

Time [min]	Water + 0.1% FA [%]	MeCN + 0.1% FA [%]
0.00	95	5
1.00	5	95
2.25	5	95
2.27	95	5
3.50	95	5

LC-MS system (**2**) A 2795 separation module connected to an LCT Premier mass spectrometer (Waters), a 1050 UV multiwavelength detector (HP, Palo Alto, USA), and an Aeris^{TM} widepore XB-C18 column (50 x 2.1 mm, particle size: 3.6 µm, Phenomenex (Aschaffenburg, Germany)). Runs (**01-90_5 min**) employed a standard gradient, as listed in **Table 3**, at a flow rate of 0.6 mL/min. Electrospray ionization (ESI) was used for ionization, and the M/z range of 100-2500 was detected. MassLynx 4.1 (Waters) software was used for analysis.

Table 3. The Solvent gradient used for the composite HPLC system.

Time [min]	Water+ 0.1% FA [%]	MeCN + 0.1% FA [%]
0.00	99	1
4.00	10	90
5.00	10	90

LC-MS system (**3**) An UltiMate 30000 ultra-high performance liquid chromatography system coupled to an ISQ EC single quadrupole mass spectrometer with an integrated UV-detector (Thermo Fisher Scientific), equipped with a Nucleodur PFP column (50 x 2.0 mm, particle size: 3.0 µm) with the corresponding precolumn cartridge (Machery-Nagel). Runs (**05-95_13 min**) followed an equilibration (5 min) and employed a standard gradient as listed in **Table 4** at a flow rate of 0.3 mL/min. Electrospray ionization (ESI) was used for ionization, and the M/z range of 100-1250 was detected. Chromeleon CDS software (Thermo Fisher Scientific) was used for analysis.

Table 4. Solvent gradient used for the Thermo Fisher Scientific UltiMate 30000 UHPLC System.

Time [min]	Water + 0.1% FA [%]	MeCN + 0.1% FA [%]
-5	95	5
0	95	5
8	5	95
13	5	95

Microwave Assisted Synthesis

Reactions under microwave irradiation were performed using the Initiator+ (Biotage, Uppsala, Sweden).

Solid Phase Peptide Synthesis (SPPS)

Peptide synthesis was performed on a Liberty BlueTM automated microwave peptide synthesizer (CEM, Charlotte, NC, USA). The reagents used are listed in Table 5. In the synthetic procedures, L-amino acids are labeled with capital and D-amino acids with small letters.

Table 5. Overview of (amino) acids used for solid phase peptide synthesis.

Amino Acid	Three / Single Letter Code	Reagent
Cysteine	Cys / C	Fmoc-Cys(Trt)-OH
Lysine	Lys / K	Fmoc-Lys(Boc)-OH
Phenylalanine	Phe / F	Fmoc-Phe-OH
Threonine	Thr / T	Fmoc-Thr(tBu)-OH
Tryptophan	Trp / W	Fmoc-Trp(Boc)-OH
Tyrosine	Tyr / Y	Fmoc-Tyr(tBu)-OH
Further Building Blocks	**Abbreviation**	**Reagent**
Threonol	Thr(ol)	Fmoc-Thr(tBu)-ol
Lysinol	Lys(ol)	Fmoc-Lys(Boc)-ol
N_3-PEG(3)-CO_2H	N_3-PEG	n. a.

Synthesis was performed following a standard Fmoc protocol at a 0.1 mmol scale. The 2-chlorotrityl chloride resin (200-400 mesh, loading 1.5-1.9 mmol/g, Bachem, Bubendorf, Switzerland) was used as solid support and was manually preloaded. Therefore, the following procedure was followed:

- Swelling (CH_2Cl_2, 0.5 h)
- Activation (dest. AcCl (1 mL/g resin), toluene, 60 °C, 3 h, Ar)
- Loading (2.0 equiv. protected amino acid, 5.0 equiv. dest. DIPEA, CH_2Cl_2, rt, 2.0 h)
- 2 x Capping (5 mL CH_2Cl_2/MeOH/DIPEA (8/1.5/0.5), rt, 0.5 h)
- Drying to constant mass in order to determine the loading efficacy

Stock solutions of (amino) acids (0.2 M in DMF), DIC (0.5 M in DMF), Oxyma® (1 M in DMF), and a deprotection solution (10% (w/v) piperazine in EtOH:NMP (1:9) were prepared and provided to the instrument. Couplings were performed with a fivefold excess (compared to the resin) of (amino) acids as well as coupling and deprotection reagents. Instrument settings for deprotection and coupling are summarized in Table 6.

Table 6. Overview of the deprotection and coupling settings used for automated peptide synthesis.

Method	Temperature [°C]	Performance [W]	Hold Time [s]	ΔT [°C]
standard deprotection	75	155	15	2
	85	30	50	1
standard coupling	75	160	15	2
	90	3	110	1

After completing peptide synthesis, the suspension was transferred to a 20 mL syringe reactor. The resin-bound peptide was filtered and washed with DMF (3x 5 mL) and CH_2Cl_2 (3x 5 mL). For resin-cleavage and removal of the protecting groups, the resin-bound peptide was incubated with 10 mL TFA/H_2O/DODT/TIS (94%/2.5%/2.5%/1%, v/v/v/v) at rt and 600 rpm on a Rotamax 120 (Heidolph, Schwabach, Germany) for a minimum of 4 h. The solution was filtered off and portioned onto two 40 mL Greiner tubes filled with 35 mL of ice-cold diethyl ether. The tubes were centrifuged (4000 rpm, 4 °C, 4 min), and the supernatants were discarded. The precipitates were washed two times with diethyl ether, dissolved in MeCN, combined, diluted with H_2O, and lyophilized. Further purification is described in the synthetic procedures.

Labeling of Panitumumab

For Panitumumab-IRDye800 conjugation, the Li-Cor protein label kit was followed. Briefly, a 20 mg/ml commercial panitumumab stock solution was diluted with PBS in a 1.5-ml microcentrifuge tube to yield a 1 mg/mL working concentration. The pH was adjusted to 8.5 by adding 1 M potassium phosphate buffer (K_2HPO_4, pH 9). In a separate microcentrifuge tube, IRDye800-NHS ester was resuspended in water (4µg/µl) and the appropriate amount of dye transferred to the panitumumab solution based on the formula = 116.6/molecular weight of the protein (147 kDa), for obtaining a DOL of 1.57. The solution was vortexed and incubated at room temperature in the dark for 1 h.

For panitumumab-sNIR conjugation, panitumumab (100 µL of a 1 mg/mL dilution in 1 M PBS pH 7.4, 0.7 nmol) was added to 100 µL of 50 mM PBS pH 7.5 in a 1.5 mL microcentrifuge tube. In a separate microcentrifuge tube, a 1 mM sNIR-NHS-ester solution in PBS (50 mM, pH 7.5) was prepared, and 7.2 equiv. were added to the panitumumab solution to yield a final DOL of 1.7. The diluted dye solution was vortexed and incubated at room temperature in the dark for 1 h.

Following incubation, the reactive dye/antibody solutions were eluted through a Zeba spin desalting column (molecular weight cutoff of 7 kDa, Thermo Fisher Scientific) to remove unreacted free dye and their absorption spectra acquired. UV/VIS of the filtrate dilution was acquired directly and used to calculate the density of labeling (DOL), as described in **1.2.1**.

Antibody fluorophore conjugates were used for animal studies within 1 week after labeling.

1.1.2 Synthetic Procedures

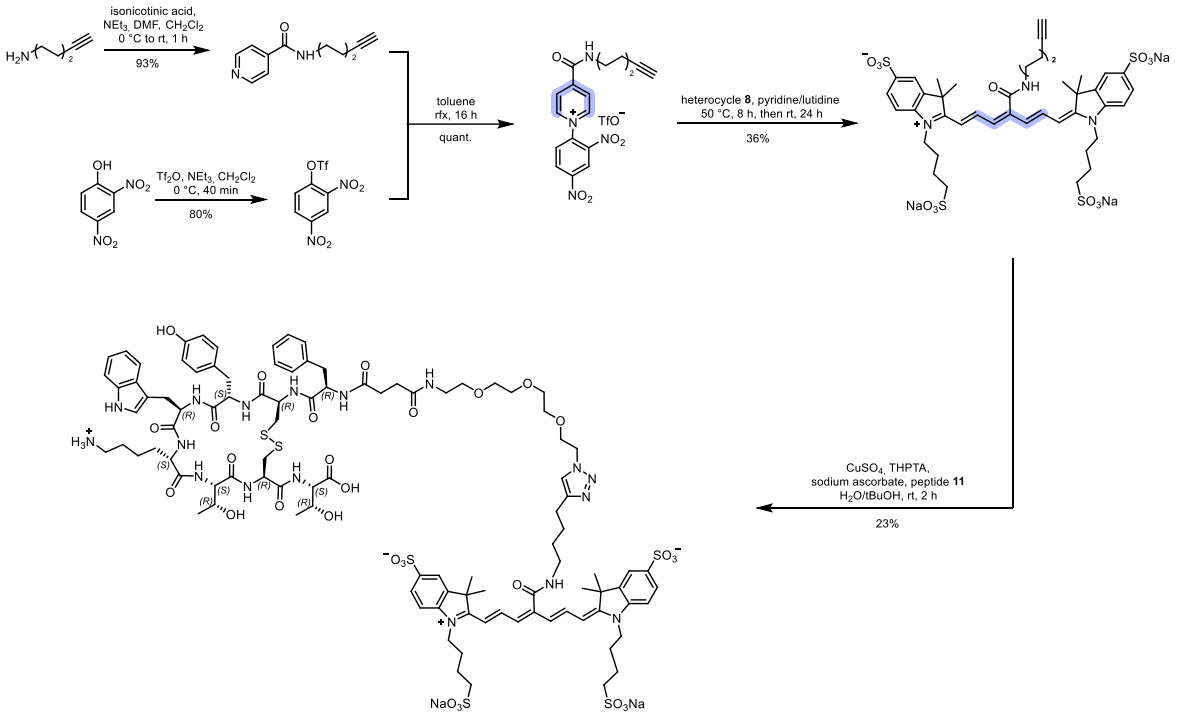

Scheme S1. Synthetic access to TATE-sNIR.

***N*-(hex-5-yn-1-yl)isonicotinamide (2)**

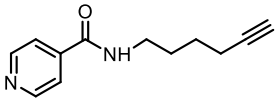

To an oven-dried two-neck flask was added isonicotinic acid (**1**, 750 mg, 6.10 mmol, 1.0 equiv.), a cat. amount of dry DMF (five drops) and dry CH_2Cl_2 (12.2 mL, 0.5 M) under argon. The solution was cooled to 0 °C, oxalyl chloride (627 µL, 7.32 mmol, 1.2 equiv.) was added dropwise, and the reaction mixture was stirred at rt for 1 h. The volatiles were removed at reduced pressure, and the residue was dissolved in CH_2Cl_2 (30.5 mL, 0.2 M). The solution was cooled to 0 °C, and hexynamine (826 µL, 7.32 mmol, 1.2 equiv.) and distilled triethylamine (2.55 mL, 18.3 mmol, 3.0 equiv.) were added. After 5 min, the ice bath was removed, and stirring was continued at rt for 1 h. The reaction mixture was quenched by the addition of saturated aqueous $NaHCO_3$, washed with saturated aqueous $NaHCO_3$, and extracted with CH_2Cl_2 three times. The combined organic layers were dried over Na_2SO_4, filtered, concentrated under reduced pressure, and the crude was purified by flash column chromatography (silica, 0% - 2% MeOH/CH_2Cl_2, main separation step at 2%). Alkyne **2** (1.16 g, 5.72 mmol, 93%) was obtained as a brown oil.

R_f (10% MeOH/CH_2Cl_2 + 0.5% NEt_3) = 0.60; **^{1}H NMR** (400 MHz, $CDCl_3$): δ = 8.61 (d, *J* = 5.9 Hz, 2H), 7.58 (dd, *J* = 4.5, 1.6 Hz, 2H), 7.16 (s, 1H), 3.44–3.36 (m, 2H), 2.17 (td, *J* = 6.9, 2.6 Hz, 2H), 1.92 (t, *J* = 2.7 Hz, 1H), 1.69 (ddd, *J* = 14.6, 9.8, 7.1 Hz, 2H), 1.55 (ddd, *J* = 10.6, 7.2, 2.2 Hz, 2H) ppm; **^{13}C{^{1}H} NMR** (101 MHz, $CDCl_3$): δ = 165.8, 150.3, 141.9, 121.1, 83.9, 69.0, 39.7, 28.4, 25.7, 18.1 ppm; **LC-MS system (1)** (05-95_3.5 min): *m/z* 203 $[M+H]^+$, t_R = 0.99 min; **HRMS (ESI+):** calculated for $C_{12}H_{15}N_2O^+$ $[M+H]^+$ 203.1184, observed 203.1186.

2,4-dinitrophenyl trifluoromethane sulfonate (4)

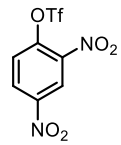

2,4-dinitrophenol (**3**, 70% in H_2O, 5.00 g, 19.0 mmol, 1.0 equiv.) and distilled triethylamine (5.30 mL, 38.0 mmol, 2.0 equiv.) were dissolved in CH_2Cl_2 (100 mL, 0.2 M). The solution was cooled to 0 °C, and Tf_2O (6.4 mL, 38.0 mmol, 2.0 equiv.) was added. The reaction mixture was stirred at 0 °C for 90 min. The mixture was diluted with CH_2Cl_2, quenched with saturated aqueous $NaHCO_3$, and extracted with CH_2Cl_2 three times. The combined organic layers were dried over Na_2SO_4, filtered, and evaporated. Triflate **4** (5.39 g, 17.1 mmol, 89%) was obtained as a yellow oil.

R_f (50% EtOAc/PE) = 0.75; **^{1}H NMR** (400 MHz, $CDCl_3$): δ = 9.03 (d, *J* = 2.7 Hz, 1H), 8.62 (dd, *J* = 9.0, 2.7 Hz, 1H), 7.76–7.69 (m, 1H) ppm; **^{13}C{^{1}H} NMR** (101 MHz, $CDCl_3$): δ = 146.6, 145.1, 129.6, 125.7, 122.5, 120.1, 117.0 ppm.

1-(2,4-dinitrophenyl)-4-(hex-5-yn-1-ylcarbamoyl)pyridin-1-ium triflat (5)

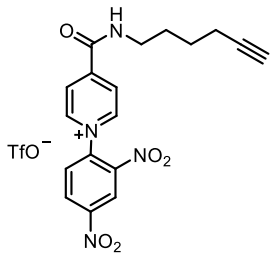

Triflate **4** (172 mg, 0.54 mmol, 1.1 equiv.) and alkyne **2** (100 mg, 0.49 mmol, 1.0 equiv.) were dissolved in toluene (3.5 mL, 0.15 M). The reaction mixture was refluxed for 16 h and left to cool to rt. The resulting precipitate was filtered, washed with toluene and Et_2O, and dissolved in MeOH. The solvent was removed under reduced pressure. Zincke salt **5** (258 mg, 0.49 mmol, quant.) was obtained as a brown solid and used without any further purification.

R_f (20% MeOH/CH_2Cl_2) = 0.70; **^{1}H NMR** (400 MHz, CD_3OD): δ = 9.44–9.41 (m, 2H), 9.29 (d, *J* = 2.5 Hz, 1H), 8.93 (dd, *J* = 8.7, 2.5 Hz, 1H), 8.67–8.63 (m, 2H), 8.32–8.28 (m, 1H), 3.57–3.49 (m, 2H), 2.31–2.21 (m, 3H), 1.88–1.77 (m, 2H), 1.70–1.60 (m, 2H) ppm; **^{13}C{^{1}H} NMR** (101 MHz, CD3OD): δ = 163.6, 153.4, 151.3, 148.4, 144.5, 139.9, 132.5, 131.2, 127.2, 123.2, 84.6, 69.9, 41.2, 29.2, 27.0, 18.7 ppm; **LC-MS system (1)** (05-95_3.5 min): *m/z* 369 $[M–OTf]^+$, t_R = 1.01 min; **HRMS (ESI+):** calculated for $C_{18}H_{17}N_4O_5^+$ $[M–OTf]^+$ 369.1187, observed 369.1199.

4-hydrazineylbenzenesulfonic acid (6)

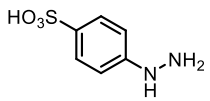

In a two-neck flask 4-aminobenzenesulfonic acid (**5**, 3.00 g, 17.3 mmol, 1.0 equiv.) was suspended in H_2O (11.5 mL, 1.5 M). The suspension was heated to 85 °C, followed by the portion-wise addition of Na_2CO_3 (973 mg, 9.18 mmol, 0.5 equiv.). The reaction mixture was cooled to 5 °C, and H_2SO_4 (1.15 mL, 1.25 mmol, 1.3 equiv.) was added dropwise. Aqueous $NaNO_2$ (6 M, 2.89 mL, 17.3 mmol, 1.0 equiv.) was added at 5 °C, causing a brownish coloration of the solution and precipitation of a white solid. The diazo compound was filtered, washed with H_2O, and added to a solution of Na_2SO_3 (4.91 g, 39.0 mmol, 2.3 equiv.) in H_2O (14.4 mL, 2.7 M) at 5 °C and stirring at this temperature was continued for 1 h. The reaction mixture was heated to reflux, followed by the addition of conc. HCl (11.6 mL, 141 mmol, 8.2 equiv.). The reaction mixture was left to cool to rt, and the resulting precipitate was filtered and washed with H_2O. Hydrazine **6**

(2.11 g, 11.2 mmol, 65%) was obtained as a white solid and used without any further purification.

R_f (10% MeOH/CH_2Cl_2) = 0.40; **^{1}H NMR** (400 MHz, DMSO-d_6): δ = 7.51 (d, *J* = 8.3 Hz, 2H), 8.38 (d, *J* = 6.6 Hz, 2H) ppm; **^{13}C{^{1}H} NMR** (101 MHz, DMSO-d_6): δ = 145.7, 141.4, 126.2, 113.0 ppm; **LCMS system (1)** (05-95_3.5 min): *m/z* 189 $[M+H]^+$, t_R = 0.17 min; **HRMS (ESI–):** calculated for $C_6H_7N_2O_3S^-$ $[M–H]^-$ 187.0177, observed 187.0172.

potassium 2,3,3-trimethyl-3H-indole-5-sulfonate (7)

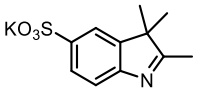

To a suspension of hydrazine **6** (2.11 g, 11.2 mmol, 1.0 equiv.) in acetic acid (11.2 mL, 1 M) was added 3-methyl-2-butanone (3.6 mL, 33.7 mmol, 3.0 equiv.). The reaction mixture was refluxed for 3 h and then cooled to 5 °C. Et_2O (10 mL) was added, causing precipitation. The solid was filtered, washed with Et_2O, dissolved in MeOH, and concentrated under reduced pressure. The red ammonium salt was dissolved in MeOH/*i*PrOH (1/1, 40 mL, 1 M), followed by the addition of grounded KOH (0.71 g, 12.7 mmol, 1.2 equiv.), causing a yellow coloration. Sulfonated indole **7** (1.98 g, 7.2 mmol, 67%) was obtained as a hygroscopic yellow solid and used without any further purification.

R_f (20% MeOH/CH_2Cl_2) = 0.15; **^{1}H NMR** (400 MHz, DMSO-d_6): δ = 7.91 (dd, *J* = 1.6, 0.6 Hz, 1H), 7.73 (dd, *J* = 8.1, 1.6 Hz, 1H), 7.56 (dd, *J* = 8.1, 0.6 Hz, 1H), 2.63 (s, 3H), 1.47 (s, 6H) ppm; **^{13}C{^{1}H} NMR** (101 MHz, DMSO-d_6): δ = 197.3, 148.2, 142.9, 142.2, 126.2, 120.6, 116.0, 54.0, 22.1, 15.1 ppm; **LC-MS system (1)** (05-95_3.5 min): *m/z* 240 $[M–K+2H]^+$, t_R = 0.45 min; **HRMS (ESI–):** calculated for $C_{11}H_{12}NO_3^-$ $[M–K]^-$ 238.0538, observed 238.0529.

potassium 2,3,3-trimethyl-1-(4-sulfonatobutyl)-3*H*-indol-1-ium-5-sulfonate (8)

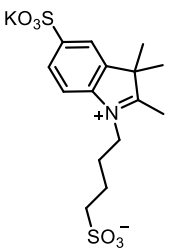

Sulfonated indole **7** (2.20 g, 7.9 mmol, 1.0 equiv.) was suspended in 1,4-butane sultone (16.1 mL, 158.8 mmol, 20 equiv.), heated to 120 °C and stirred at this temperature for 12 h. The reaction mixture was left to cool to rt, and the resulting precipitate was filtered, washed with EtOAc, dissolved in MeOH, and concentrated under reduced pressure. Purification by flash column chromatography (C8, 2% - 95% MeCN+0.05% TFA/H_2O+0.05% TFA, main separation step at 2%) afforded heterocycle **8** (1.14 g, 3.0 mmol, 38%) as a gray-brown solid.

^{1}H NMR (400 MHz, DMSO-d_6): δ = 8.01 (s, 1H), 7.96 (d, *J* = 8.4 Hz, 1H), 7.81 (dd, *J* = 8.4, 1.6 Hz, 1H), 4.46 (t, *J* = 7.9 Hz, 2H), 2.84 (s, 3H), 2.53 (t, *J* = 7.3 Hz, 2H), 1.95 (p,

J = 7.8 Hz, 2H), 1.75 (p, *J* = 7.3 Hz, 2H), 1.54 (s, 6H) ppm; **$^{13}C\{^{1}H\}$ NMR** (101 MHz, DMSO-d_6): δ = 197.2, 149.5, 141.5, 141.0, 126.3, 120.7, 115.0, 69.8, 54.2, 50.1, 26.0, 22.1, 21.91, 13.9 ppm; **LC-MS system (1)** (05-95_3.5 min): *m/z* 376 $[M–K+2H]^+$, t_R = 0.2 min; **HRMS (ESI–):** calculated for $C_{15}H_{20}NO_6S_2^-$ $[M–K]^-$ 374.0732, observed 374.0719.

sodium 2-((1*E*,3*Z*,5*E*)-7-((*E*)-3,3-dimethyl-5-sulfonato-1-(4-sulfonatobutyl)indolin-2-ylidene)-4-(hex-5-yn-1-ylcarbamoyl)hepta-1,3,5-trien-1-yl)-3,3-dimethyl-1-(4-sulfonatobutyl)-3*H*-indol-1-ium-5-sulfonate (sNIR-alkyne)

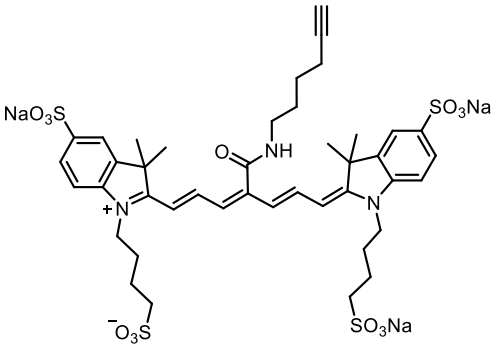

To a microwave reaction vial, Zincke salt **5** (100 mg, 0.19 mmol, 1.0 equiv.) was dissolved in 3 mL (0.06 M) of dry pyridine containing 1% (v/v) lutidine. The solution was degassed by applying vacuum, and subsequently purged with argon. Heterocycle **8** (175 mg, 0.425 mmol, 2.2 equiv.) was then added, and the reaction mixture was heated at 50 °C in a microwave reactor for 8 h, followed by stirring at room temperature for 24 h. The reaction mixture was then washed with cold Et_2O (3x), water was added and the resulting green aqueous phase was collected, lyophilized, and purified by flash column chromatography (C18 Aq gold, 0% - 95% MeCN+0.05% TFA/H_2O+0.05% TFA, main separation step at 25%) afforded cyanine **sNIR-alkyne** (72 mg, 0.07 mmol, 36%) as a green solid.

R_f (50% MeOH/CH_2Cl_2) = 0.40, **^{1}H NMR** (400 MHz, D_2O): δ = 7.83–7.70 (m, 4H), 7.63 (bd, *J* = 11.1 Hz, 2H), 7.28 (d, *J* = 8.2 Hz, 2H), 6.38 (bd, *J* = 12.3 Hz, 2H), 3.98 (s, 4H), 3.47 (t, *J* = 7.2 Hz, 2H), 2.89 (t, *J* = 7.3 Hz, 5H), 2.40 (t, *J* = 2.6 Hz, 1H), 2.27 (td, *J* = 6.9, 2.6 Hz, 2H), 1.93–1.70 (m, 10H), 1.65–1.57 (m, 2H), 1.54 (s, 12H) ppm; **$^{13}C\{^{1}H\}$ NMR** (101 MHz, D_2O): δ = 172.7, 169.5, 157.0, 146.7, 144.2, 141.6, 139.0, 126.6, 122.8, 119.7, 111.1, 105.0, 85.5, 69.8, 50.3, 49.0, 43.7, 39.5, 28.4, 27.1, 25.5, 25.3, 21.6, 17.4 ppm; **LC-MS system (2)** (01-95_5 min): *m/z* 934 $[M–2Na]^-$, t_R = 3.22 min; **HRMS (ESI–):** calculated for $C_{42}H_{50}N_3Na_2O_{13}S_4^-$ $[M–Na]^-$ 978.2022, observed 978.2070.

sodium 2-((*E*)-2-((*E*)-3-(2-((*E*)-3,3-dimethyl-5-sulfonato-1-(4-sulfonatobutyl)indolin-2-ylidene)ethylidene)-2-(4-sulfonatophenoxy)cyclohex-1-en-1-yl)vinyl)-1-(6-(hex-5-yn-1-ylamino)-6-oxohexyl)-3,3-dimethyl-3*H*-indol-1-ium-5-sulfonate (IRdye800-alkyne)

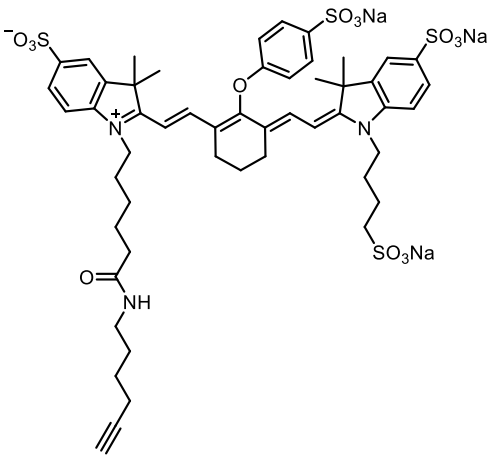

To a solution of IRDye800 carboxylate (**IRDye800**, 10 mg, 9.36 µmol, 1.0 equiv.) in DMF (1.9 mL, 5 mM) were added DIPEA (3.2 µL, 18.7 µmol, 2.0 equiv.) and TSTU (5.6 mg, 18.7 µmol, 2.0 equiv.). The solution was stirred under light exclusion at rt for 30 min until LCMS indicated complete conversion. The reaction mixture was inversely added to ice-cold Et_2O (2 mL), resulting in a green precipitate. After centrifugation, the supernatant was discarded, and the pellet was dissolved in 50 mM pH = 7.5 PBS (1.9 mL, 5 mM). Hexynamine (1 µL, 10.3 µmol, 1.1 equiv.) was added, and the reaction mixture was stirred at rt for 30 min. The reaction mixture was directly purified by flash column chromatography (C18 gold, 1% - 95% MeCN+0.05% TFA/H_2O+0.05% TFA, main separation step at 15%). Cyanine **IRDye800-alkyne** (11.0 mg, 9.36 µmol, quant.) was obtained as a green solid.

^{1}H NMR (600 MHz, DMSO-d_6): δ = 7.90 – 7.84 (m, 1H), 7.84 – 7.74 (m, 2H), 7.66 – 7.58 (m, 6H), 7.35 (d, *J* = 8.3 Hz, 1H), 7.30 – 7.24 (m, 1H), 7.10 (d, *J* = 8.2 Hz, 2H), 6.25 (d, *J* = 14.3 Hz, 1H), 6.14 (dt, *J* = 14.3, 4.0 Hz, 1H), 4.10 (dt, *J* = 28.8, 7.2 Hz, 4H), 3.24 – 3.14 (m, 2H), 3.02 (dq, *J* = 12.8, 6.4 Hz, 2H), 2.76 – 2.67 (m, 4H), 2.56 – 2.52 (m, 1H), 2.27 – 2.11 (m, 4H), 2.02 (q, *J* = 7.3 Hz, 2H), 1.96 – 1.91 (m, 2H), 1.78 – 1.70 (m, 4H), 1.69 – 1.61 (m, 2H), 1.56 – 1.48 (m, 2H), 1.48 – 1.38 (m, 4H), 1.31 (s, 12H) ppm; **^{13}C{^{1}H} NMR** (150 MHz, DMSO-d_6): 174.4, 172.1, 172.0, 171.9, 171.3, 171.2, 170.2, 162.8, 159.4, 145.3, 145.0, 142.8, 142.3, 142.0, 141.0, 140.5, 140.3, 140.0, 128.0, 126.2, 122.2, 122.0, 119.6, 113.8, 110.7, 110.2, 101.2, 100.3, 84.5, 71.2, 50.7, 48.7, 48.5, 43.8, 43.6, 37.9, 37.8, 35.5, 35.2, 28.3, 28.3, 27.3, 27.3, 26.6, 26.0, 25.5, 23.8, 22.5, 20.8, 17.5 ppm; **LC-MS system (2)** (05-95_5 min): *m/z* 1081 $[M–3Na+4H]^–$, t_R = 3.38 min; **HRMS (ESI–):** *m/z* calculated for $C_{52}H_{60}N_3O_{14}S_4^{3–}$ $[M–3Na]^{3–}$ 359.4319 (*z*=3, triply charged ion), observed 359.4319.

2-(2-(2-(2-azidoethoxy)ethoxy)ethoxy)ethan-1-amine (9)

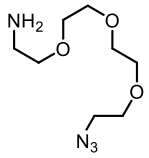

Tetraethylene glycol (15.0 g, 77.2 mmol, 1.0 equiv.) was co-evaporated with toluene, dissolved in dry THF (60 mL, 1.3 M), and cooled to 0 °C. Mesylchloride (13.3 mL, 171 mmol, 2.2 equiv.) was added by syringe, followed by the dropwise addition of Et_3N (23.7 mL, 171 mmol, 2.2 equiv.) in 5 mL THF, forming a precipitate. After 1 h, the ice bath was removed, and the solution was stirred for a further 4 h. The reaction mixture was diluted with H_2O (36 mL) and basified to pH = 8 by the addition of sat. $NaHCO_3$. THF was removed under reduced pressure, and NaN3 (10.3 g, 158 mmol, 2.1 equiv.) was added. The reaction mixture was refluxed for 16 h, cooled to rt, and extracted with Et_2O five times. The combined organic layers were washed using sat. saline, dried over Na_2SO_4, filtered, and concentrated under reduced pressure. The crude diazide (13.5 g, 55.3 mmol 1.0 equiv.) was dissolved in 0.65 M aqueous H_3PO_4 (126 mL) and Ph_3P (12.5 g, 47.6 mmol, 0.9 equiv.) in 94 mL Et_2O was added dropwise over 45 min (leaking dropping funnel, possible explanation for bad yield). The reaction mixture was stirred for 24 h, and the aqueous layer was extracted with CH_2Cl_2 until triphenylphosphine oxide was no longer detected. The aqueous layer was adjusted to pH=12 using KOH, and the product was extracted using CH_2Cl_2. Azide **9** (3.2 g, 14.7 mmol, 19%) was obtained as an amber oil and used without further purification.

R_f (50% EtOAc/PE) = 0.20; **^{1}H NMR** (400 MHz, $CDCl_3$): δ = 3.89 – 3.83 (m, 2H), 3.75 – 3.64 (m, 10H), 3.46 (dd, *J* = 5.6, 4.5 Hz, 2H), 3.24 (p, *J* = 5.6 Hz, 2H), 2.45 (s, 1H) ppm; **^{13}C{^{1}H} NMR** (101 MHz, $CDCl_3$): δ = 70.5, 70.5, 70.5, 70.3, 70.0, 66.8, 50.9, 39.9 ppm; **LC-MS system (2)** (05-95_5 min): *m/z* 219 $[M+H]^+$, t_R = 0.52 min; **HRMS (ESI+):** calculated for $C_8H_{19}N_4O_3^+$ $[M+H]^+$ 219.1457, observed 219.1448.

1-azido-13-oxo-3,6,9-trioxa-12-azahexadecan-16-oic acid (10)

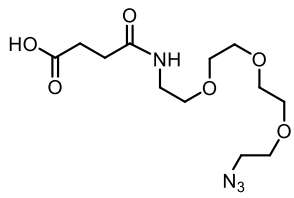

Azide **9** (300 mg, 1.38 mmol, 1.0 equiv.) and dihydrofuran-2,5-dione (151 mg, 1.51 mmol, 1.1 equiv.) were dissolved in CH_2Cl_2 (3.8 mL, 0.4 M) and heated to reflux for 1.5 h. The reaction mixture was cooled to rt, concentrated under reduced pressure, and the crude was purified by flash column chromatography (silica, 0% - 20% MeOH/CH_2Cl_2, main separation step at 10%). Azide **10** (320 mg, 1.01 mmol, 73%) was obtained as a colorless oil.

R_f (10% MeOH/CH_2Cl_2) = 0.20; **^{1}H NMR** (400 MHz, $CDCl_3$): δ = 6.81 (t, *J* = 5.5 Hz, 1H), 3.56–3.47 (m, 10H), 3.42 (dd, *J* = 5.7, 4.7 Hz, 2H), 3.32–3.24 (m, 4H), 2.52 (t, *J* = 7.0 Hz, 2H), 2.39 (t, *J* = 6.6 Hz, 2H) ppm; **^{13}C{^{1}H} NMR** (101 MHz, $CDCl_3$): δ = 175.2, 172.4, 70.2, 70.2, 70.1, 69.8, 69.7, 69.3, 50.3, 39.2, 30.4, 29.4 ppm; **LC-MS system (1)** (05-95_3.5 min): *m/z* 317 $[M–H]^–$, t_R = 0.8 min; **HRMS (ESI–):** calculated for $C_{12}H_{21}N_4O_6^–$ $[M–H]^–$ 317.1416, observed 317.1456; **IR**: $\tilde{\nu}$[cm^{-1}] = 2098.55 (azide).

$N_3(CH_2)_2(OCH_2CH_2)_3NHCO(CH_2)_2CO$-phe-cyclo(Cys-Tyr-trp-Lys-Thr-Cys)-Thr (11)

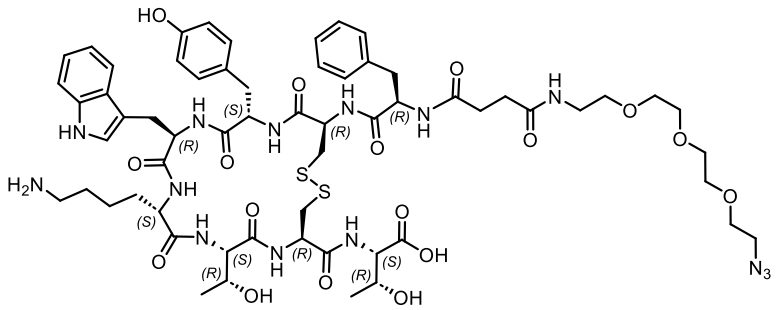

The linker-peptide conjugate was automatically synthesized, cleaved, and precipitated as described in **1.1.1**, implementing the following specifications: Bachem's 2-chlorotrityl chloride resin was manually preloaded with Thr and provided to the synthesizer. Standard settings were chosen for deprotection and coupling. The crude (77.6 mg) was purified by flash column chromatography (C18 gold, 1% - 95% MeCN+0.05% TFA/H_2O+0.05% TFA, main separation step at 30%). The linear peptide (26.7 mg) was obtained with minor impurities. For disulfide cyclization, the linear precursor was dissolved in THF (1 mL/mg peptide), and 5 mM ammonium acetate (0.1 mL/mg peptide) was added. The solution was buffered to pH=7 with saturated $NaHCO_3$, and H_2O_2 (30%, 0.5 µL/mg peptide) was added subsequently. Cyclization was completed within 30 min. THF was evaporated, and the mixture was diluted with H_2O and lyophilized. The residue was purified by flash column chromatography (C18 gold, 1% - 95% MeCN+0.05% TFA/H_2O+0.05% TFA, main separation step at 35%). Lower yield was accepted in favor of purity. Cyclized peptide **11** (9.37 mg, 6.94 µmol, 7%) was obtained as a white solid.

^{1}H NMR (500 MHz, DMSO-d_6): δ = 12.72 (bs, 1H, CO_2H), 10.77 (d, *J* = 2.4 Hz, 1H, NH), 9.16 (s, 1H, OH), 8.97 (d, *J* = 9.3 Hz, 1H, NH), 8.77 (d, *J* = 5.5 Hz, 1H, NH), 8.53 (dd, *J* = 15.0, 8.4 Hz, 2H, NH), 8.38 (d, *J* = 8.2 Hz, 1H, NH), 8.31 (d, *J* = 8.7 Hz, 1H, NH), 7.87 – 7.81 (m, 2H, NH), 7.58 (s, 4H, NH), 7.57 – 7.52 (m, 1H, CH), 7.44 (d, *J* = 7.9 Hz, 1H, CH), 7.33 (d, *J* = 8.1 Hz, 1H, CH), 7.30 – 7.26 (m, 2H, CH), 7.24 (t, *J* = 7.5 Hz, 2H, CH), 7.22 – 7.14 (m, 1H, CH), 7.11 – 7.03 (m, 2H, CH), 7.03 – 6.97 (m, 1H, CH), 6.93 – 6.88 (m, 2H, CH), 6.64 – 6.59 (m, 2H, CH), 5.46 – 5.37 (m, 1H, $C_\alpha H$), 5.37 – 5.29 (m, 1H, $C_\alpha H$), 4.83 –

4.74 (m, 2H, $C_\alpha H$, OH), 4.59 – 4.51 (m, 2H, $C_\alpha H$), 4.32 – 4.27 (m, 1H, $C_\beta H$), 4.27 – 4.18 (m, 2H, $C_\alpha H$), 4.04 – 3.96 (m, 1H, $C_\alpha H$), 3.98 – 3.89 (m, 1H, $C_\beta H$), 3.61 – 3.56 (m, 2H, CH_2), 3.56 – 3.45 (m, 8H, CH_2), 3.40 – 3.33 (m, 4H, CH_2), 3.19 – 3.11 (m, 3H. CH_2, OH), 3.03 (dd, *J* = 14.2, 9.5 Hz, 1H, CH_2), 2.91 – 2.81 (m, 3H, CH_2), 2.81 – 2.66 (m, 5H, CH_2), 2.56 – 2.51 (m, 2H, CH_2), 2.31 – 2.23 (m, 1H, CH_2), 2.25 – 2.11 (m, 3H, CH_2), 1.76 – 1.66 (m, 1H, CH_2), 1.34 – 1.22 (m, 4H, CH_2), 1.18 (d, *J* = 6.3 Hz, 3H, CH_3), 1.06 (d, *J* = 6.3 Hz, 3H, CH_3), 0.75 – 0.62 (m, 2H, CH_2) ppm; **$^{13}C\{^1H\}$ NMR** (150 MHz, DMSO-d_6): δ = 172.9 (C_q), 171.9 (C_q), 171.8 (C_q), 171.4 (C_q), 171.0 (C_q), 170.9 (C_q), 170.8 (C_q), 170.4 (C_q), 169.9 (C_q), 168.9 (C_q), 155.8 (C_q), 137.9 (C_q), 136.1 (C_q), 129.9 (CH), 129.3 (CH), 127.9 (CH), 127.0 (C_q), 127.0 (C_q), 126.2 (CH), 123.7 (CH), 120.9 (CH), 118.3 (CH), 118.2 (CH), 114.9 (CH), 111.3 (CH), 109.1 (C_q), 69.8 (CH_2), 69.7 (CH_2), 69.7 (CH_2), 69.6 (CH_2), 69.2 (CH_2), 69.0 (CH_2), 67.4 (CH), 66.1 ($C_\beta H$), 58.2 ($C_\beta H$), 58.1 ($C_\alpha H$), 55.4 ($C_\alpha H$), 54.2 ($C_\alpha H$), 53.4 ($C_\alpha H$), 52.4 ($C_\alpha H$), 52.3 ($C_\alpha H$), 51.9 ($C_\alpha H$), 50.0 (CH_2), 45.7 (CH_2), 44.7 (CH_2), 38.5 (CH_2), 38.5 (CH_2), 38.1 (CH_2), 30.7 (CH_2), 30.6 (CH_2), 30.5 (CH_2), 26.4 (CH_2), 26.0 (CH_2), 21.7 (CH_2), 20.3 (CH_3), 19.4 (CH_3)ppm; **LC-MS system (3)** (05-95_13 min): *m/z* 675.28 $[M+2H]^{2+}$, t_R = 7.05 min, **HRMS (ESI-):** calculated for $C_{61}H_{83}N_{14}O_{17}S_2^-$ $[M–H]^-$ 1347.5502, observed 1347.5497.

$N_3(CH_2)_2(OCH_2CH_2)_3NHCO(CH_2)_2CO$-trp-cyclo(Cys-Thr-phe-Thr-Tyr-Cys)-Lys (12)

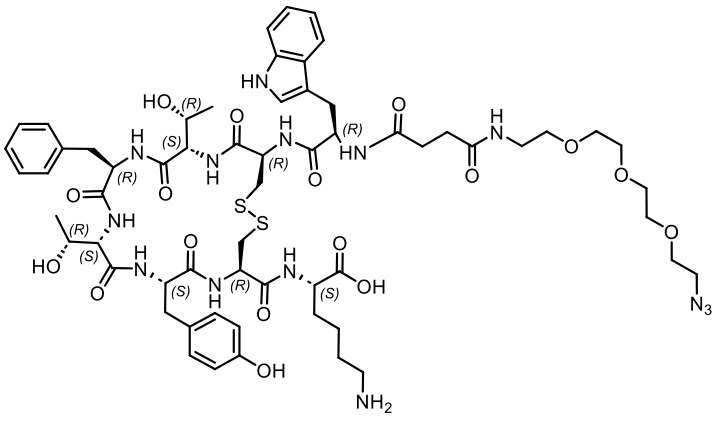

The linker-peptide conjugate was automatically synthesized, cleaved, and precipitated as described in **1.1.1**, implementing the following specifications: Bachem's 2-chlorotrityl chloride resin was manually preloaded with Lys and provided to the synthesizer. Standard settings were chosen for deprotection and coupling. The crude (80 mg) was purified by flash column chromatography (C18 gold, 1% - 95% MeCN+0.05% TFA/H_2O+0.05% TFA, main separation step at 30%). The linear peptide (35.6 mg) was obtained with minor impurities. For disulfide cyclization, the linear precursor was dissolved in MeCN/H_2O (1/1, 7 mL, 4 mM) and treated with 0.2 M aqueous ammonium acetate (23 mL)

and DMSO (5 mL). The reaction mixture was stirred overnight at rt, diluted with H_2O (25 mL) and lyophilized. The residue was purified by flash column chromatography (C18 gold, 1% - 95% MeCN+0.05% TFA/H_2O+0.05% TFA, main separation step at 35%). Lower yield was accepted in favor of purity. Cyclized peptide **12** (10 mg, 7.41 µmol, 7%) was obtained as a white solid.

LC-MS system (2) (05-95_5 min): *m/z* 1350 $[M+H]^+$, t_R = 2.99 min; **HRMS (ESI+):** calculated for $C_{61}H_{84}N_{14}NaO_{17}S_2^+$ $[M+Na]^+$ 1371.5478, observed 1371.5483.

sNIR-triazole-$(CH_2)_2(OCH_2CH_2)_3NHCO(CH_2)_2$CO-phe-cyclo(Cys-Tyr-trp-Lys-Thr-Cys)-Thr (TATE-sNIR)

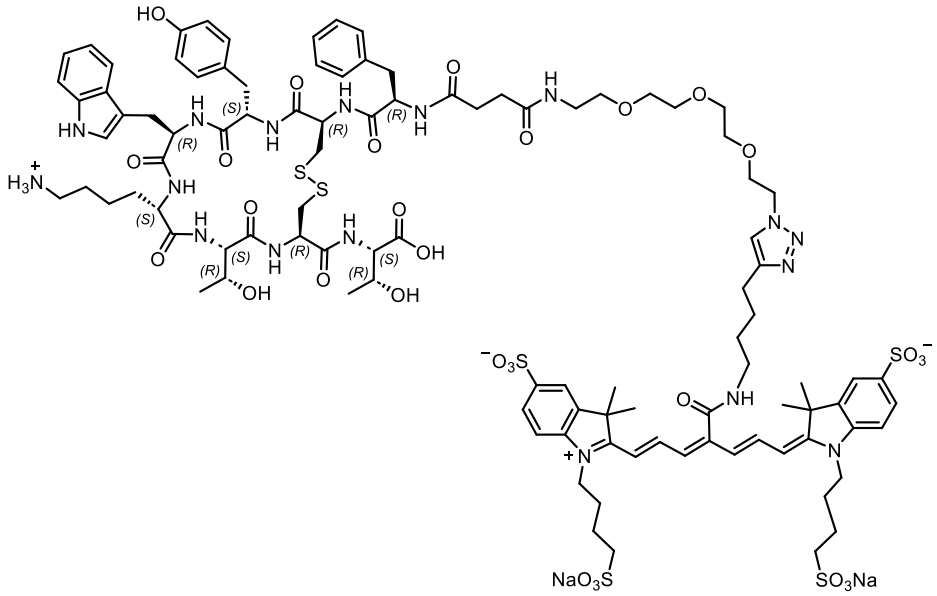

To the degassed aqueous solution of $CuSO_4$ (50 mM, 1.3 mL, 61.9 µmol, 4.0 equiv.) were added THPTA (26.9 mg, 61.9 µmol, 4.0 equiv.), sodium ascorbate (15.3 mg, 77.4 µmol, 5.0 equiv.), *t*BuOH (0.4 mL), and cyclized peptide **11** (19.8 mg, 14.7 µmol, 0.95 equiv.). Under light exclusion, the peptide-containing solution was added to a solution of cyanine **sNIR-alkyne** (15.5 mg, 15.5 µmol, 1.0 equiv.) in degassed H_2O (2.0 mL). The reaction mixture was flushed with argon, sonicated for 1 min, stirred at rt for 2 h, and then directly purified by flash column chromatography (C18 gold, 5% - 95% MeCN+0.05% TFA/H_2O+0.05% TFA, main separation step at 25%). Following semipreparative HPLC (PFP, 5% - 95% MeCN+0.1% FA / H_2O+0.1% FA), **TATE-sNIR** (8.3 mg, 3.56 µmol, 23%) was obtained as a green solid. Low yield was accepted in favor of purity.

^{1}H NMR (500 MHz, DMSO-d_6): δ = 10.77 (d, *J* = 2.3 Hz, 1H, NH), 9.16 (bs, 1H, OH), 8.91 – 8.84 (m, 2H, NH), 8.74 (d, *J* = 5.5 Hz, 1H, NH), 8.49 (d, *J* = 8.5 Hz, 2H, NH), 8.34 (t, *J* = 7.8 Hz, 2H, NH), 7.90 – 7.84 (m, 2H, NH), 7.84 (s, 1H, CH), 7.75 (d, *J* = 1.7 Hz, 2H, CH), 7.71 – 7.66 (m, 2H, CH), 7.63 (dd, *J* = 8.2, 1.6 Hz, 2H), 7.60 – 7.52 (m, 3H, NH), 7.44 (d, *J* = 7.8 Hz, 1H, CH), 7.35 – 7.30 (m, 3H, CH), 7.30 – 7.26 (m, 2H, CH), 7.23 (t, *J* = 7.6 Hz, 2H, CH), 7.20 – 7.13 (m, 1H, CH), 7.10 – 7.02 (m, 2H, CH), 7.02 – 6.96 (m, 1H, CH), 6.92 – 6.86 (m, 2H, CH), 6.64 – 6.58 (m, 2H, CH), 6.52 (d, *J* = 13.6 Hz, 2H, CH), 6.45 (d, *J* = 12.7 Hz, 2H, CH), 5.41 – 5.34 (m, 1H, CH), 5.30 – 5.26 (m, 1H, CH), 4.79 – 4.71 (m, 1H, CH), 4.53 (dd, *J* = 8.7, 5.8 Hz, 2H, CH), 4.47 (t, *J* = 5.2 Hz, 2H, CH_2), 4.34 – 4.27 (m, 1H, CH), 4.27 – 4.20 (m, 2H, CH), 4.12 – 4.05 (m, 4H, CH_2), 4.02 – 3.96 (m, 1H, CH), 3.98 – 3.89 (m, 1H, CH), 3.76 (t, *J* = 5.3 Hz, 2H, CH_2), 3.35 – 3.32 (m, 4H, CH_2) 3.19 – 3.09 (m, 3H, CH_2, OH), 3.02 (dd, *J* = 14.3, 9.4 Hz, 1H, CH_2), 2.88 – 2.83 (m, 2H, CH_2), 2.80 – 2.74 (m, 3H, CH_2), 2.74 – 2.67 (m, 4H, CH_2), 2.58 – 2.53 (m, 1H, CH_2), 2.52 – 2.51 (m, 2H, CH_2), 2.32 – 2.23 (m, 1H, CH_2), 2.23 – 2.10 (m, 3H, CH_2), 2.04 – 1.94 (m, 1H, CH_2), 1.80 – 1.67 (m, 8H, CH_2), 1.67 – 1.60 (m, 2H, CH_2), 1.51 (s, 12H, CH_3), 1.48 – 1.42 (m, 2H, CH_2), 1.36 – 1.21 (m, 8H, CH_2), 1.18 (d, *J* = 6.3 Hz, 3H, CH_3), 1.05 (d, *J* = 6.2 Hz, 3H, CH_3), 0.69 – 0.65 (m, 2H, CH_2) ppm; **^{13}C{^{1}H} NMR** (150 MHz, DMSO-d_6): δ = 176.3 (C_q), 172.8 (C_q), 171.8, (C_q), 171.4 (C_q), 171.1 (C_q), 171.0 (C_q), 170.8 (C_q), 170.4 (C_q), 170.0 (C_q), 168.9 (C_q), 166.6 (C_q), 158.7 (C_q), 155.8, (C_q), 146.4 (CH), 146.3 (C_q), 145.3 (C_q), 142.0 (C_q), 140.3 (C_q), 138.0 (C_q), 136.0 (C_q), 129.9 (CH), 129.3 (CH), 127.9, (CH), 127.0 (C_q), 127.0 (C_q), 126.2 (CH), 126.2 (CH), 123.7 (CH), 122.2 (CH), 122.2 (CH), 120.9 (CH), 119.8 (CH), 118.3 (CH), 118.1 (CH), 114.9 (CH), 111.3 (CH), 110.5 (CH), 109.1 (C_q), 104.9 (CH), 69.6 (CH_2), 69.6 (CH_2), 69.5 (CH_2), 69.5 (CH_2), 69.0 (CH_2), 68.8 (CH_2), 67.4 (CH), 66.1 (CH), 58.1 (CH), 58.1 (CH), 55.3 (CH), 54.2 (CH), 53.5 (CH), 52.4 (CH), 52.4 (CH), 51.9 (CH), 50.7 (CH_2), 49.2 (CH_2), 48.6 (C_q), 45.4 (CH_2), 44.3 (CH_2), 43.8 (CH_2), 38.9 (CH_2), 38.7 (CH_2), 38.5 (CH_2), 37.9 (CH_2), 30.6 (CH_2), 30.5 (CH_2), 30.4 (CH_2), 29.2 (CH_2), 28.7 (CH_2), 27.3 (CH_3), 26.6 (CH_2), 26.4 (CH_2), 26.2 (CH_2), 25.1 (CH_2), 24.7 (CH_2), 22.4 (CH_2), 21.7 (CH_2), 20.4 (CH_3), 19.4 (CH_3) ppm; **LC-MS system (3)** (05-95_13 min): *m/z* 1143 $[M–2Na+4H]^{2+}$ t_R = 6.45 min, **HRMS (ESI-):** *m/z* calculated for $C_{103}H_{134}N_{17}O_{30}S_2^{3-}$ $[M–2Na–H]^{3-}$ 760.2602 (*z*=3, triply charged ion), observed 760.2604. *8H (CH_2) under water peak (δ = 3.43 ppm).

sNIR-triazole-$(CH_2)_2(OCH_2CH_2)_3NHCO(CH_2)_2$CO-trp-cyclo(Cys-Thr-phe-Thr-Tyr-Cys)-Lys (scTATE-sNIR)

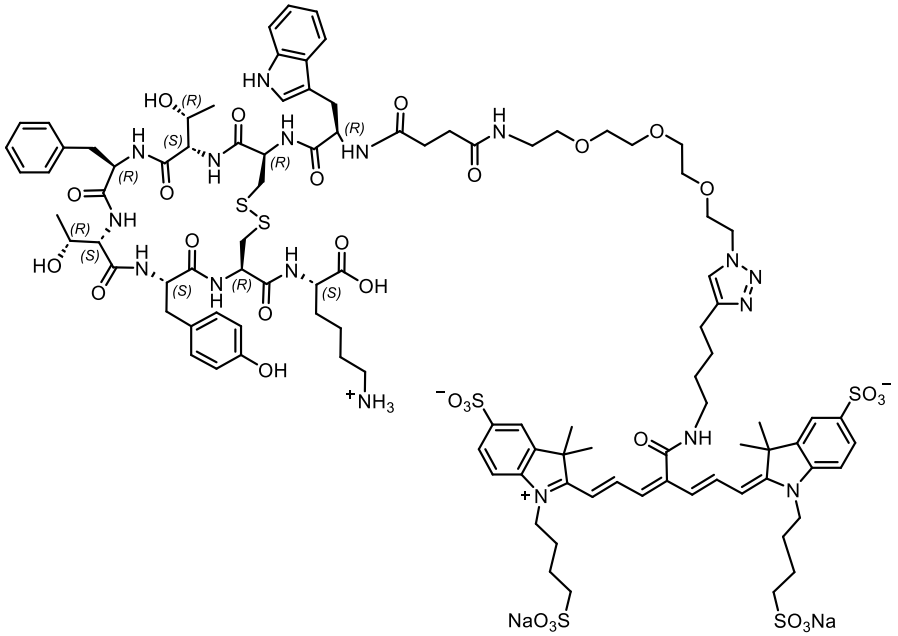

To the degassed aqueous solution of $CuSO_4$ (50 mM, 0.3 mL, 12.8 µmol, 4.0 equiv.) were added THPTA (5.6 mg, 12.8 µmol, 4.0 equiv.), sodium ascorbate (3.2 mg, 16.0 µmol, 5.0 equiv.), *t*BuOH (0.5 mL), and cyclized peptide **12** (4.1 mg, 3.04 µmol, 0.95 equiv.). Under light exclusion, the peptide-containing solution was added to a solution of cyanine **sNIR-alkyne** (3.2 mg, 3.2 µmol, 1.0 equiv.) in degassed H_2O (0.5 mL). The reaction mixture was flushed with argon, sonicated for 1 min, stirred at rt for 2 h, and then directly purified by flash column chromatography (C18 gold, 5% - 95% MeCN+0.05% TFA/H_2O+0.05% TFA, main separation step at 25%). Following semipreparative HPLC (PFP, 5% - 95% MeCN+0.1% FA/H_2O+0.1% FA), **scTATE-sNIR** (2.5 mg, 1.1 µmol, 34%) was obtained as a green solid. Low yield was accepted in favor of purity.

^{1}H NMR (600 MHz, DMSO-d_6)*: δ = 10.80 (d, *J* = 2.3 Hz, 1H), 9.15 (s, 1H), 8.88 – 8.85 (m, 1H), 8.74 (d, *J* = 4.4 Hz, 1H), 8.40 (d, *J* = 8.4 Hz, 1H), 8.22 (d, *J* = 8.4 Hz, 1H), 8.10 (d, *J* = 8.0 Hz, 1H), 8.06 – 7.97 (m, 3H), 7.93 – 7.85 (m, 2H), 7.83 (s, 1H), 7.74 (d, *J* = 1.6 Hz, 2H), 7.70 – 7.65 (m, 2H), 7.65 – 7.60 (m, 5H), 7.35 (d, *J* = 8.4 Hz, 2H), 7.31 (d, *J* = 8.1 Hz, 1H), 7.27 – 7.20 (m, 4H), 7.19 – 7.13 (m, 2H), 7.08 – 7.02 (m, 3H), 6.98 – 6.93 (m, 1H), 6.64 – 6.59 (m, 2H), 6.51 (d, *J* = 13.6 Hz, 2H), 6.49 – 6.43 (m, 2H), 5.08 (s, 1H), 4.85 (s, 1H), 4.59 (td, *J* = 8.5, 5.2 Hz, 1H), 4.55 – 4.49 (m, 2H), 4.46 (t, *J* = 5.2 Hz, 2H), 4.37 (dd, *J* = 8.6, 6.2 Hz, 1H), 4.19 (td, *J* = 8.4, 5.2 Hz, 1H), 4.10 – 4.05 (m, 4H), 4.05 – 4.02 (m, 1H), 3.82 – 3.77 (m, 2H), 3.75 (t, *J* = 5.2 Hz, 2H), 3.18 – 3.12 (m, 3H), 3.04 – 2.82 (m, 8H), 2.78

– 2.74 (m, 2H), 2.70 (t, *J* = 7.3 Hz, 2H), 2.55 – 2.52 (m, 4H), 2.32 – 2.20 (m, 4H), 1.81 – 1.67 (m, 11H), 1.65 – 1.60 (m, 3H), 1.57 – 1.52 (m, 2H), 1.51 (s, 12H), 1.41 – 1.31 (m, 3H), 1.27 – 1.21 (m, 5H), 0.99 (dd, *J* = 6.2, 1.6 Hz, 3H), 0.57 (d, *J* = 6.3 Hz, 3H) ppm; **^{13}C{^{1}H} NMR** (150 MHz, DMSO-d_6): δ = 176.3, 173.3, 172.6, 172.4, 171.9, 171.6, 171.6, 170.8, 170.5, 169.8, 169.3, 166.7, 158.9, 155.7, 146.5, 146.4, 145.1, 142.1, 140.4, 136.8, 136.1, 130.1, 129.4, 128.2, 128.1, 127.2, 126.5, 126.3, 123.8, 122.3, 120.9, 119.8, 118.5, 118.2, 115.0, 111.3, 110.6, 110.1, 105.0, 104.1, 69.7, 69.6, 69.6, 69.6, 69.0, 68.9, 67.0, 65.2, 59.2, 57.9, 55.7, 54.7, 53.7, 52.1, 51.9, 51.6, 50.8, 49.3, 48.6, 43.8, 39.0, 38.7, 38.6, 36.5, 36.0, 30.7, 30.6, 30.5, 29.3, 28.6, 28.1, 27.4, 26.6, 26.5, 26.2, 24.8, 22.5, 22.4, 19.8, 19.6 ppm; **LC-MS system (3)** (05-95_13 min): *m/z* 1143 $[M–2Na+4H]^{2+}$ t_R = 6.45 min; **HRMS (ESI-):** *m/z* calculated for $C_{103}H_{135}N_{17}O_{30}S_2^{2–}$ $[M–2Na]^{2–}$ 1140.8943 (*z*=2, doubly charged ion), observed 1140.8931. * 12H (CH_2) under water peak (δ = 3.43 ppm).

IRDye800-triazole-$(CH_2)_2(OCH_2CH_2)_3NHCO(CH_2)_2CO$-phe-cyclo(Cys-Tyr-trp-Lys-Thr-Cys)-Thr (TATE-IRDye800)

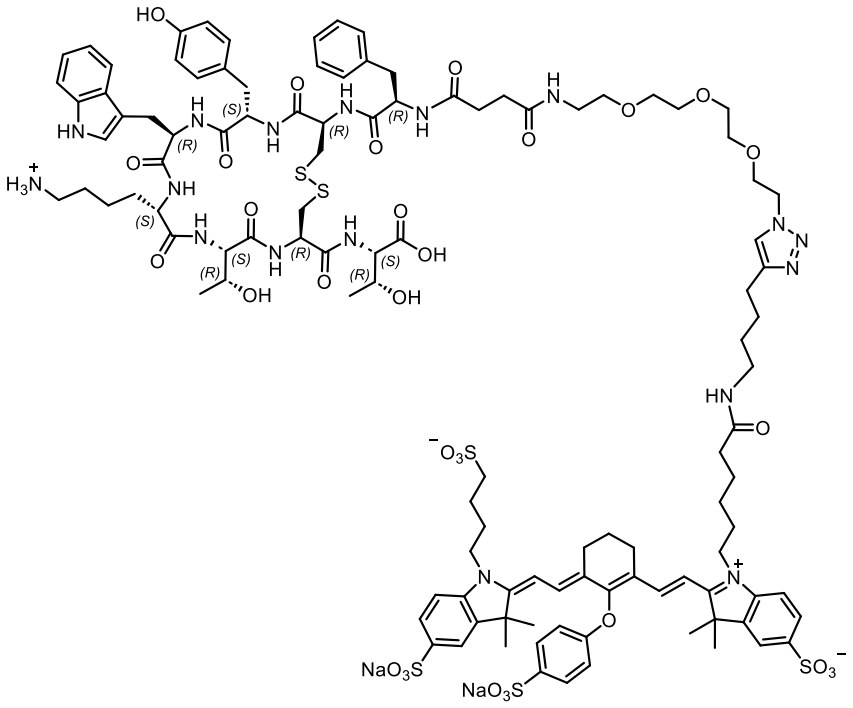

Cyclized peptide **11** (3.50 mg, 2.59 µmol, 1.0 equiv.) and cyanine **IRDye800-alkyne** (2.83 mg, 2.46 µmol, 0.95 equiv.) were under light exclusion dissolved in degassed H_2O/*t*BuOH (1/1, v/v, 820 µL, 3 mM). In parallel, THPTA (4.51 mg, 10.4 µmol, 4.0 equiv.) and sodium ascorbate (1.54 mg, 7.78 µmol, 3.0 equiv.) were added to degassed aqueous $CuSO_4$ (50 mM, 207 µL, 10.4 µmol, 4.0 equiv.). The copper (I) containing solution was transferred to the solution of azide and alkyne. The reaction mixture was flushed with argon, sonicated for 1 min, stirred at rt for 2 h, and then directly purified by flash column chromatography (C18 gold, 5% - 95% MeCN+0.05% TFA/H_2O+0.05% TFA, main separation step at 35%), followed by a semipreparative HPLC (PFP, 5% - 95% MeCN+0.1% FA/H_2O+0.1% FA). **TATE-IRDye800** (3.50 mg, 1.44 µmol, 59%) was obtained as a green solid.

LC-MS system (3) (05-95_13 min): *m/z* 1216 $[M–2Na+4H]^{2+}$ t_R = 7.68 min.

tri-*tert*-butyl (9S,13S)-3,11-dioxo-1-phenyl-2-oxa-4,10,12-triazapentadecane-9,13,15-tricarboxylate (13)

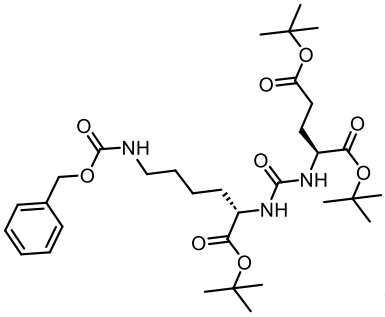

Under argon atmosphere, a suspension of L-H-Glu(O*t*Bu)-O*t*Bu *HCl (1.00 g, 3.38 mmol, 1.0 equiv.) in anhydrous CH_2Cl_2 (11 mL, 0.3 M) was cooled to 0 °C. NEt_3 (0.47 mL, 3.38 mmol, 1.0 equiv.) and 4-DMAP (12.2 mg, 0.1 mmol, 3 mol%) were added, and the mixture was stirred at 0 °C for 5 min. CDI (687 mg, 4.18 mmol, 1.1 equiv.) was added, and the mixture was stirred for 18 h with warming to room temperature. The mixture was diluted with CH_2Cl_2 and washed with sat. $NaHCO_3$, water, and brine. The organic layer was dried over Na_2SO_4, filtered, and the solvent was evaporated. Without purification, the crude imidazole was dissolved in CH_2ClCH_2Cl (12 mL, 0.3 M) at cooled to 0 °C. NEt_3 (0.94 mL, 6.76 mmol, 2.0 equiv.) and MeOTf (0.42 mL, 3.72 mmol, 1.1 equiv.) were added and the mixture was stirred for 30 min, followed by the addition of L-H-Lys(Cbz)-O*t*Bu*HCl (1.26 g, 3.38 mmol, 1.0 equiv.) and stirring at 40 °C for 4 h. The mixture was concentrated, and the crude material was purified by flash column chromatography (silica, 0% - 100% EtOAc/PE, main separation step at 40%). Urea **13** (2.0 mg, 3.22 mmol, 95% o2s) was obtained as a colorless oil.

R_f (40% EtOAc/PE) = 0.40; **^{1}H NMR** (400 MHz, $CDCl_3$): δ = 7.35 (d, *J* = 4.2 Hz, 4H), 7.32 − 7.28 (m, 1H), 5.13 − 5.03 (m, 4H), 4.36 − 4.30 (m, 2H), 3.20 − 3.15 (m, 2H), 2.37 − 2.22 (m, 2H), 1.88 − 1.73 (m, 2H), 1.69 − 1.48 (m, 4H), 1.46–1.44 (m, 18H), 1.43 (s, 9H) ppm; **^{13}C{^{1}H} NMR** (101 MHz, $CDCl_3$): δ = 172.6, 172.5, 172.3, 156.9, 156.7, 136.8, 128.6, 128.2, 128.2, 82.2, 81.9, 80.7, 53.4, 53.2, 40.7, 31.7, 29.5, 28.5, 28.2, 28.2, 28.1, 22.4, 14.3 ppm; **LC-MS** (01-90_5min): *m/z* 623 $[M+H]^+$, t_R = 4.00 min; **HRMS (ESI+):** calculated for $C_{32}H_{51}N_3O_9Na^+$ $[M+Na]^+$ 644.3523, observed 644.1819.

NMR spectra contain ethyl acetate.

di-*tert*-butyl (((*S*)-6-amino-1-(*tert*-butoxy)-1-oxohexan-2-yl)carbamoyl)-L-glutamate (14)

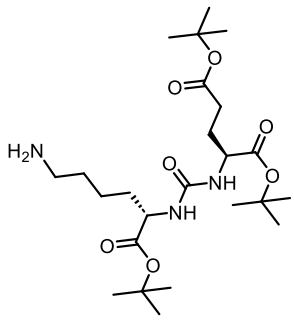

Under argon atmosphere, urea **13** (2.00 g, 3.22 mmol, 1.0 equiv.) was dissolved in MeOH (20 mL, 0.16 M). The solution was purged with argon. 3 Spatula pints of palladium on activated charcoal (10%) were added. After purging the flask with H_2, the mixture was stirred at rt for 18 h under light H_2-pressure (balloon). The product-containing suspension was filtered over a plug of sand and celite to remove the palladium catalyst, followed by evaporation of the solvent. Purification of the crude material by flash column chromatography (C18 gold, 5% - 95% MeCN/H_2O, main separation step at 65%) afforded amine **14** (1.31 g, 2.86 mmol, 83%) as a colorless oil.

R_f (40% EtOAc/PE) = 0.20; **^{1}H NMR** (400 MHz, $CDCl_3$): δ = 5.39 − 5.35 (m, 2H), 4.30 (m, 2H), 2.64 (d, *J* = 7.4 Hz, 2H), 2.34 − 2.19 (m, 2H), 2.07 − 1.98 (m, 1H), 1.85 − 1.77 (m, 1H), 1.75 − 1.68 (m, 1H), 1.62 − 1.54 (m, 3H), 1.46–1.44 (m, 18H) 1.39 (s, 8H) ppm; **^{13}C{^{1}H} NMR** (101 MHz, $CDCl_3$): δ = 172.6, 172.5, 172.4, 157.1, 82.0, 81.7, 80.5, 53.5, 53.0, 41.9, 33.3, 33.1, 31.7, 28.5, 28.1, 28.1, 28.1, 22.5 ppm; **LC-MS** (01-90_5min): *m/z* 488 $[M+H]^+$, t_R = 2.88 min; **HRMS (ESI+):** calculated for $C_{24}H_{45}N_3O_7Na^+$ $[M+Na]^+$ 510.3155, observed 510.3158.

2,5-dioxopyrrolidin-1-yl 6-azidohexanoate (15)

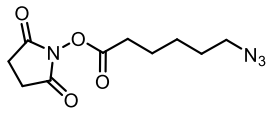

6-Azidohexanoic acid (100 mg, 0.64 mmol, 1.0 equiv.) was dissolved in DMF (4 mL, 0.16 M) and TSTU (230 mg, 0.76 mmol, 1.2 equiv.) and DIPEA (130 µL, 0.76 mmol, 1.2 equiv.) were added. The reaction mixture was stirred at rt for 18 h, followed by evaporation of the solvent. The crude material was dissolved in $CHCl_3$ and washed with brine. The organic layer was dried over Na_2SO_4, filtered, and concentrated. The crude material was purified by flash column chromatography (silica, 0% - 100% EtOAc/PE, main separation step at 50%). Carboxy-activated linker **15** (114 mg, 0.45 mmol, 71%) was obtained as a colorless oil.

^{1}H NMR (400 MHz, $CDCl_3$): δ = 3.29 (t, *J* = 6.8 Hz, 2H), 2.84 (bs, 4H), 2.63 (t, *J* = 7.3 Hz, 2H), 1.85 − 1.79 (m, 2H), 1.67 − 1.60 (m, 2H), 1.54 − 1.48 (m, 2H) ppm; **^{13}C{^{1}H} NMR** (101 MHz, $CDCl_3$): δ = 169.1, 168.4, 51.1, 30.8, 28.4, 25.9, 25.6, 24.1 ppm; **HRMS (ESI+):** calculated for $C_{10}H_{14}N_4O_4Na^+$ $[M+Na]^+$ 277.0913, observed 277.0910.

di-*tert*-butyl (((*S*)-6-(6-azidohexanamido)-1-(*tert*-butoxy)-1-oxohexan-2-yl)carbamoyl)-L-glutamate (16)

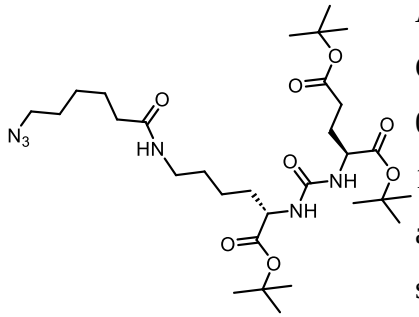

Amine **14** (190 mg, 0.39 mmol, 1.0 equiv.) was dissolved in $CHCl_3$ (2 mL, 0.1 M), carboxy-activated linker **15** (100 mg, 0.39 mmol, 1.0 equiv.) and DIPEA (100 µL, 0.59 mmol, 1.5 equiv.) were added, and the reaction mixture was stirred at rt for 3 h. The solvent was removed under reduced pressure and the crude material was purified by flash column chromatography (C18 gold, H_2O/MeCN, 5%-95%, main separation step at 80%). Urea **16** (223 mg, 0.36 mmol, 91%) was obtained as a colorless oil.

^{1}H NMR (400 MHz, $CDCl_3$): δ = 4.34 − 4.24 (m, 2H), 3.27 (t, *J* = 6.5 Hz, 3H), 2.39 − 2.26 (m, 2H), 2.20 (t, *J* = 7.7 Hz, 2H), 2.12 − 2.03 (m, 1H), 1.90 − 1.73 (m, 2H), 1.69 − 1.58 (m, 5H), 1.54 − 1.36 (m, 33H) ppm; **^{13}C{^{1}H} NMR** (101 MHz, $CDCl_3$): δ = 173.2, 1773.1, 172.9, 172.5, 157.2, 82.4, 81.9, 80.8, 53.6, 53.3, 51.5, 39.1, 36.5, 32.7, 31.8, 28.9, 28.8, 28.3, 28.2, 28.1, 26.5, 25.4, 24.3 ppm; **LC-MS** (01-90_5min): *m/z* 628 $[M+H]^+$, t_R = 3.80 min; **HRMS (ESI+):** calculated for $C_{30}H_{54}N_6O_8Na^+$ $[M+Na]^+$ 649.3901, observed 649.3890.

(((*S*)-5-(6-azidohexanamido)-1-carboxypentyl)carbamoyl)-L-glutamic acid (17)

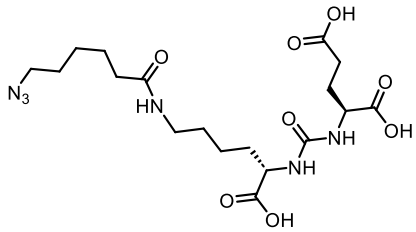

Urea **16** (52.0 mg, 83.0 µmol, 1.0 equiv.) was dissolved in CH_2Cl_2/TFA (1/1, v/v, 4 mL, 0.02 M) and stirred at rt for 18 h. The reaction mixture was concentrated, and the crude material was purified by flash column chromatography (C18 gold, H_2O + 0.05% TFA/MeCN + 0.05% TFA, 5%-95%, main separation step at 40%). Azide **17** (5.0 mg, 10.9 µmol, 13%) was obtained as a yellow oil.

^{1}H NMR (500 MHz, CD_3OD): δ = 4.33 (q, *J* = 4.9 Hz, 1H), 4.28 (q, *J* = 4.9 Hz, 1H), 3.37 (s, 1H), 3.34 − 3.29 (m, 1H), 3.19 (t, *J* = 6.9 Hz, 2H), 2.46 − 2.41 (m, 2H), 2.23 − 2.12 (m, 3H), 1.96 − 1.82 (m, 2H), 1.73 − 1.61 (m, 5H), 1.59 − 1.51 (m, 2H), 1.48 − 1.39 (m, 4H) ppm; **^{13}C{^{1}H} NMR** (125 MHz, CD_3OD): δ = 176.4, 176.4, 176.0, 175.8, 160.1, 53.9, 53.5, 52.3, 40.1, 36.9, 33.2, 31.1, 29.9, 29.6, 28.9, 27.4, 26.5, 24.0 ppm; **LC-MS** (01-90_5min): *m/z* 459 $[M+H]^+$, t_R = 2.39 min; **HRMS (ESI+):** calculated for $C_{18}H_{30}N_6O_8Na^+$ $[M+Na]^+$ 481.2023, observed 481.2018.

sodium 2-((1*E*,3*Z*,5*E*)-4-((4-(1-(6-(((*S*)-5-carboxy-5-(3-((*S*)-1,3-dicarboxypropyl)ureido)pentyl)amino)-6-oxohexyl)-1*H*-1,2,3-triazol-4-yl)butyl)carbamoyl)-7-((*E*)-3,3-dimethyl-5-sulfonato-1-(4-sulfonatobutyl)indolin-2-ylidene)hepta-1,3,5-trien-1-yl)-3,3-dimethyl-1-(4-sulfonatobutyl)-3*H*-indol-1-ium-5-sulfonate (EuK-Ahx-sNIR)

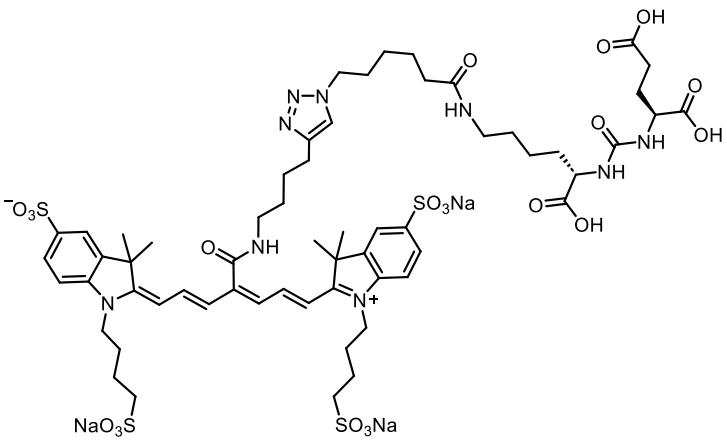

Azide **17** (5.0 mg, 10.9 µmol, 1.0 equiv.) was under light exclusion dissolved in degassed *t*BuOH/H_2O (3/1, v/v, 800 µL, 0.01 M), and **sNIR-alkyne** (10.4 mg, 10.3 µmol, 0.95 equiv.) was added. In parallel, THPTA (23.7 mg, 54.6 µmol, 5.0 equiv.) and sodium ascorbate (15.1 mg, 76.4 µmol, 7.0 equiv.) were added to degassed aqueous $CuSO_4$ (50 mM, 873 µL, 43.7 µmol, 4.0 equiv.). The copper(I)-containing solution was transferred to the solution of azide and alkyne, and the reaction mixture was stirred at rt for 2 h. Subsequently, the reaction mixture was directly purified by flash column chromatography (C18 gold, 2% - 95% MeCN+0.05% TFA/H_2O+0.05% TFA, main separation step at 20%), followed by a semipreparative HPLC (PFP, 5% - 95% MeCN+0.05% FA/H_2O+0.05% FA). Lower yield was accepted in favor of purity. **EuK-Ahx-sNIR** (4.0 mg, 2.87 µmol, 28%) was obtained as a green solid.

^{1}H and **^{13}C{^{1}H} NMR** were not acquired due to limited substance quantities; **LC-MS** (05-95_13min): *m/z* 695.8 $[M-3Na+H]^{2-}$, t_R = 5.86 min; **HRMS (ESI-)**: *m/z* calculated for $C_{60}H_{80}N_9NaO_{21}S_4^{2-}$ $[M-2Na]^{2-}$ 706.7023, observed 706.7117.

The LC-MS spectrum is attached in the appendix.

sodium 1-(6-(((1-(6-(((S)-5-carboxy-5-(3-((S)-1,3-dicarboxypropyl)ureido)pentyl)amino)-6-oxohexyl)-1H-1,2,3-triazol-4-yl)methyl)amino)-6-oxohexyl)-2-((E)-2-((E)-3-(2-((E)-3,3-dimethyl-5-sulfonato-1-(4-sulfonatobutyl)indolin-2-ylidene)ethylidene)-2-(4-sulfonatophenoxy)cyclohex-1-en-1-yl)vinyl)-3,3-dimethyl-3H-indol-1-ium-5-sulfonate (EuK-Ahx-IRDye800)

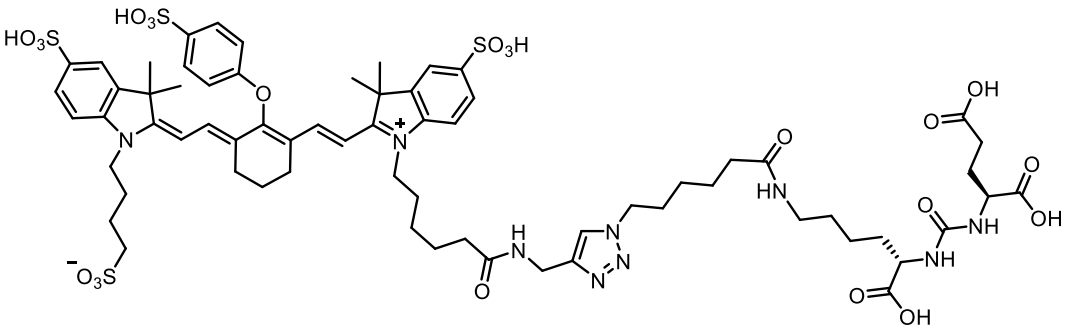

The solvents used were degassed for 15 min in a sonication bath prior to use. Azide **17** (1.9 mg, 4.0 µmol, 1.0 eq) and IRDye800-alkyne (4.6 mg, 4.0 µmol, 0.95 eq) were dissolved in 0.4 ml of tBuOH/water (1:1). Then, the catalyst solution containing copper sulfate pentahydrate (4.2 mg, 17.0 µmol, 4.0 eq), THPTA (7.2 mg, 17.0 µmol, 4.0 eq), and sodium ascorbate (6.6 mg, 33.0 µmol, 5.0 eq) in 0.4 ml of water was added. The mixture was stirred for 30 min at rt. After completion of the reaction, the crude was directly purified via column chromatography (C18, 5% - 95% MeCN+0.05% TFA/H_2O+0.05% TFA) to obtain **EuK-Ahx-IRDye800** as a green solid (0.3 mg, 0.192 µmol, 5%).

^{1}H and **^{13}C{^{1}H} NMR** were not acquired due to limited substance quantities; **LC-MS** (05-95_13min): *m/z* 749.9 $[M-3Na+5H]^{2+}$, t_R = 6.2 min; **HRMS (ESI+)**: *m/z* calculated for $C_{67}H_{88}N_9O_{22}S_4^{2+}$ $[M\ radical+2H^+]^{2+}$ 749.2463, observed 749.2462.

The LC-MS spectrum is attached in the appendix.

1.1.3 NMR spectra

^{1}H NMR (400 MHz, $CDCl_3$) of **2**

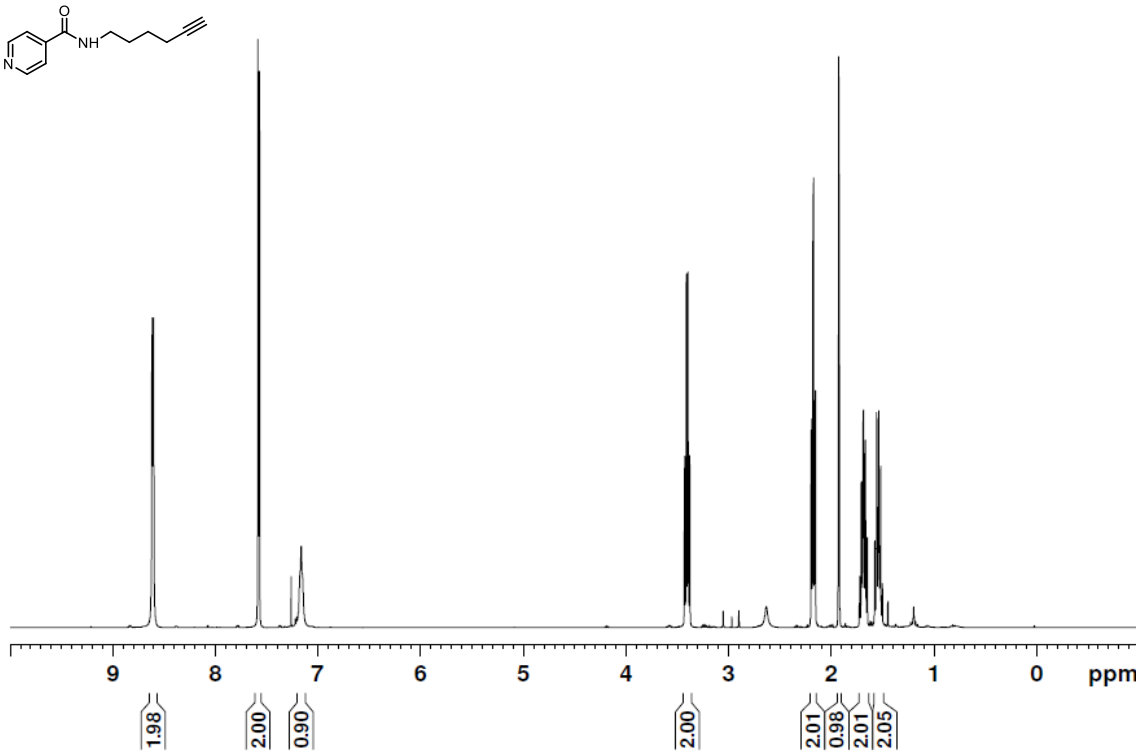

^{13}C{^{1}H} NMR (101 MHz, $CDCl_3$) of **2**

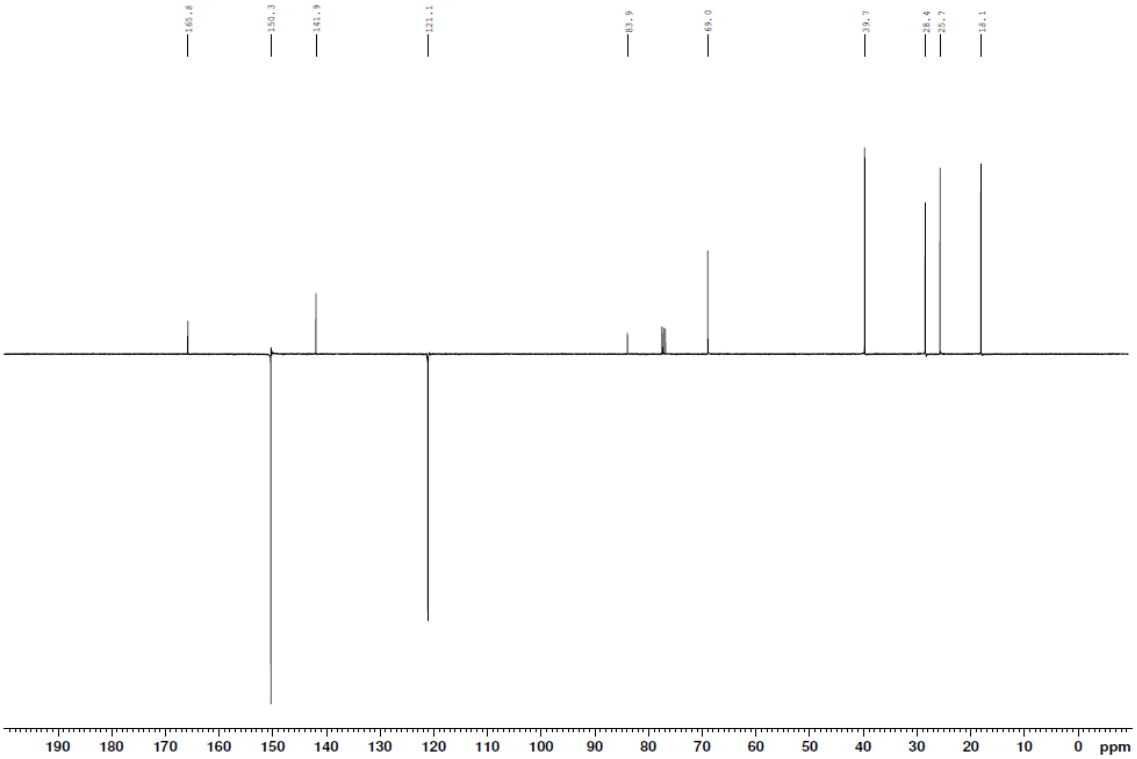

^{1}H NMR (400 MHz, $CDCl_3$) of **4**

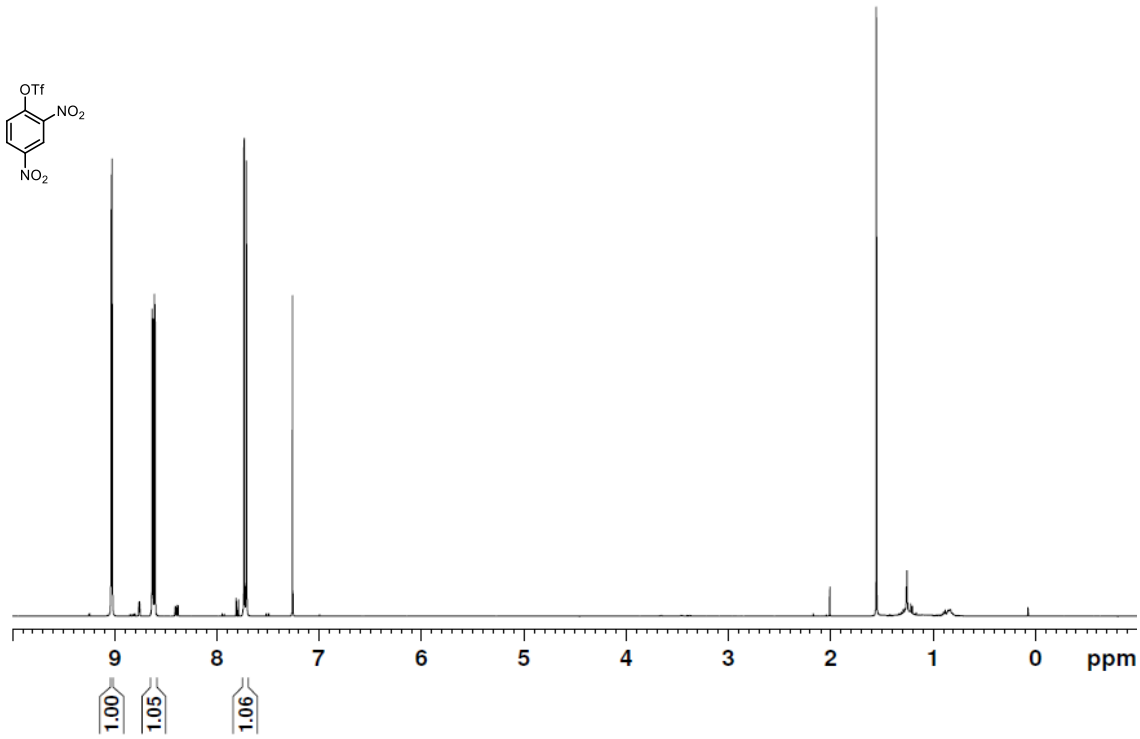

^{13}C{^{1}H} NMR (101 MHz, $CDCl_3$) of **4**

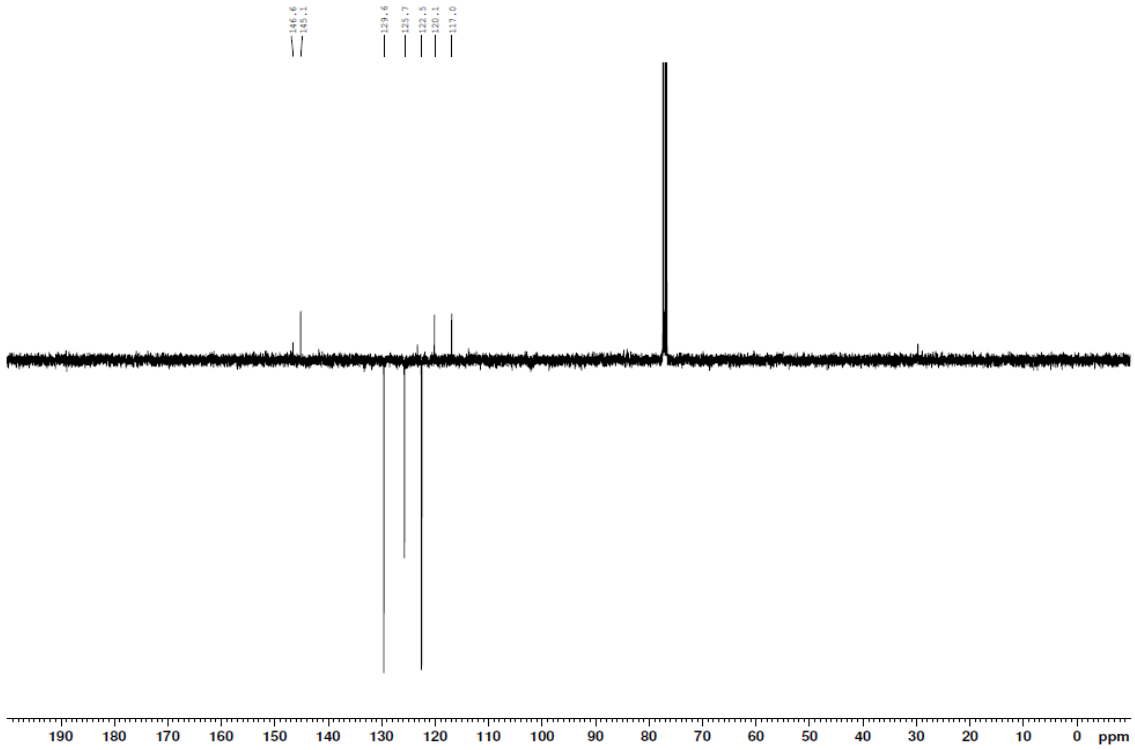

^{1}H NMR (400 MHz, CD_3OD) of **5**

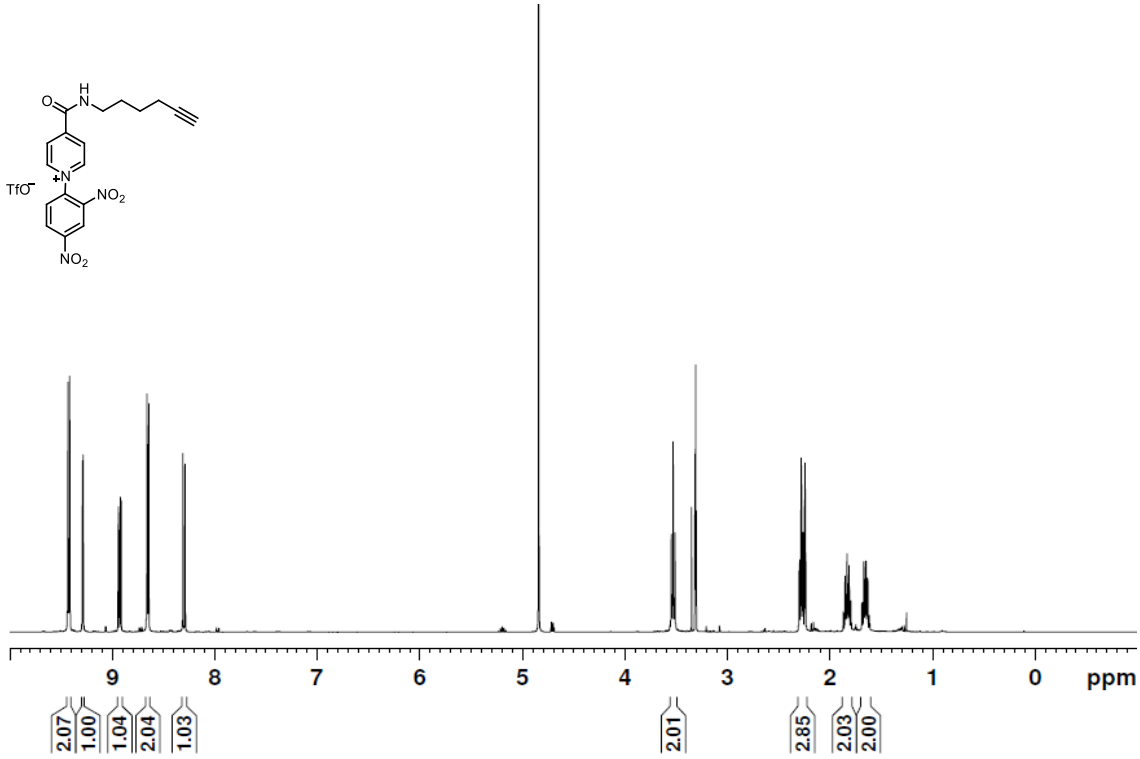

^{13}C{^{1}H} NMR (101 MHz, CD_3OD) of **5**

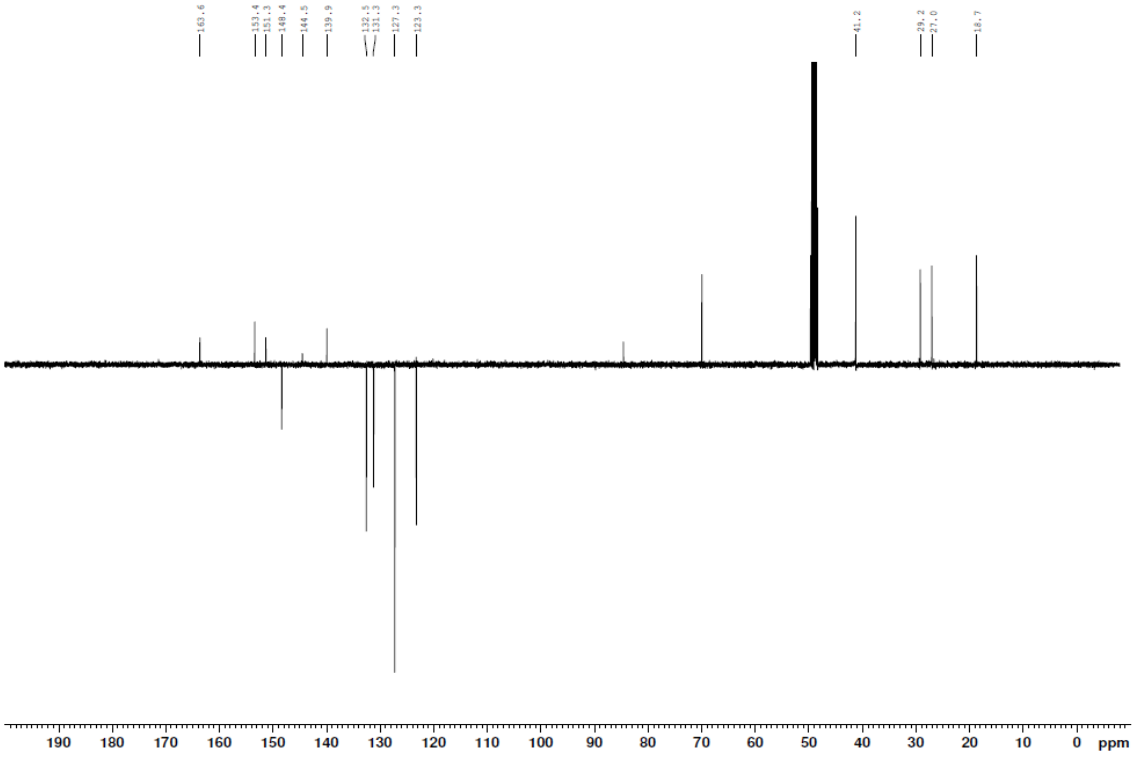

^{1}H NMR (400 MHz, DMSO-d_6) of **6**

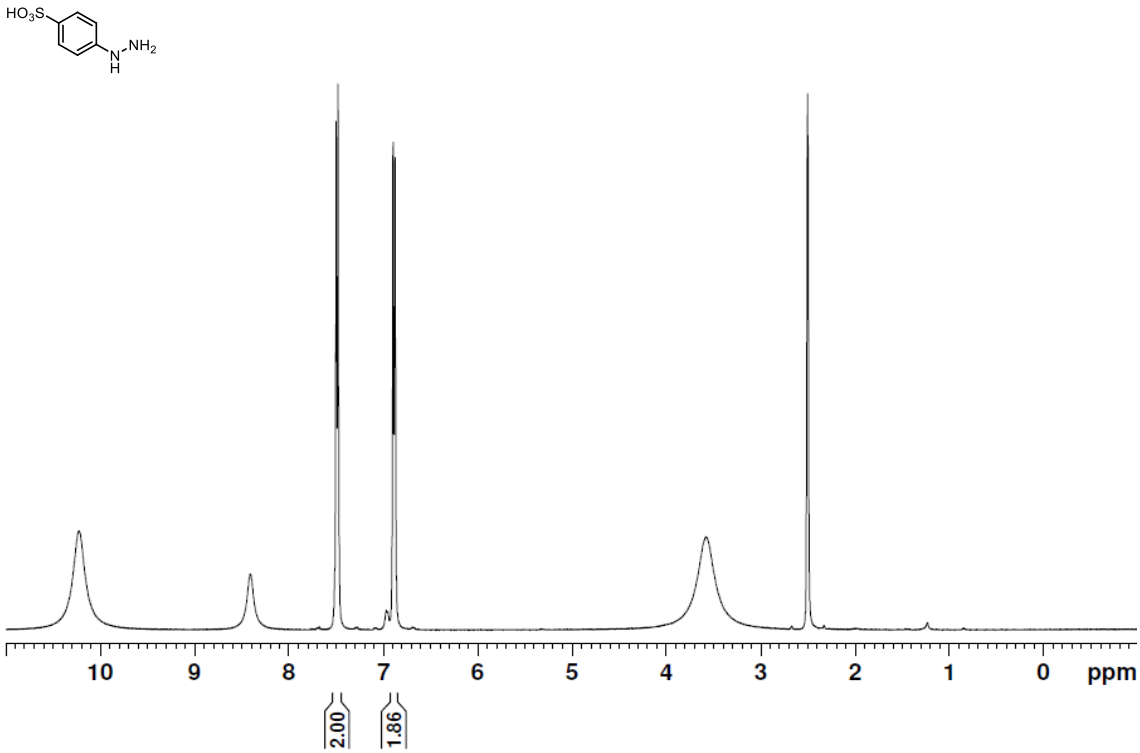

^{13}C{^{1}H} NMR (101 MHz, DMSO-d_6) of **6**

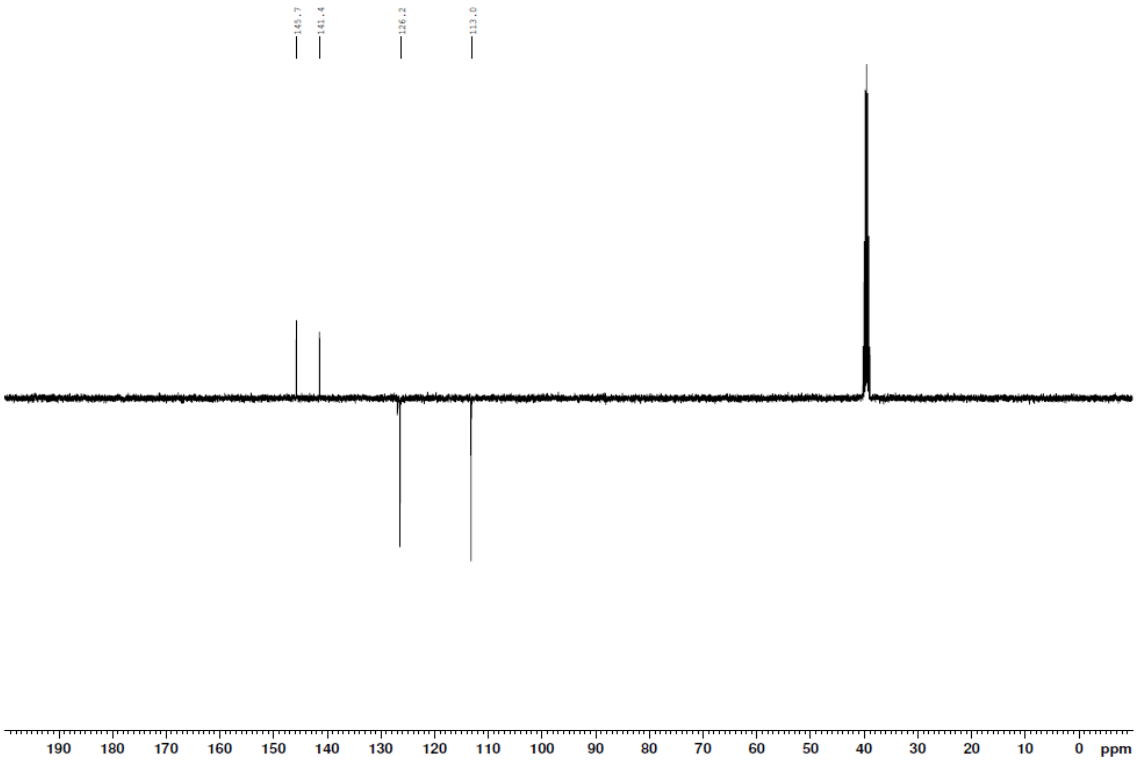

^{1}H NMR (400 MHz, DMSO-d_6) of **7**

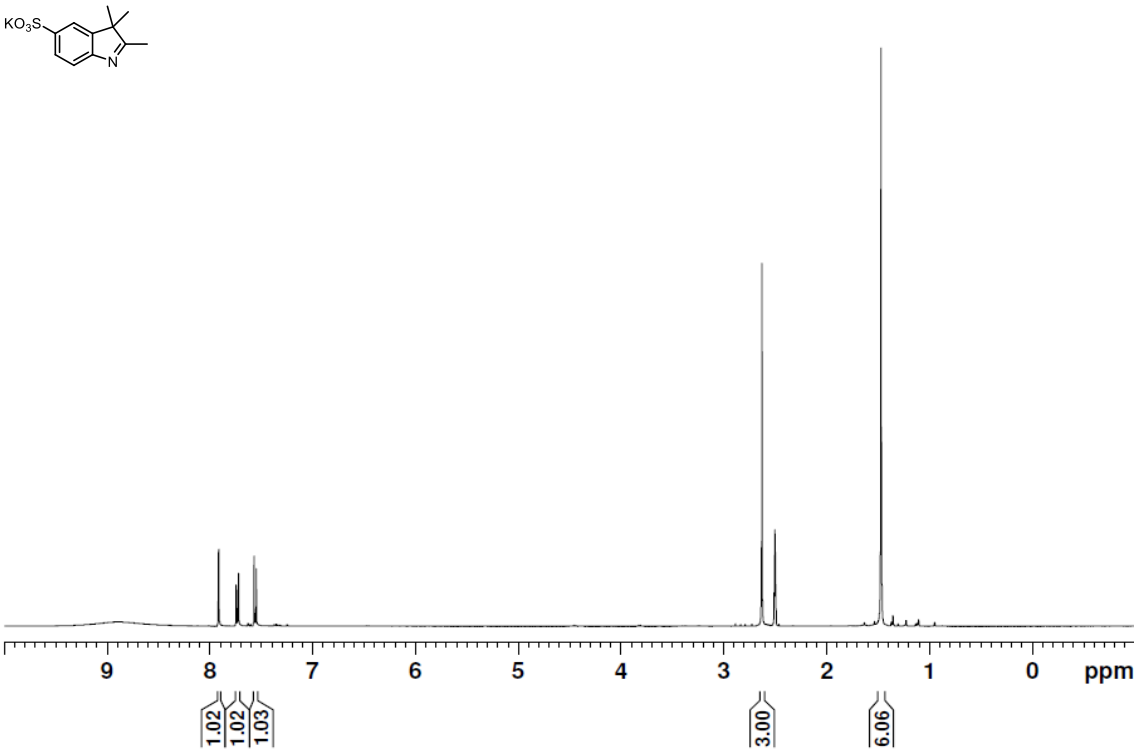

^{13}C{^{1}H} NMR (101 MHz, DMSO-d_6) of **7**

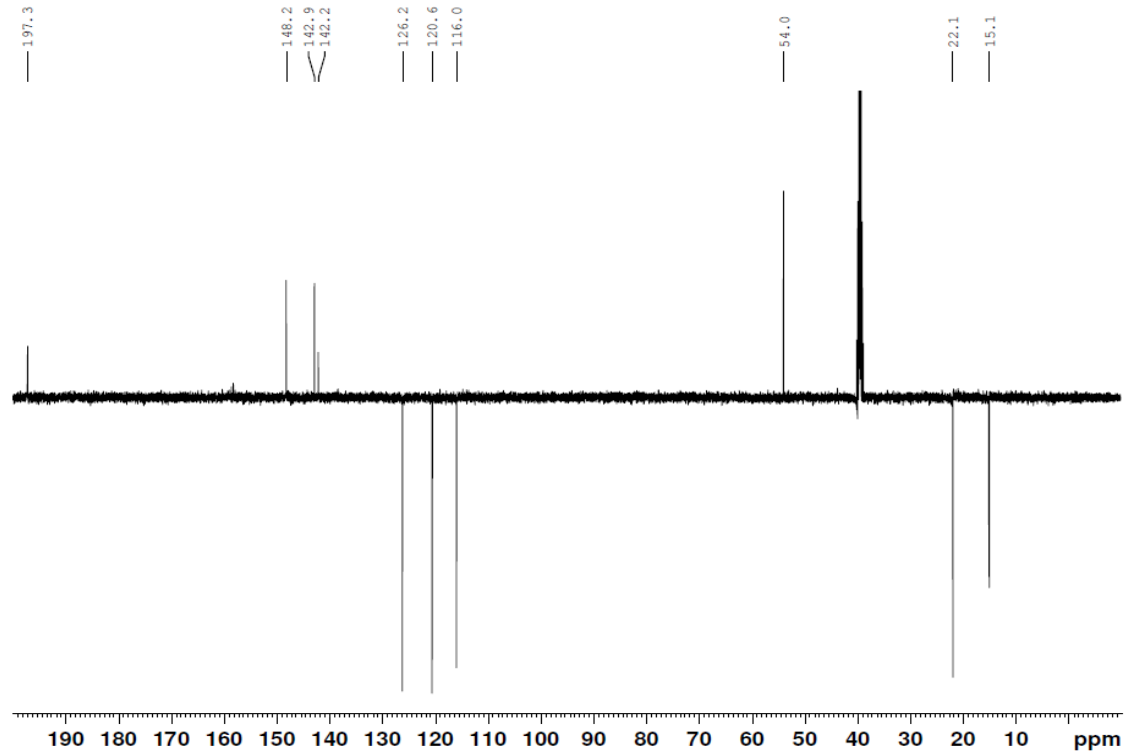

^{1}H NMR (400 MHz, DMSO-d_6) of **8**

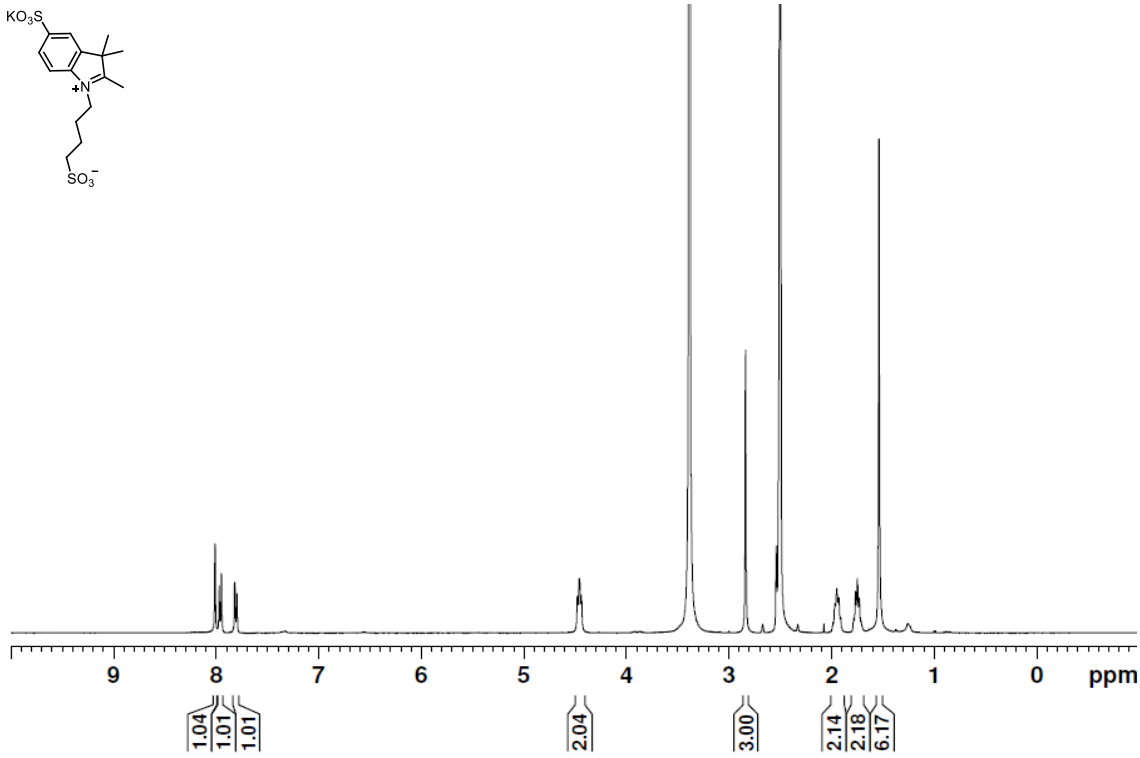

^{13}C{^{1}H} NMR (101 MHz, DMSO-d_6) of **8**

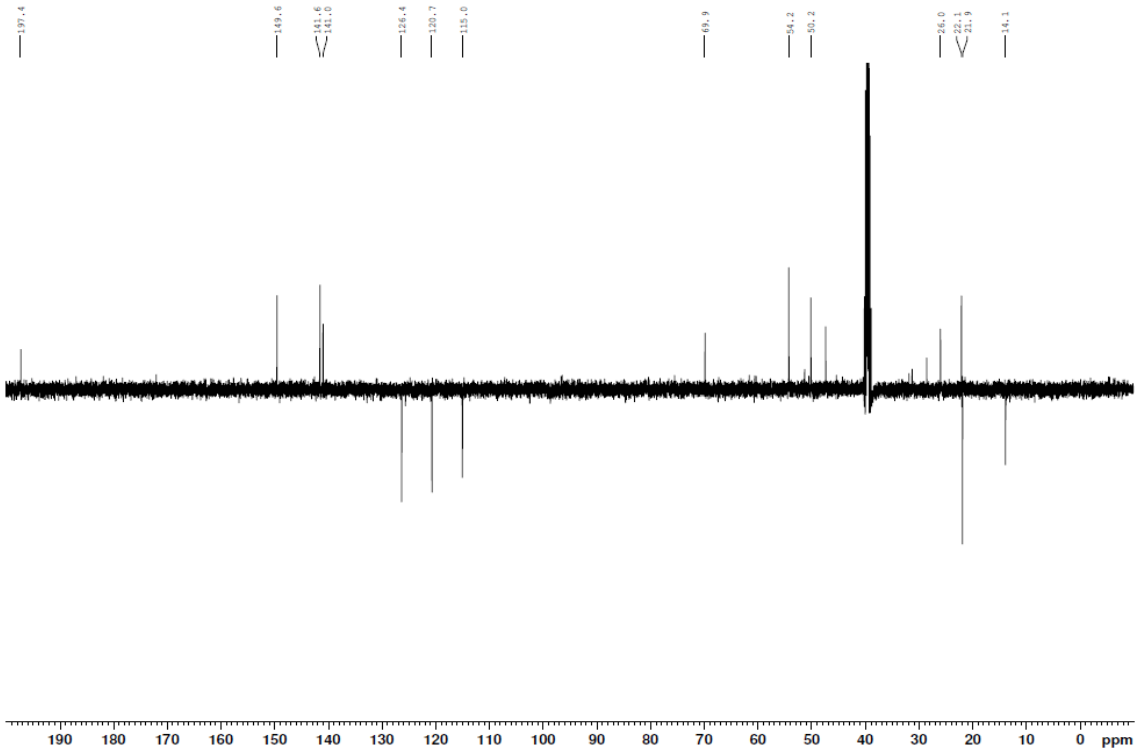

^{1}H NMR (400 MHz, D_2O) of **sNIR-alkyne**

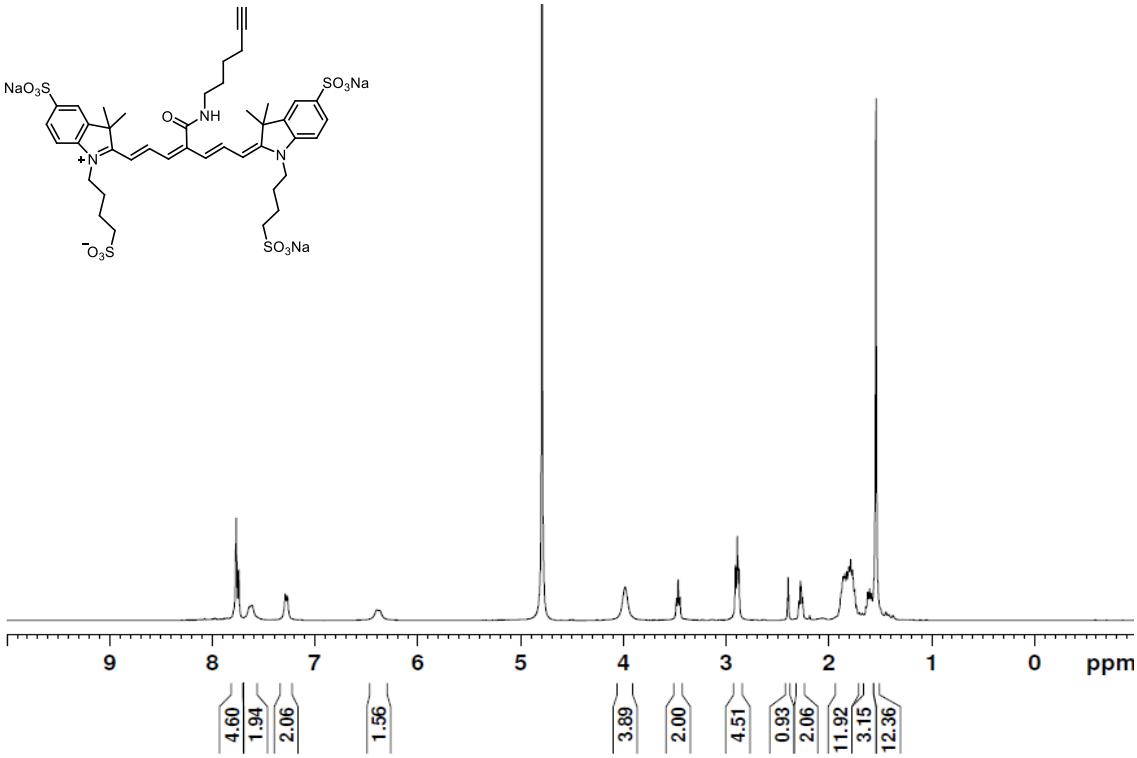

^{13}C{^{1}H} NMR (101 MHz, D_2O) of **sNIR-alkyne**

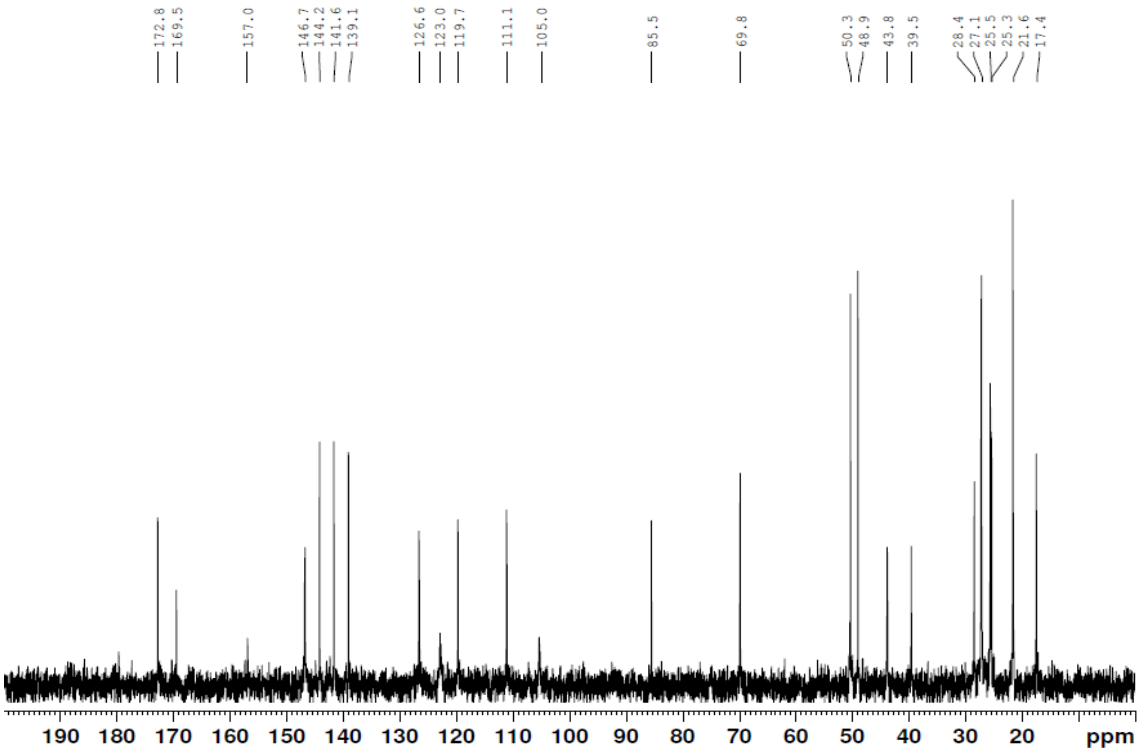

^{1}H NMR (600 MHz, DMSO-d_6) of **IRDye800-alkyne**

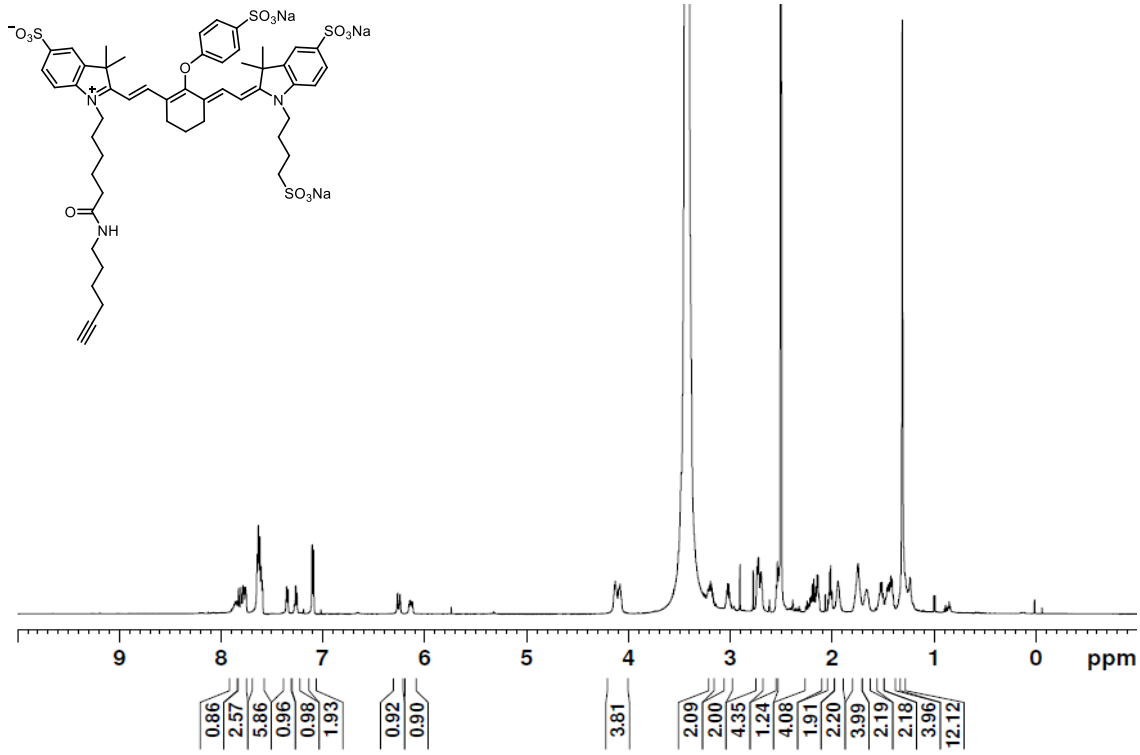

^{13}C{^{1}H} NMR (150 MHz, DMSO-d_6) of **IRDye800-alkyne**

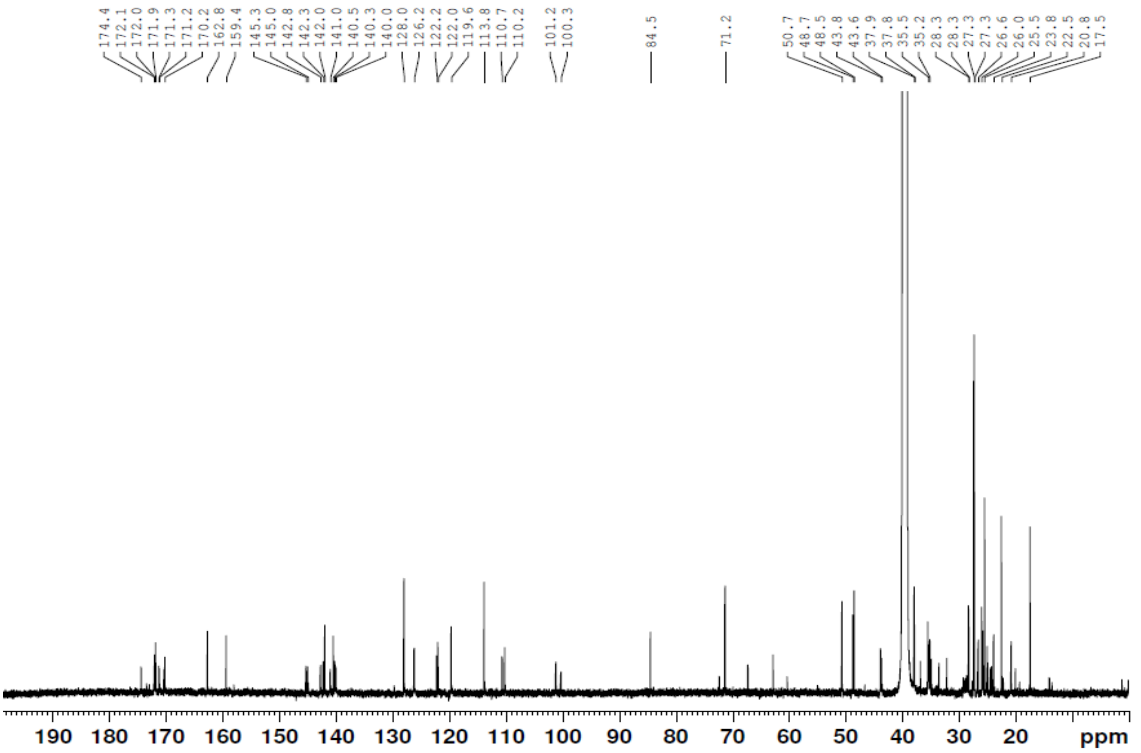

^{1}H NMR (400 MHz, $CDCl_3$) of **9**

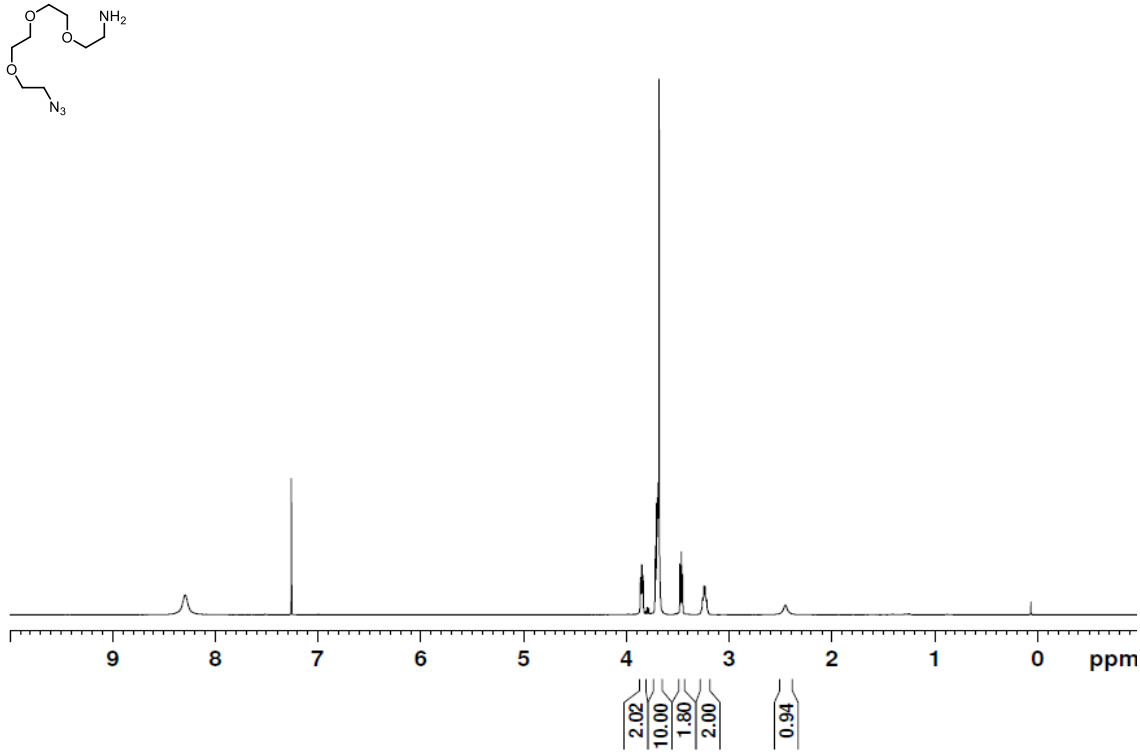

^{13}C{^{1}H} NMR (101 MHz, $CDCl_3$) of **9**

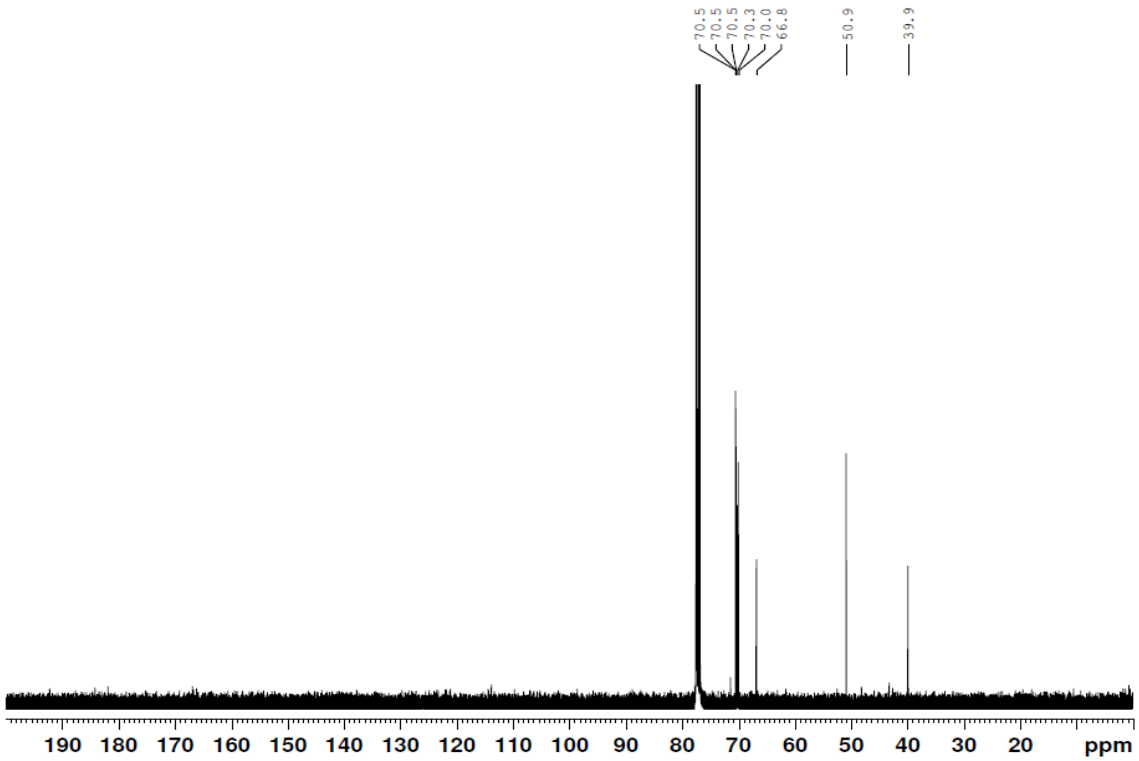

^{1}H NMR (400 MHz, $CDCl_3$) of **10**

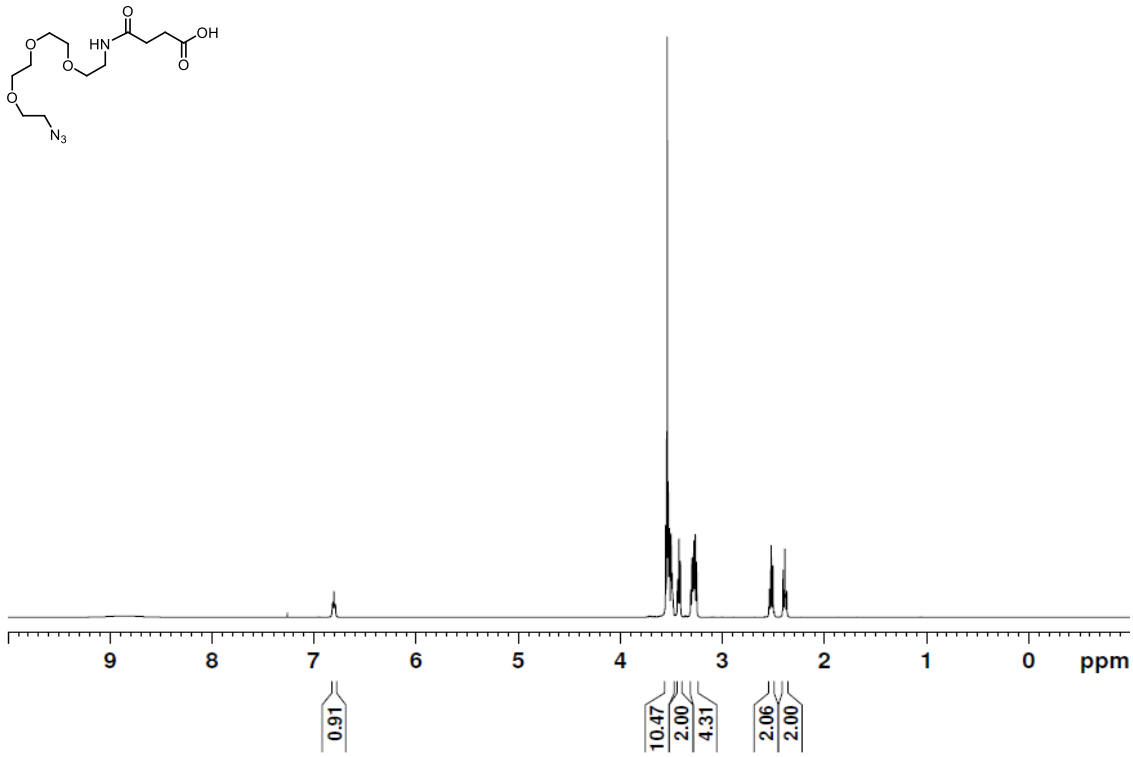

^{13}C{^{1}H} NMR (101 MHz, $CDCl_3$) of **10**

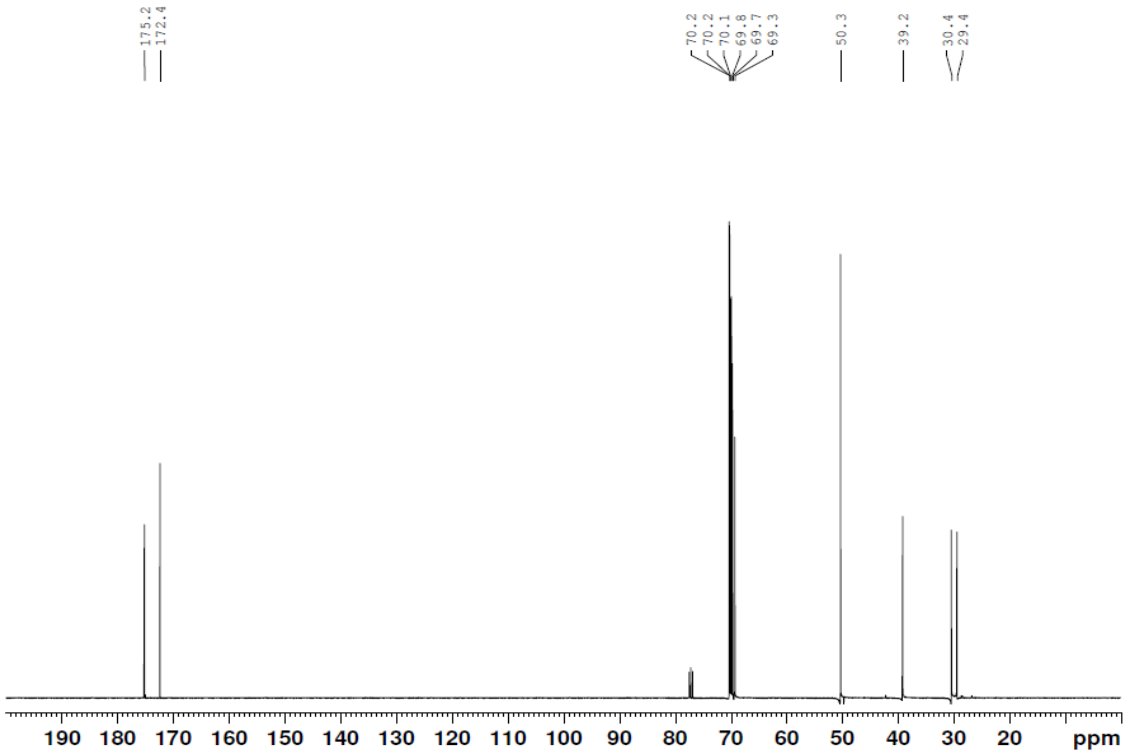

^{1}H NMR (500 MHz, DMSO-d_6) of **11**

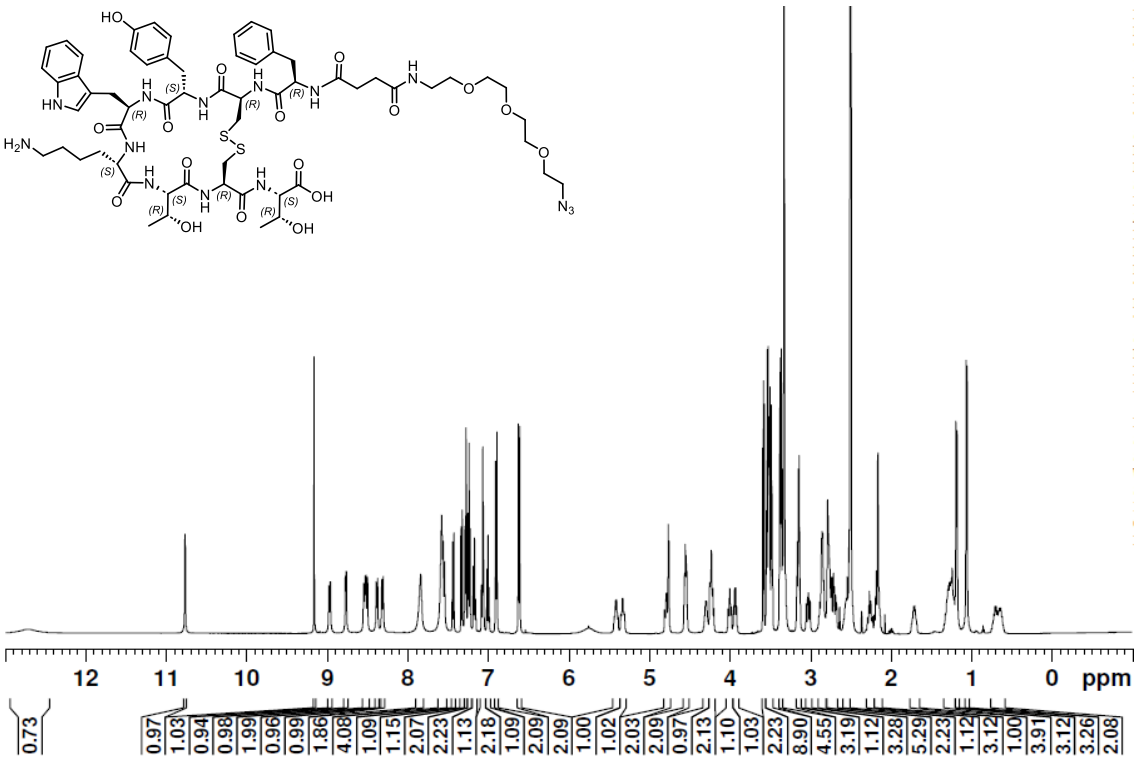

^{13}C{^{1}H} NMR (125 MHz, DMSO-d_6) of **11**

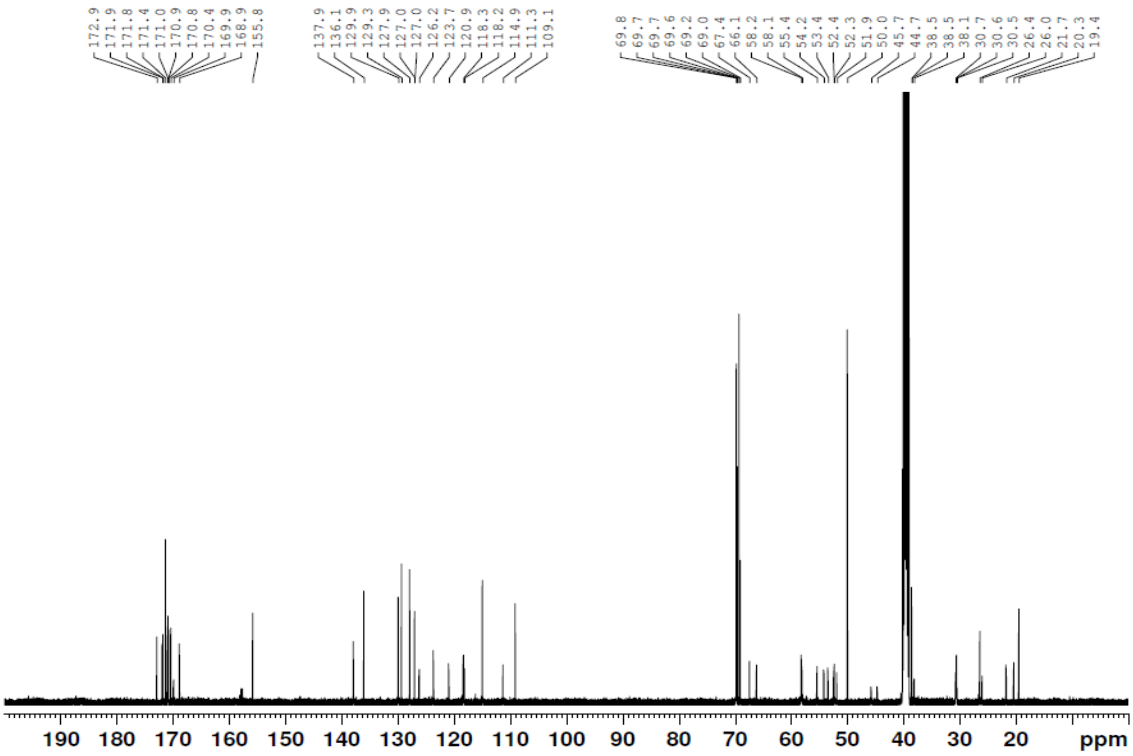

^{1}H NMR (500 MHz, DMSO-d_6) of **TATE-sNIR**

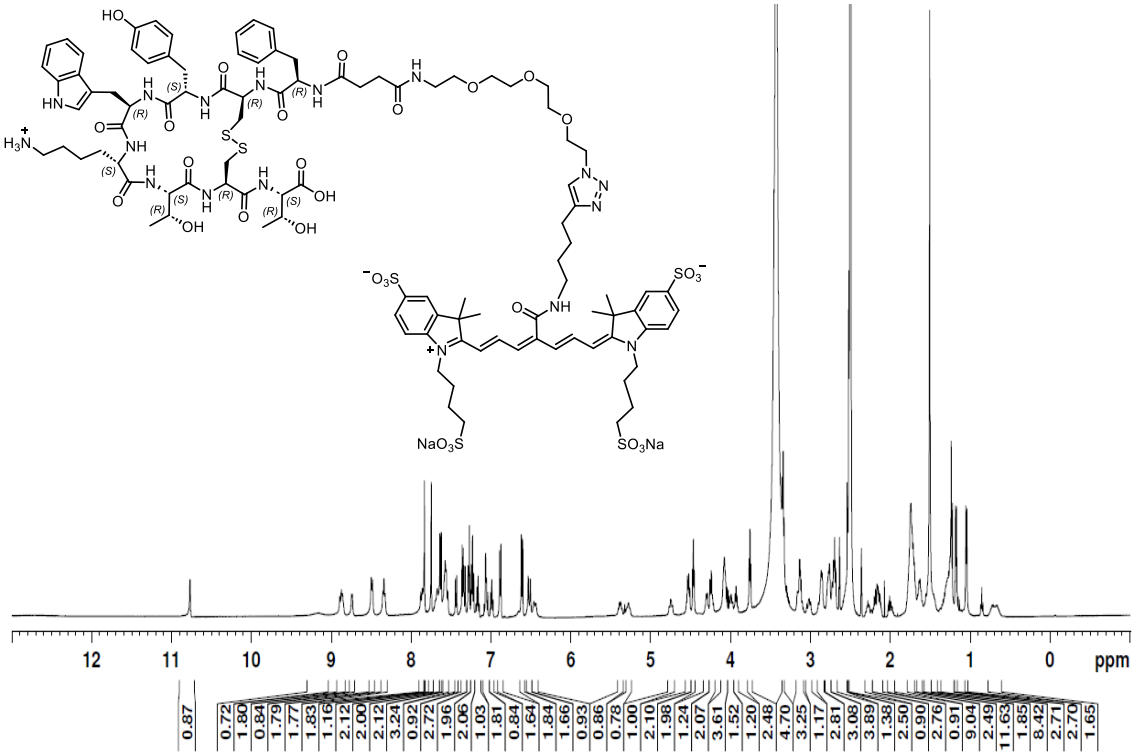

^{13}C{^{1}H} NMR (150 MHz, DMSO-d_6) of **TATE-sNIR**

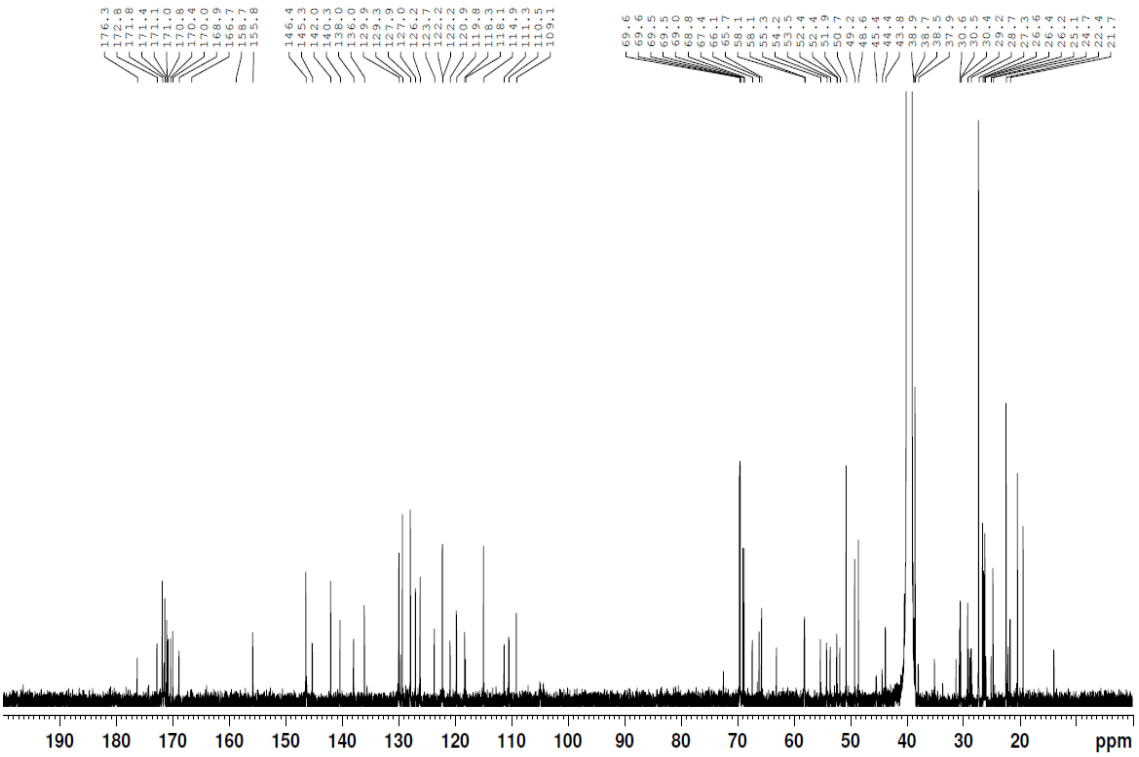

^{1}H NMR (600 MHz, DMSO-d_6) of **scTATE-sNIR**

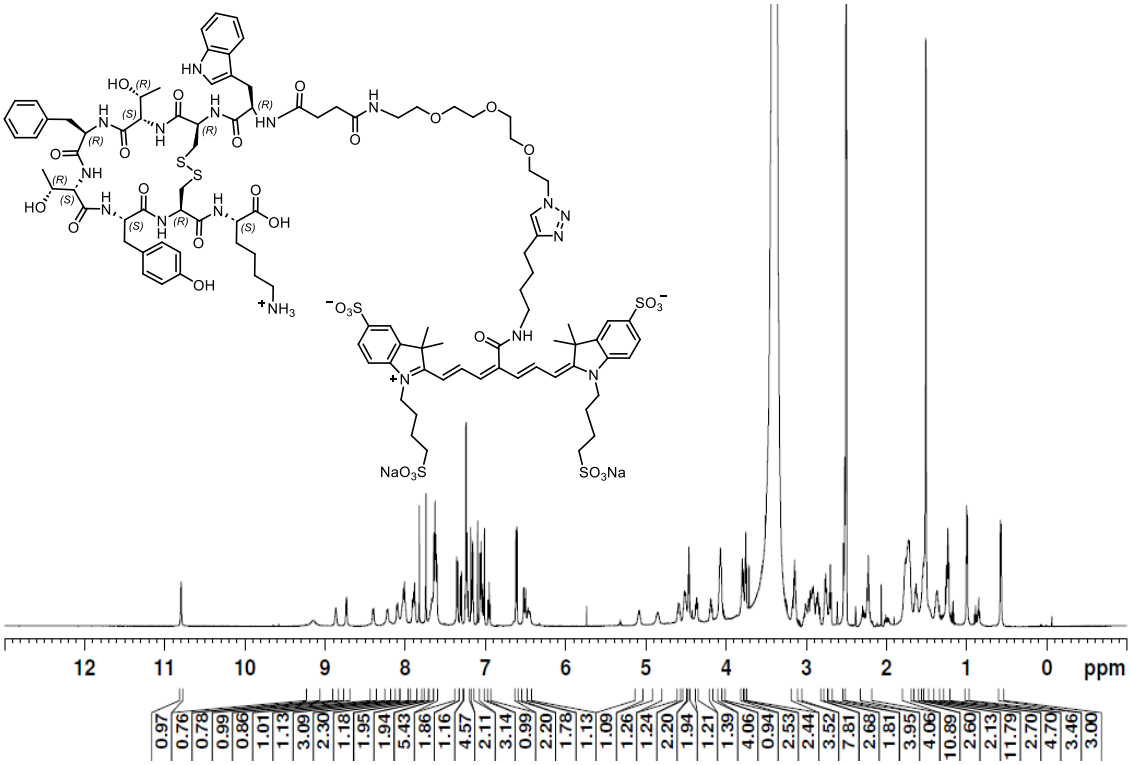

^{13}C{^{1}H} NMR (150 MHz, DMSO-d_6) of **scTATE-sNIR**

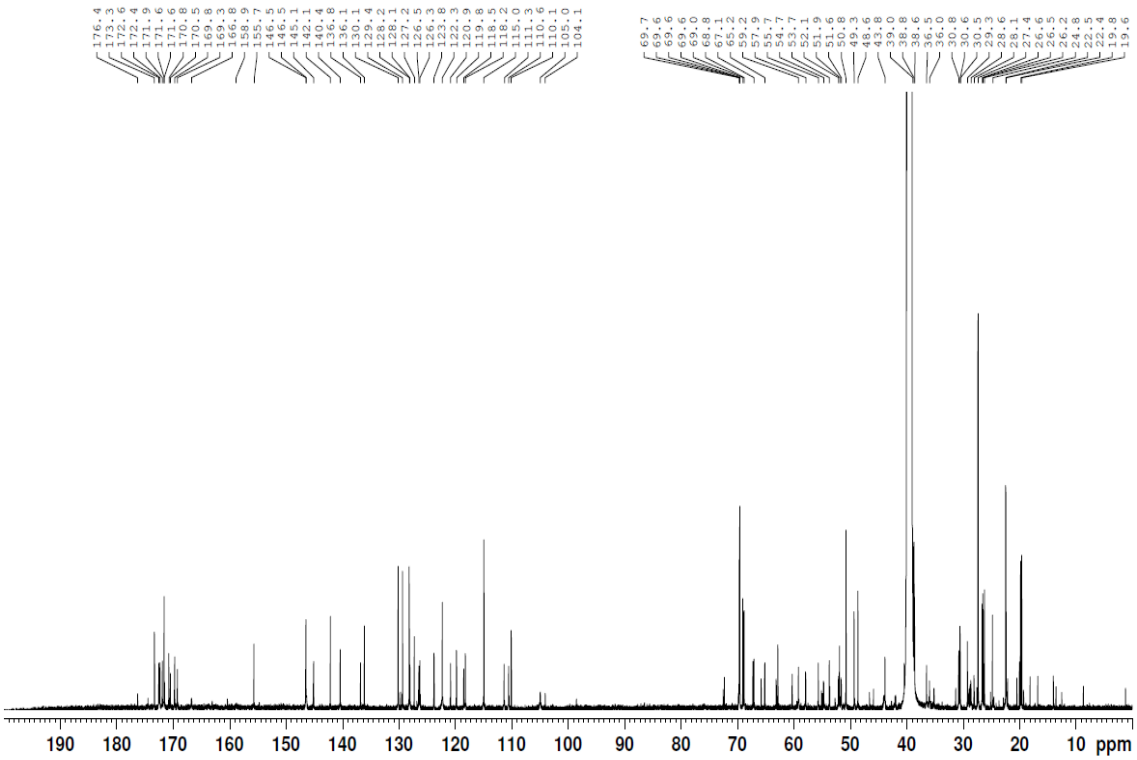

^{1}H NMR (400 MHz, $CDCl_3$) of **13**

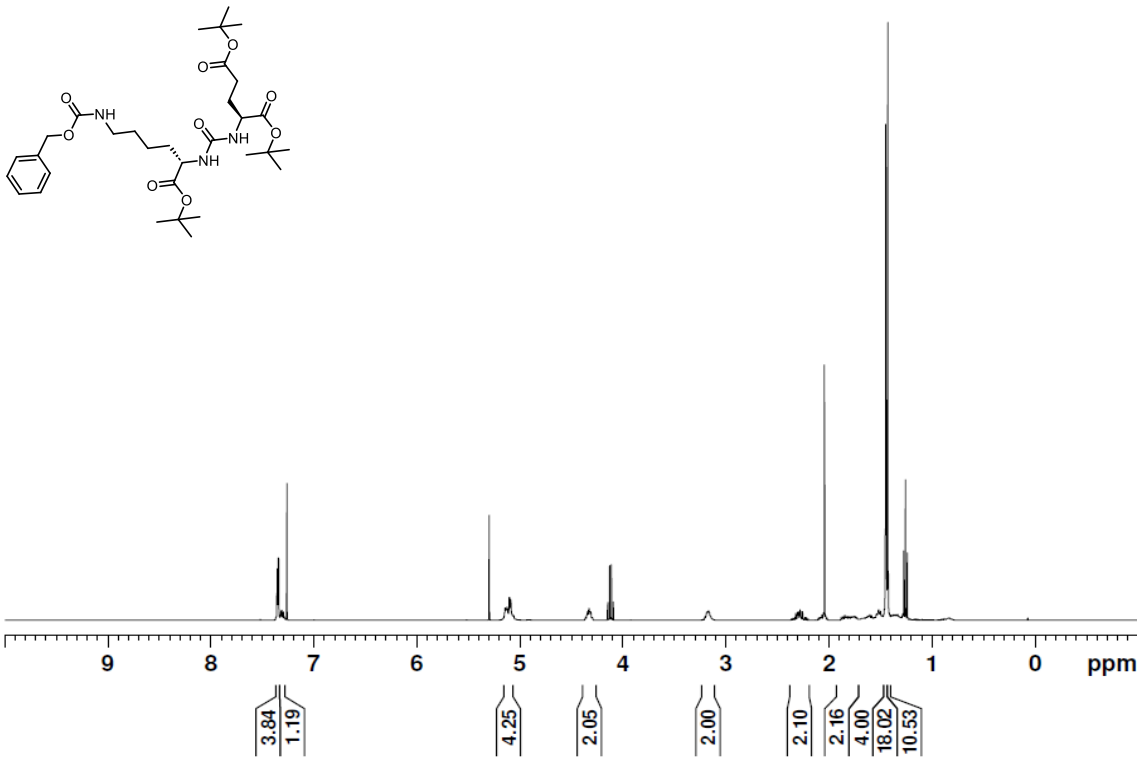

^{13}C{^{1}H} NMR (101 MHz, $CDCl_3$) of **13**

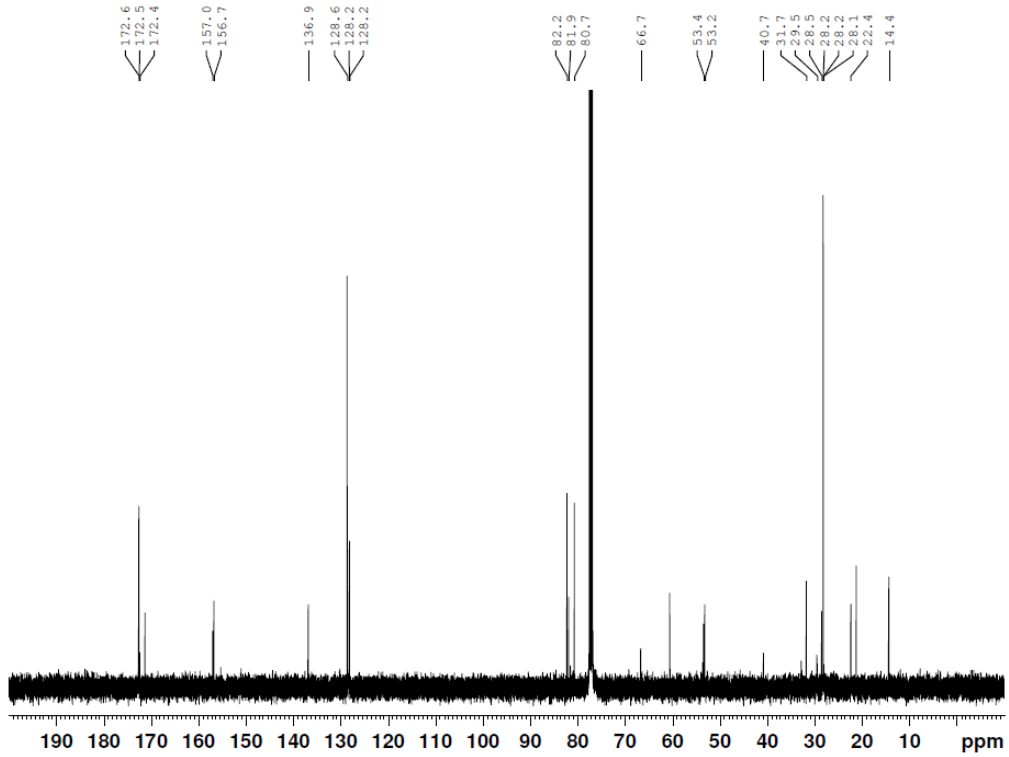

^{1}H NMR (400 MHz, $CDCl_3$) of **14**

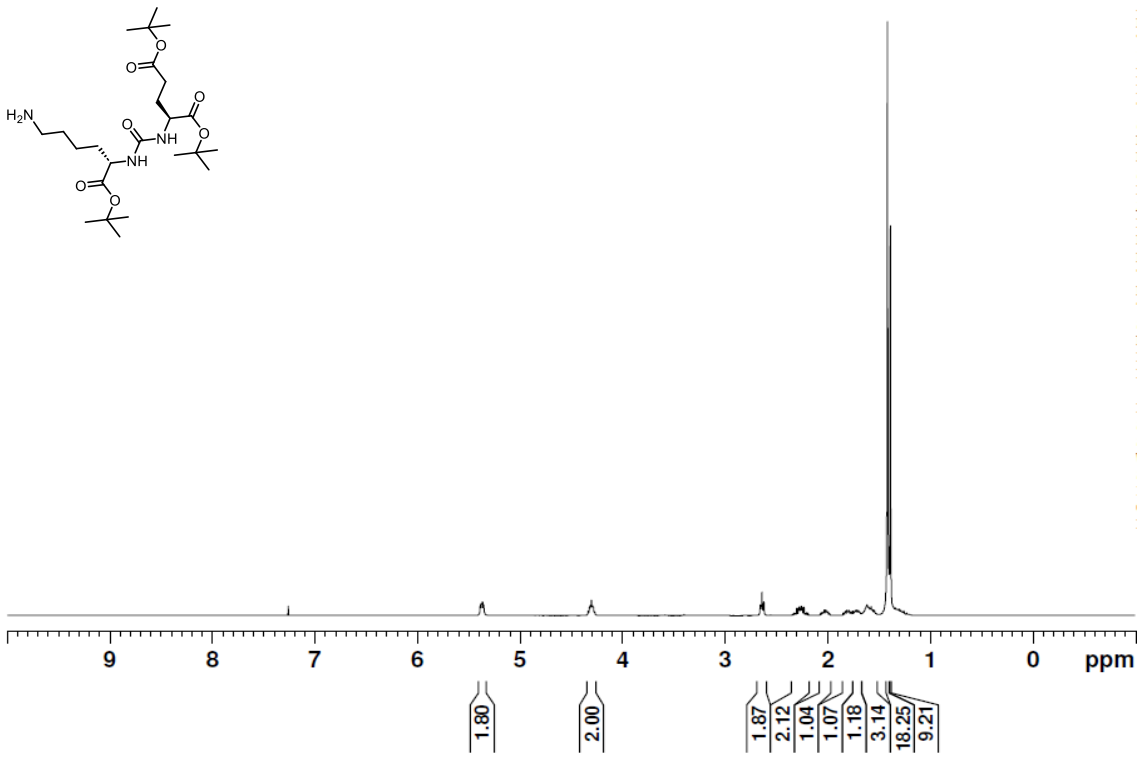

^{13}C{^{1}H} NMR (101 MHz, $CDCl_3$) of **14**

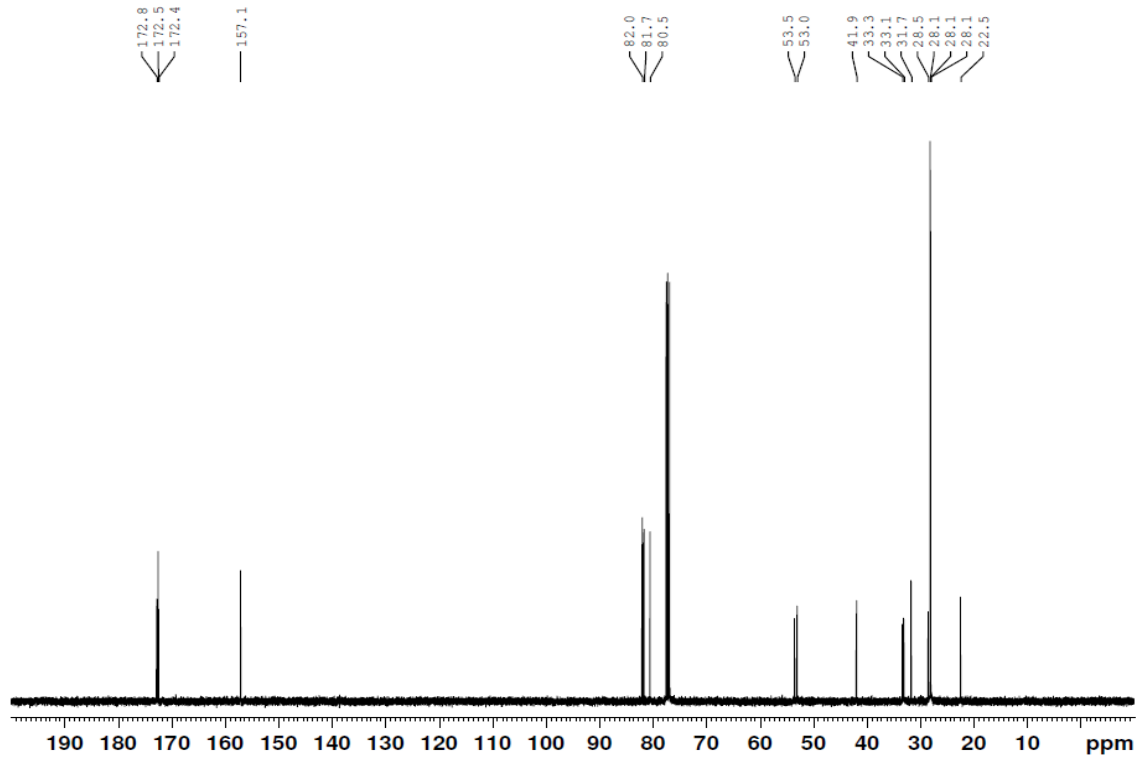

^{1}H NMR (400 MHz, $CDCl_3$) of **15**

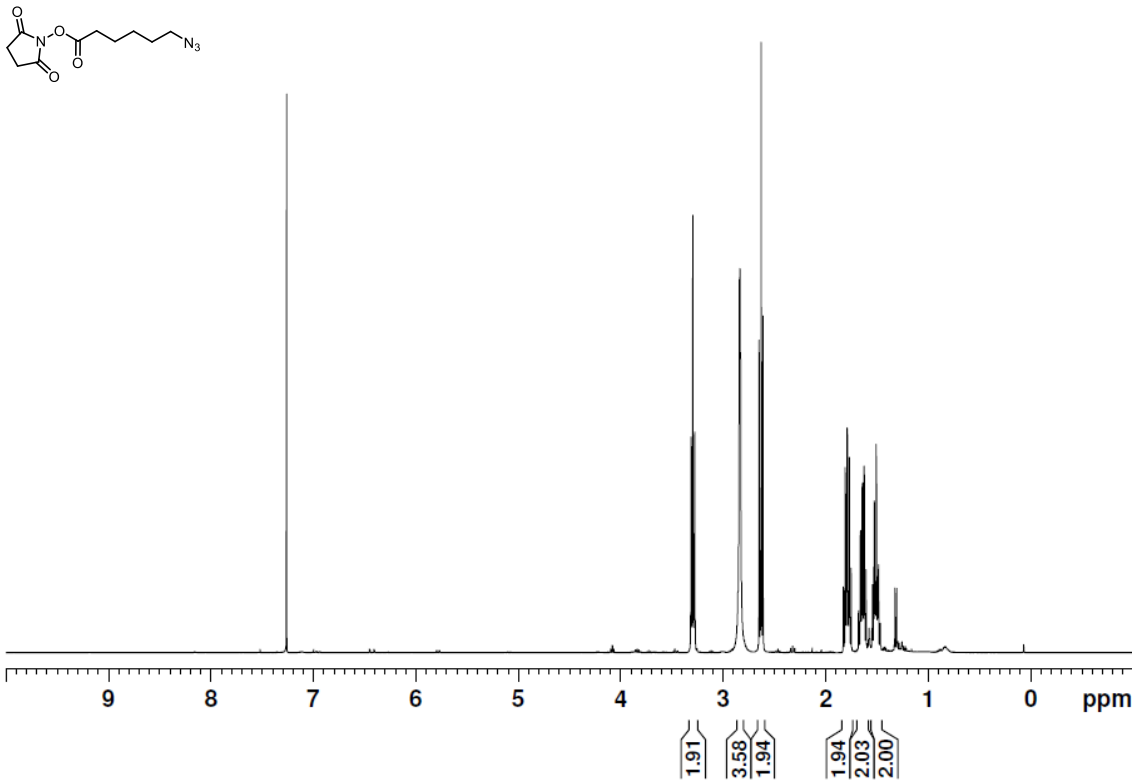

^{13}C{^{1}H} NMR (101 MHz, $CDCl_3$) of **15**

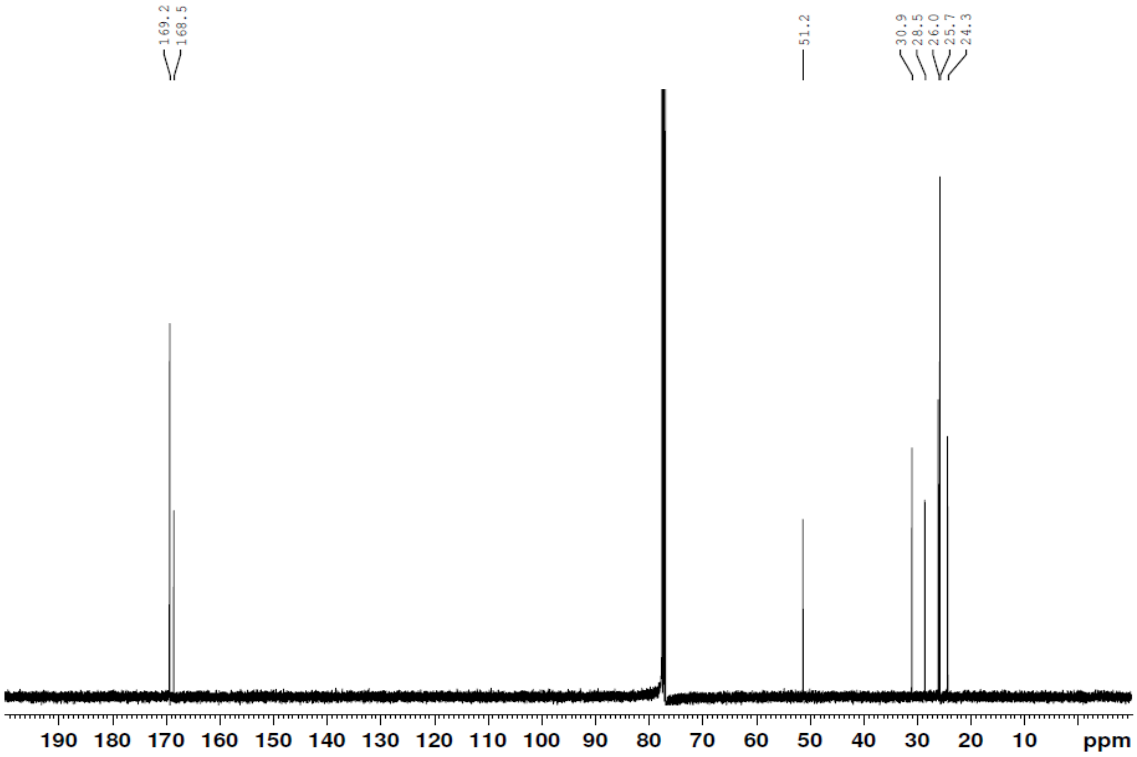

^{1}H NMR (400 MHz, $CDCl_3$) of **16**

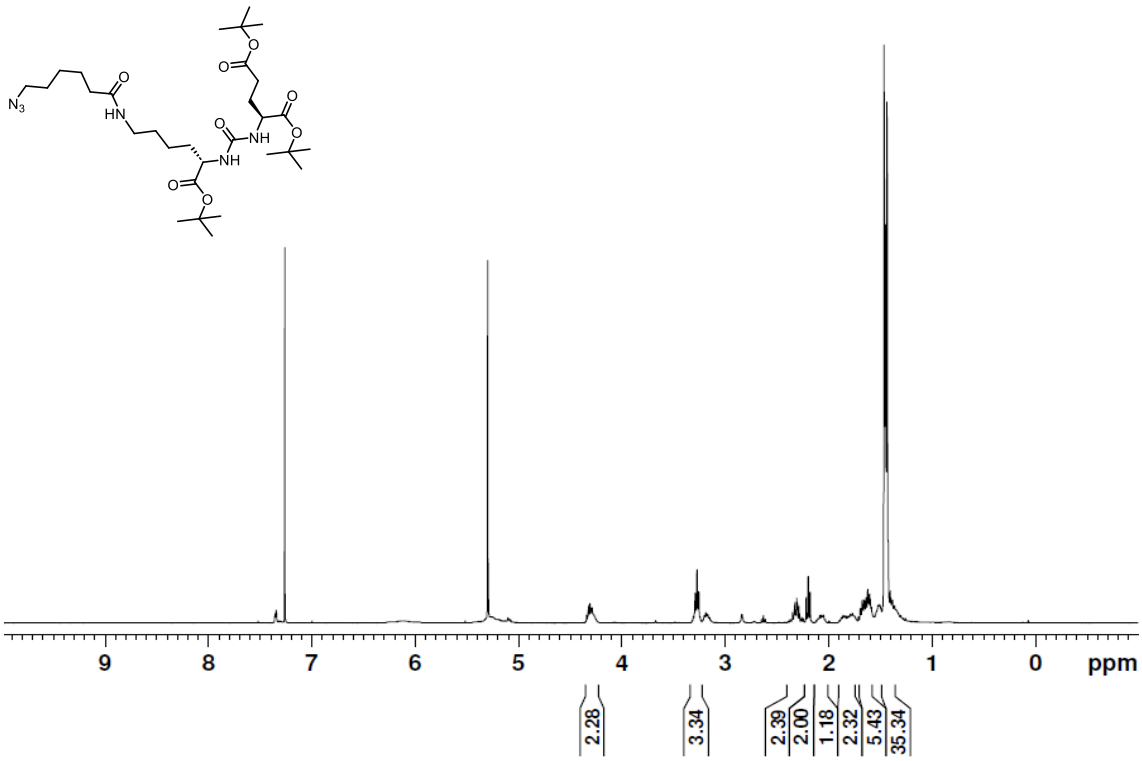

^{13}C{^{1}H} NMR (101 MHz, $CDCl_3$) of **16**

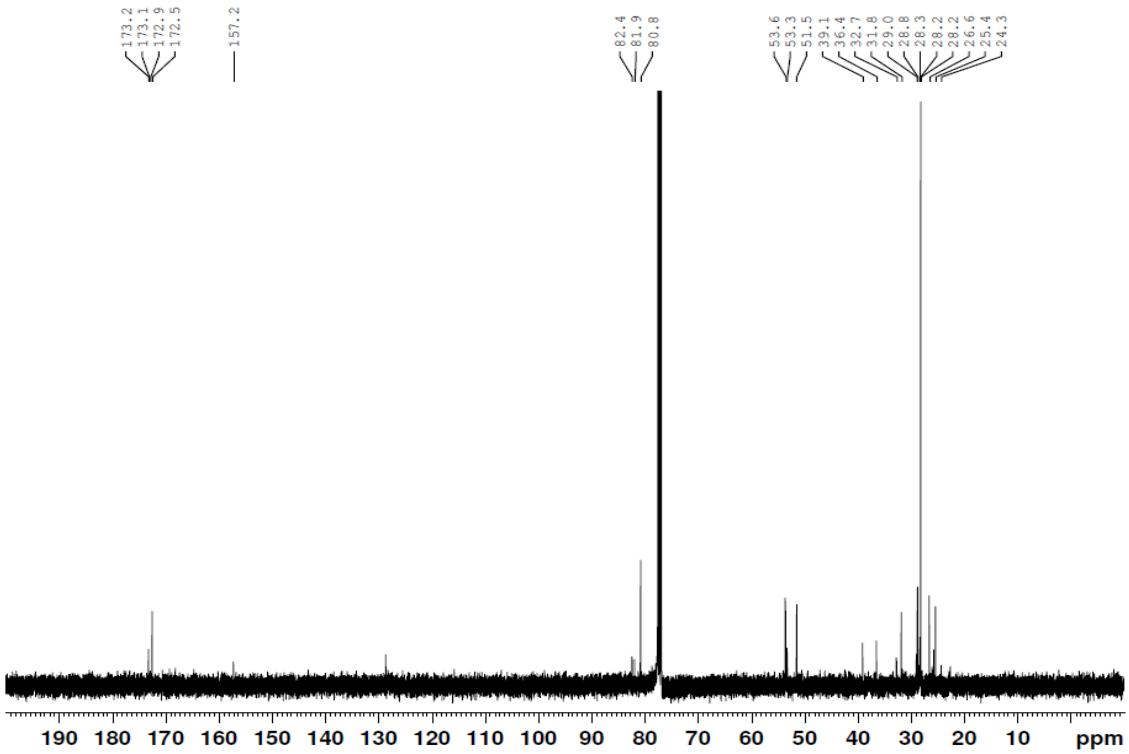

^{1}H NMR (500 MHz, CD_3OD) of **17**

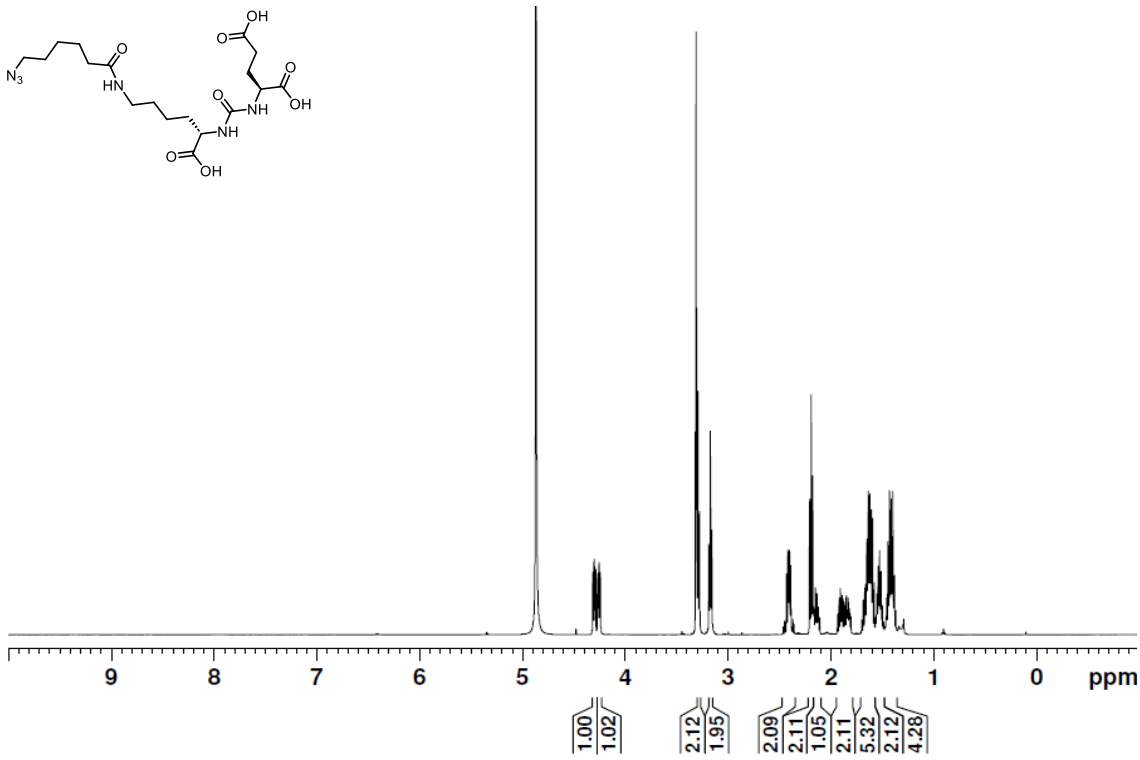

^{13}C{^{1}H} NMR (125 MHz, CD_3OD) of **17**

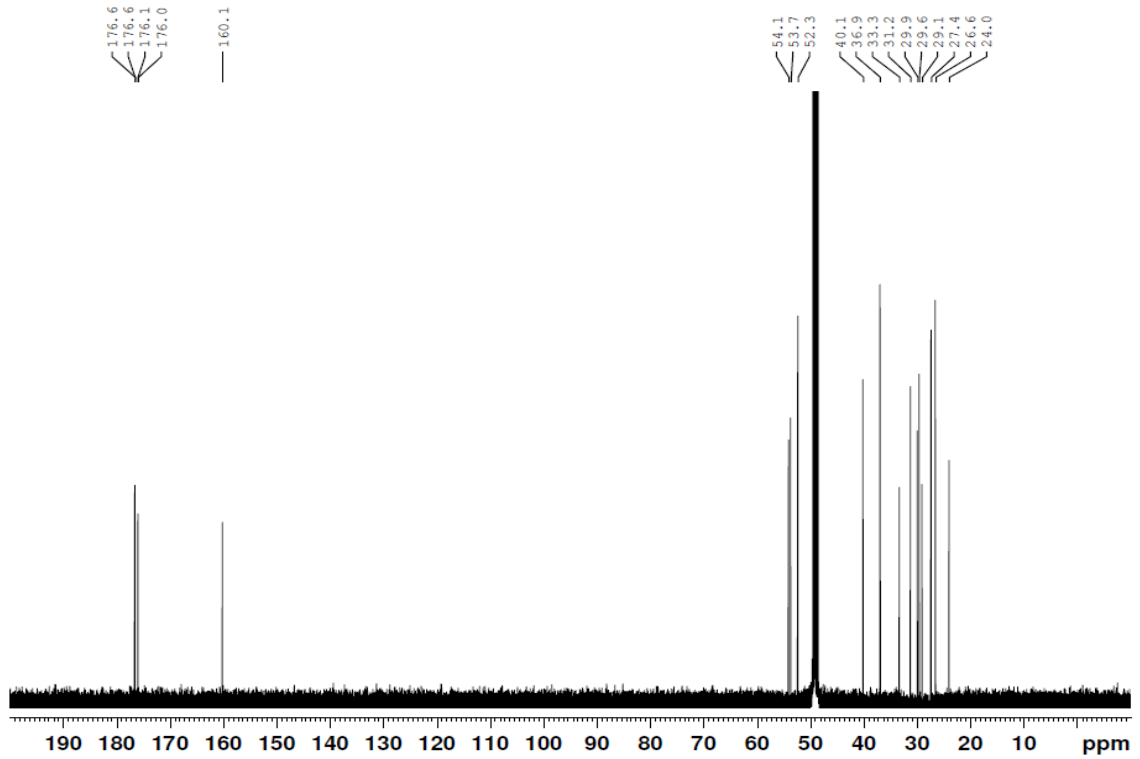

1.1.4 HPLC-MS spectra

HPLC-MS of **TATE-sNIR** (05-95_13 min): *m/z* 1143 $[M–2Na^{+}+4H^{+}]^{2+}$ t_R = 6.45 min.

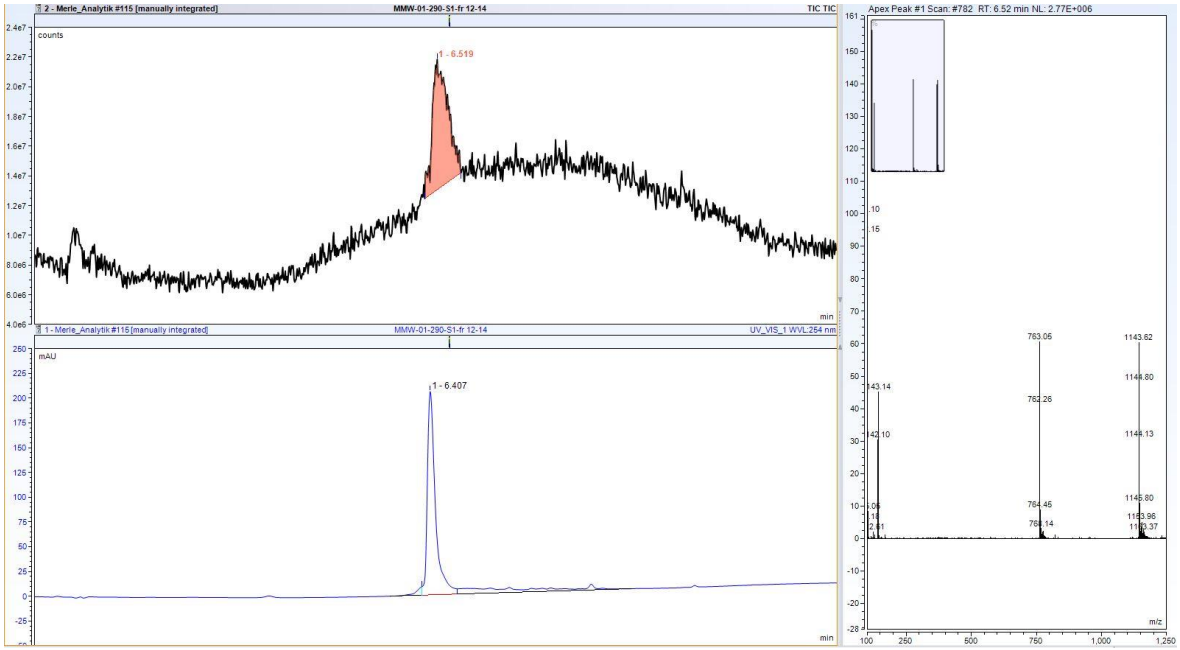

HPLC-MS of **scTATE-sNIR** (05-95_13 min): *m/z* 1143 $[M–2Na^{+}+4H^{+}]^{2+}$ t_R = 6.45 min.

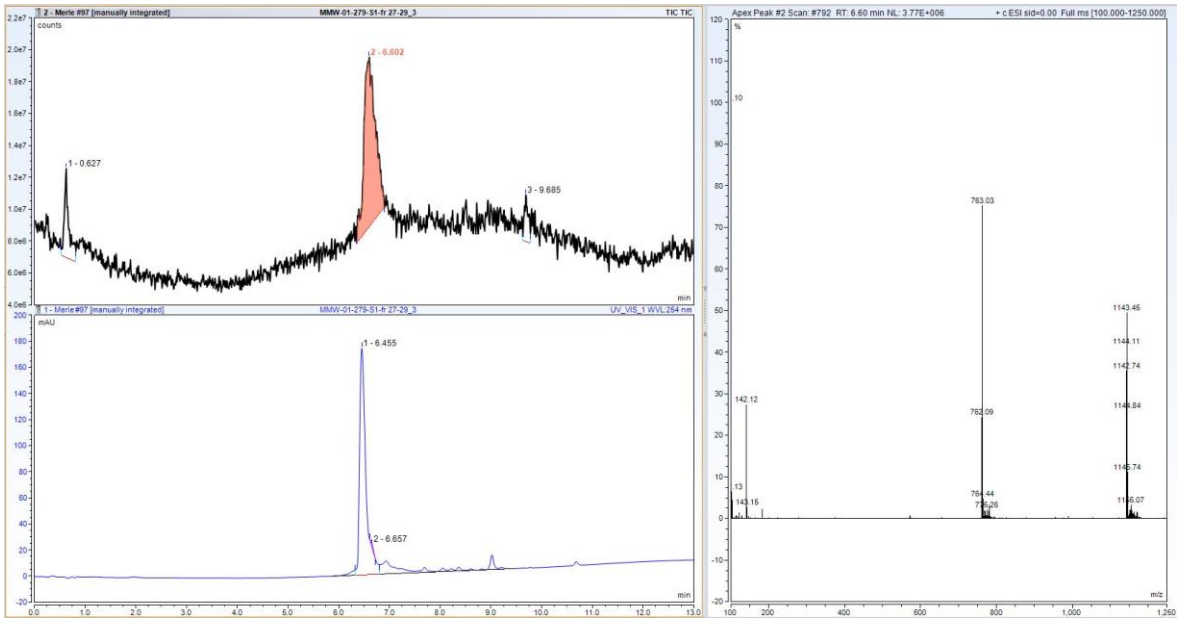

HPLC-MS of **TATE-IRDye800** (05-95_13 min): *m/z* 1216 $[M–2Na^{+}+4H^{+}]^{2+}$

t_R = 7.68 min.

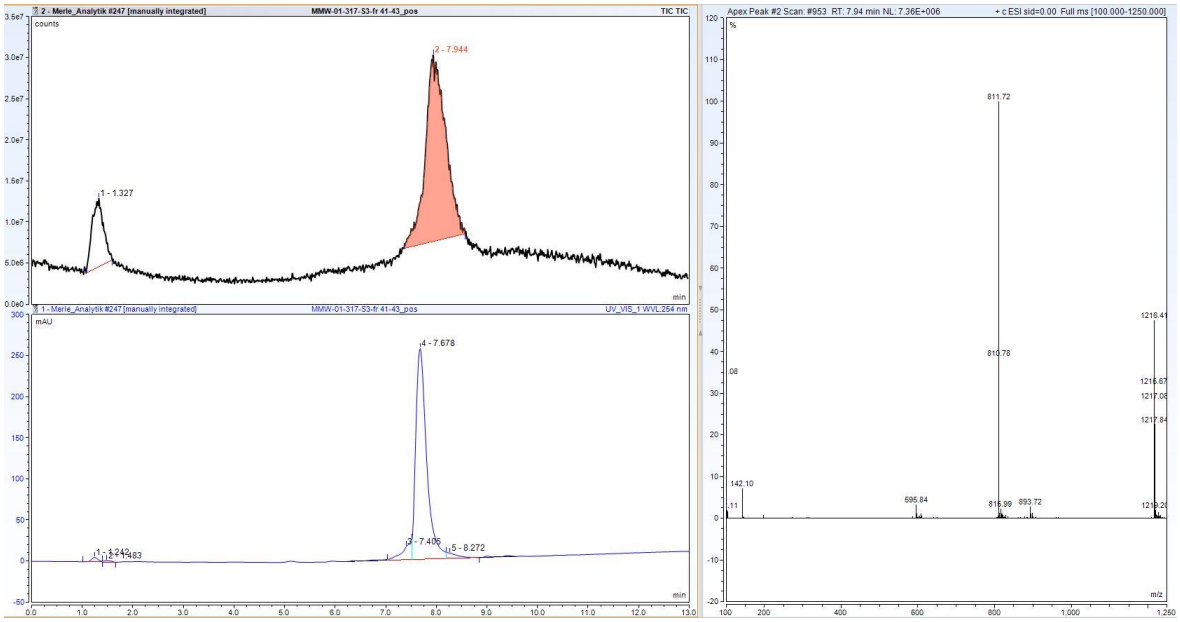

HPLC-MS of **EuK-Ahx-sNIR** (05-95_13 min): *m/z* 695.8 $[M-3Na+H]^{2-}$, t_R = 5.86 min.

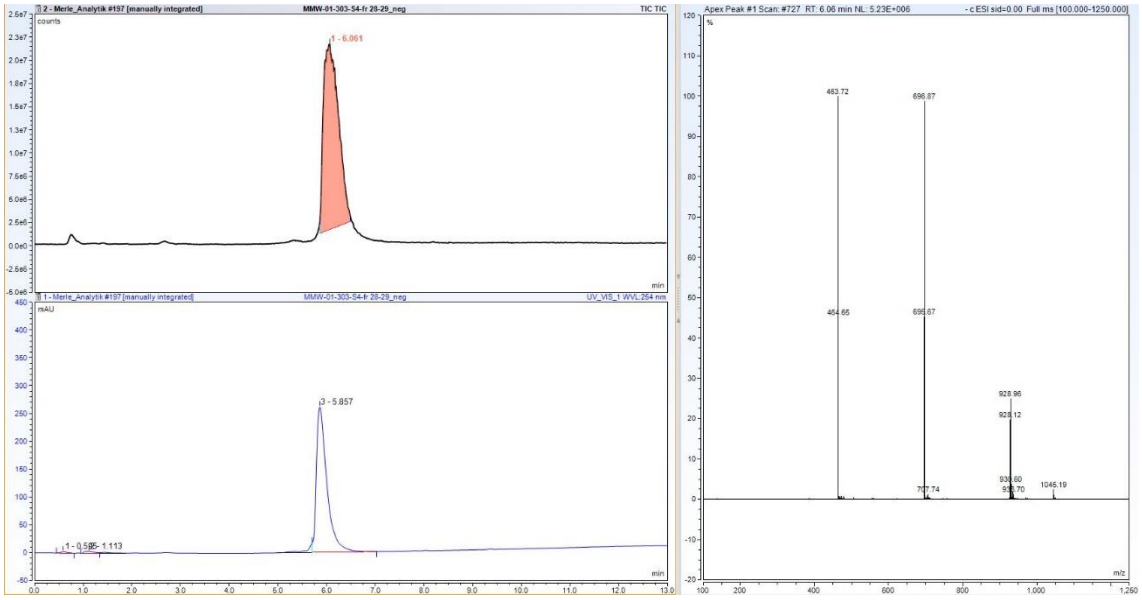

HPLC-MS of EuK-Ahx-IRDye800 (05-95_13min): *m/z* 749.9 $[M-3Na+5H]^{2+}$,

t_R = 6.2 min

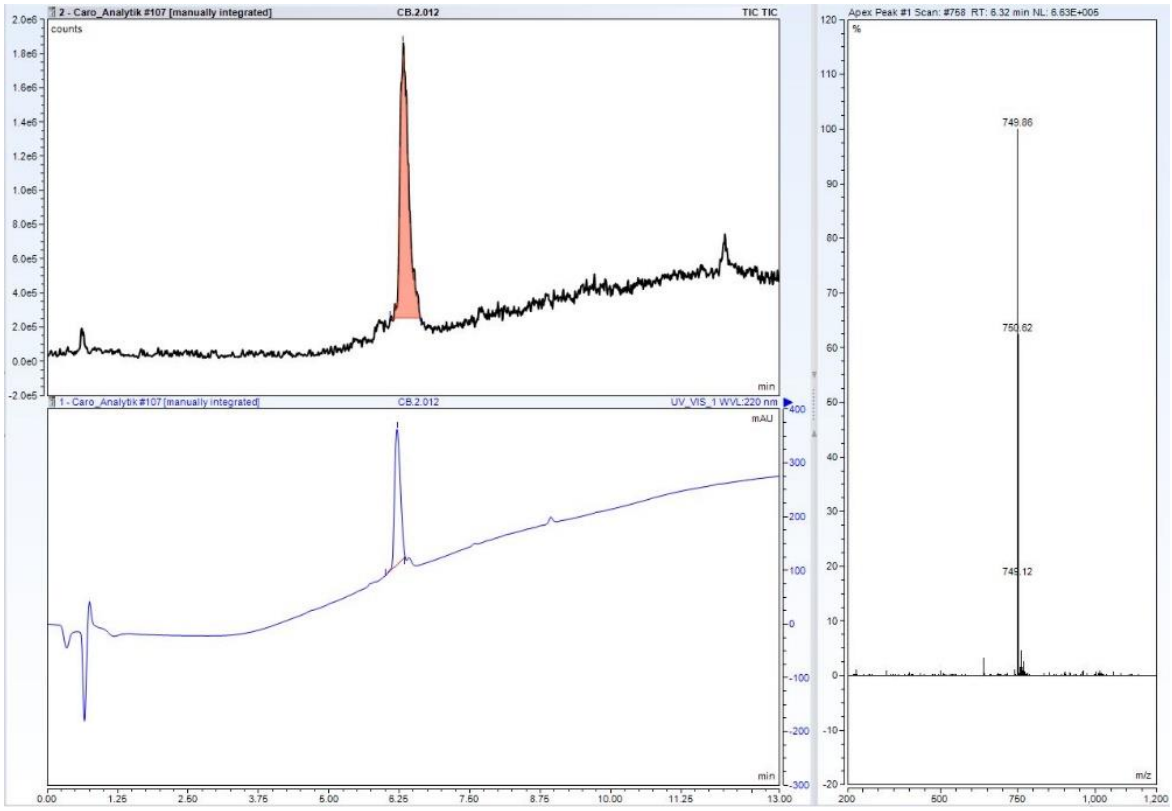

1.2 Experimental Procedures

For optical and *in vitro* characterization, 1x Dulbecco's phosphate buffered saline without calcium and magnesium (Gibco 14190144, Thermo Fisher Scientific, Waltham, MA, USA, referred to as PBS), heat-inactivated fetal bovine serum (F9665, Merck Millipore, Burlington, VT, USA, referred to as FBS), and ethanol for spectroscopy (Uvasol, Merck Millipore) were used.

1.2.1 Optical Properties

Absorption and Emission Measurements

111-QS Quartz cuvettes (Hellma, Müllheim, Germany) were used for absorption and emission measurements. All spectra were obtained at ambient temperature. Normalized spectra are displayed for clarity.

Absorption spectra were obtained using a Lambda 1050+ (Perkin Elmer, Waltham, USA) with solvent in the reference beam path, applying the following specification: scan rate: 176 nm/min, PMT slits: fixed, 2.5 nm, PMT gain: auto, PMT response: 0.2 s, InGaAs gain: 2, InGaAs response: 0.2 s. The spectrophotometer was operated by UV WinLab software (Perkin Elmer, Waltham, USA). Absorbance at the absorption maxima was in the dynamic range of 0.1 – 1.0.

Emission spectra were recorded using a custom-built system designed by Dr. Jakob Lingg. Emission in the visible wavelength range was detected with a Pixis:400BR camera (Teledyne Princeton Instruments, Trenton, USA) cooled to -70 °C attached to a SpectraPro HRS-300-SS spectrograph (Teledyne Princeton Instruments, Trenton, USA). Emission in the near and shortwave infrared wavelength range was detected with a Pylon-IR:1024 line camera (Teledyne Princeton Instruments, Trenton, USA) cooled to -100 °C attached to the same spectrograph. A grating with a density of 150 g/nm and a blaze of 800 nm was used. LightField software (Teledyne Princeton Instruments, Trenton, USA) was used to control acquisition. Excitation wavelengths were 635 nm (CPS635R with FL-635-10 clean-up filter, Thorlabs, Newton, USA) and 785 nm (Fiber-Coupled Laser S4FC785 with FL780-10 clean-up filter, Thorlabs, Newton, USA). For the excitation wavelengths, FELH0650 and FELH0800 (Thorlabs, Newton, USA) were used as emission filters, respectively. For the acquisition of emission spectra, the solutions were diluted so that the absorbance in the absorption maxima did not exceed 0.1 to minimize the effects of reabsorption. The exposure times for both detectors were set to 1000 ms. Five frames per detector per spectrum were

acquired. The frames were background-, flatfield-corrected, and averaged. The sum of the rows of frames acquired with the Pixis:400BR was taken. The resulting spectra were intensity-corrected using a stabilized Fiber-Coupled Light Source (SLS201L/M, Thorlabs, Newton, USA). The intensity-corrected spectra from both detectors were stitched, resulting in the final spectrum.

Determination of Molar Absorption Coefficients

Molar extinction coefficients (ε) were determined in Dulbecco's PBS (PBS) using Beer's law from plots of absorbance in absorption maximum vs. concentration. Measurements were performed using the Lambda 1050+ (Perkin Elmer, Waltham, USA), as described above. Three stock solutions from independent weights were prepared per dye. Five dilutions with absorbance > 0.1 and < 1.0 were measured per stock. For each concentration, the mean absorbance and the corresponding molar absorption coefficient were calculated.

Relative Fluorescence Quantum Yield Measurement

Relative photoluminescence quantum yield measurements were carried out using IR-125 in EtOH as a reference (Φ_r= 14.87 ± 0.74). Absorption spectra were acquired using a Cary 5000 UV-Vis-NIR spectrophotometer (Agilent, Santa Clara, USA) with air in the reference beam path, applying the following specifications: detection range: 400 – 1000 nm, detector changeover: 900 nm. Emission spectra were acquired using a Photonics FSP920 spectrometer (Edinburgh Instruments, Livingston, Scotland) using the following specifications: Xe900 continuous xenon lamp, excitation wavelength: 700 ± 4 nm, NIR grating, detector: MID_R2658P, detection range: 710 – 1010 nm. For each dye-solvent combination, three dilutions with absorbance in the absorption peak < 0.1 were independently prepared, and absorption and emission were measured in a Quartz cuvette. Absorption spectra were bank-subtracted, and absorption factors f were calculated for the band-pass $\Delta\lambda_{ex}$ used for excitations as follows:

$$f = \int_{\lambda_{ex}-\frac{1}{2}\Delta\lambda_{ex}}^{\lambda_{ex}+\frac{1}{2}\Delta\lambda_{ex}} 1\text{-}10^{-A(\lambda|ex)}d\lambda_{ex}$$

Emission spectra were automatically corrected by the software for 1) fluctuations in the intensity of the lamp and 2) the instrument-specific spectral responsivity. Corrected spectra were blank-subtracted only for measurements in serum but not PBS or EtOH. Φ_{rel} of a given sample s and the corresponding standard deviation $\sigma(\Phi_{rel,s})$were calculated as follows:

$$\Phi_{rel,s}=\Phi_r\left(\frac{f_r}{f_s}\right)\left(\frac{F_s}{F_r}\right)\left(\frac{n_s}{n_r}\right)^2$$

$$\sigma(\Phi_{rel,s})=\Phi_{rel,s}*\sqrt{\left(\frac{\sigma(\Phi_r)}{\Phi_r}\right)^2+\left(\frac{\sigma\left(\frac{F_s}{f_s}\right)}{\frac{F_s}{f_s}}\right)^2+\left(\frac{\sigma\left(\frac{f_r}{F_r}\right)}{\frac{f_r}{F_r}}\right)^2}$$

where subscripts s and r refer to sample and reference, f to the absorption factor, F to the integrated area under the emission band (wavelength range = 725 – 1000 nm), n to the refractive index of the solvent and σ to the standard deviation.

Refractive indices were determined using the ABBE MARK III refractometer (Reichert Technologies, Depew, USA) and are summarized in Table 7.

Table 7. Refractive indices of PBS, FBS and EtOH.

	PBS	FBS	EtOH
n	1.3331	1.3216	1.3624

Lifetime Measurements

TCSPC lifetime measurements were performed on a confocal microscope (Olympus FV1200). Different concentrations of the fluorophore (sNIR-CO_2H, IRDye800-CO_2H) in a buffered solution (PBS) were illuminated with a pulsed laser diode of wavelength 780nm (LDH-D-C-780, PicoQuant GmbH, Berlin). The microscope was equipped with a dichroic mirror for excitation/emission clearance (T800lpxr-xt-UF2, Chroma). The fluorescence was collected through the same microscope objective (UPlanSApo 60x/1.2w, Olympus) as for the excitation laser beam and was then passed through an emission filter (800 Long Pass) before being collected by two avalanche photodiodes (Tau-SPAD, PicoQuant GmbH, Berlin). The signals from these photodiodes were streamed onto a data acquisition card for time-correlated single photon counting (TCSPC, Hydraharp 400, PicoQuant GmbH) along with the electronic sync pulses from the laser. The instrument response function was determined from the back-reflected light from the laser excitation pulses and then used for deconvolution

when fitting the fluorescence decay (TCSPC data) to an exponential decay based on nonlinear least-squares minimization (Symphotime, Picoquant GmbH).

Spectral analysis of fluorophore-antibody conjugates

The conjugates were diluted 10-15-fold into PBS and their absorption spectra were recorded on a spectrometer PerkinElmer Lamba 1050 Plus spectrometer using 111-QS Quartz cuvettes (Hellma, Müllheim, Germany). The absorption values at 280 nm (A280) and at the cyanine λ_{max} were obtained, and the relative dye and antibody concentrations were determined from Beer's law.

Panitumumab conjugates of IRDye-800 and sNIR were analyzed and DOL calculated as described previously (Bandi, Luciano, Saccomano – Nat Meth) according to the equation below.

$$\mathrm{DOL} = \frac{\left(\frac{A_{\lambda\ \max}}{\varepsilon_{dye}}\right)}{(A_{280\ nm} - \mathrm{CF} \times A_{\lambda\ \max})/\varepsilon_{\mathrm{protein}}} [\mathrm{protein}] \left(\frac{mg}{ml}\right)$$

$$= \frac{(A_{280\ nm} - \mathrm{CF} \times A_{\lambda\ \max})}{\varepsilon_{\mathrm{protein}}} \times \mathrm{MW}_{\mathrm{protein}} \times \text{dilution factor}$$

Using the following values

- ε = 270,000 M−1 cm−1 for IRDye-800 (Li-Cor protein label kit),
- ε = 250,000 M−1 cm−1 for sNIR, and
- ε antibody = 203,000 M−1 cm−1 for Panitumumab.

A correction factor of 0.03 and 0.064 for IRDye-800 and sNIR, respectively, was applied to account for the absorption contribution of the dyes at 280 nm relative to the λ_{max}.

1.2.2 Near-Infrared Fluorescence Imaging

Macroscopic imaging was mainly performed on three custom-built setups. For the pheochromocytoma allograft mouse model, however, the IVIS SpectrumCT In Vivo Imaging System (PerkinElmer, Waltham, USA) was used.

Custom-built setup #1

A laser unit LU0785DLU250-S70AN03 (25 W) "785 nm" (Lumics, Berlin, Germany) was used for excitation. The laser was externally controlled using a laser diode control system (Lumics, Berlin, Germany). Laser output was coupled in a 4x1 fan-out fiber-optic bundle (BF46LS01, Thorlabs, Newton, USA) of 600 µm core diameter for each optical path. The output from the fiber was fixed in an excitation cube (KCB1EC/M, Thorlabs, Newton, USA), reflected off of a mirror (BBE1-E03, Thorlabs, Newton, USA), and passed through a positive achromat (AC254-050-B, Thorlabs, Newton, USA), SP filter (FESH0800, 25 mm, Thorlabs, Newton, USA) and an engineered diffuser (ED1-S20-MD, Thorlabs, Newton, USA) to provide uniform illumination over the working area, which was covered by blackout fabric (BK5, Thorlabs, Newton, USA). In a typical experiment, the excitation flux in the field of view (5x5 cm) was adjusted to be close to 50 or 110 mW/cm^2 at 785 nm. The power density was determined using an energy meter console PM100D (Thorlabs, Newton, USA) in combination with an S130C sensor (Thorlabs, Newton, USA), characterized by measurement uncertainty of ± 3%. If necessary, the laser was triggered externally by the camera. Emitted light was directed through a construct consisting of the Optem Fusion SWIR 45-00-10-000 zoom lens (Excelitas, Waltham, USA) and three filters: BP825-50, 50 mm (Edmund Optics, Barrington, USA), FELH0800, 25 mm (Thorlabs, Newton, USA), and NF785-33, 25 mm (Thorlabs, Newton, USA). The construct was screwed onto a PCO Edge 4.2 (Excelitas, Waltham, USA). For organ imaging, the 0.75 or 1.0 magnification of the zoom lens was used. The distance between the imaging sample and the camera was 70 cm. The software µManager was used to control the camera externally. The assembly was partially enclosed to avoid excess light while enabling manipulation of the field of view during operation.

Custom-built setup #2

A mounted LED M780LP1 (800 mW) “780” (Thorlabs, Newton, USA) was used for excitation and controlled using a LED driver LEDD1B Thorlabs, Newton, USA). A construct consisting of an Aspheric Condenser Lens ACL25416U-B (Thorlabs, Newton, USA), a spacer, a cleanup filter (BP769-48, 25 mm, Edmund Optics, Barrington, USA), and an engineered diffuser ED1-S20-MD (Thorlabs, Newton, USA) was screwed onto the LED. Imaging samples were brought into focus using a lifting platform covered by blackout fabric (BK5, Thorlabs, Newton, USA). In a typical experiment, the excitation flux in the field of view (5x4 cm) was adjusted to be close to 1.7 or 30 mW/cm^2 at 780 nm. It was determined using an energy meter console PM100D (Thorlabs, Newton, USA) in combination with an S130C sensor (Thorlabs, Newton, USA), characterized by measurement uncertainty of ± 3%. Emitted light was directed through a construct consisting of a LM50FC24M C-Mount Lens (Kowa Optronics, Aichi, Japan) and three emission filters: 2x BP880-135, LP800 (Edmund Optics, Barrington, USA). The construct was screwed onto a PCO edge 26 (Excelitas, Waltham, USA). The distance between the imaging sample and the camera was 7 cm. The software µManager was used to control the camera externally. The assembly was partially enclosed to avoid excess light while enabling manipulation of the field of view during operation.

Custom-built setup #3:

A laser unit LU0785DLU250-U70AN (25 W) "785 nm” (Lumics, Berlin, Germany) was used for excitation. The laser was externally controlled using a laser diode control system (Lumics). Laser output was coupled in a 4x1 fan-out fiber-optic bundle (BF46LS01, Thorlabs) of 600 µm core diameter for each optical path. The output from the fiber was fixed in an excitation cube (KCB1EC/M, Thorlabs), reflected off of a mirror (PFE10-P01, Thorlabs), and passed through a positive achromat (C254-050-B, Thorlabs). Next, the beam was filtered by a laser clean-up filter combination of a BP785-10 filter (#86-739, Edmund Optics) and an SP800 filter (FESH0800, Thorlabs). Lastly, the filtered light reached an engineered diffuser (ED1-S20-MD, Thorlabs) to provide uniform illumination over the working area. In a typical experiment, the excitation flux in the field of view (around 100 cm^2) was adjusted to be 91 mW/cm^2 in the center. The power density was determined using an energy meter console PM100D (Thorlabs) in combination with an S130C sensor (Thorlabs), characterized by measurement uncertainty of ± 3%. Emitted fluorescence was directed through a construct consisting of four filters, lens and camera. A BP825-50 filter (25 mm,

#86-957, Edmund Optics) was used to set the detection window, and three additional LP800 filters were utilized to block the laser light (25 mm, dielectric glass, FELH0800, Thorlabs; 25 mm, colored glass, #66-059, Edmund Optics; and 50 mm, dielectric, #84-762, Edmund Optics). A SWIR 50 f 1.4 lens (MVL50M1_1, Navitar, Rochester, NY, USA), mounted on a Prime BSI camera (Photometrics, Tucson, AZ, USA), was placed right after the filters. The software µManager (v. 2.0.3, using the PVCAM driver) was used to control the camera. The custom-built imaging setup was fully enclosed.

Image Processing Procedures

Images were acquired as an average of 10 frames. All images and image stacks were 1) subtracted with a 10-frame averaged "dark" file to correct for current at the given exposure time and 2) divided by a "flatfield" file to account for the inhomogeneities of the power density over the field of view. For the acquisition of the "dark" frames, room light and excitation light were switched off. The "flatfield" was obtained from a 5-frame acquisition of the reverse side of blackout fabric (BK5, Thorlabs, Newton, USA), with room light off, and excitation light on. "flatfield" frames were 1) averaged, 2) dark subtracted, 3) Gaussian blurred (factor 60), and 4) divided by the maximum. Regions of interest were drawn over the corresponding organ or tumor. The mean fluorescence intensity (counts/ms) was used as a comparing parameter.

1.2.3 *In Vitro* Experiments

Preparation of Solutions with Defined Concentrations

Dye (conjugate) was dissolved in PBS. Absorption was measured using a Nanodrop ND60 (Implen, Munich, Germany), and actual concentration was calculated using the Beer-Lambert law.

Imaging and Bleaching in Capillaries

For each dye (conjugate), 50 µM stock solutions in PBS (or PBS + 1% DMSO in case of ICG) were prepared. 2.5 µM dilutions were prepared in both PBS and serum, transferred to mini caps (Code-Nr: 9000110, V = 10 µL, d = 0.0652 cm, Hirschmann Laborgeräte, Eberstadt, Germany), and closed with wax. The inclusion of bubbles was avoided. Absorbance over the capillaries was < 0.1 for all dye (conjugate) dilutions. Filled capillaries were placed on a homemade capillary holder made from acryl. Samples were imaged using custom-built setup #1 (785 nm laser, 110 mW/cm^2). To assess photostability, samples were continuously irradiated and imaged until bleaching was completed. Bleaching curves were obtained by plotting the mean counts for a capillary over time.

Stability in Solution

100 µM dye solutions in PBS were measured in regular intervals using **LC-MS system (3)**. Between the measurements, the solutions were either stored at rt and the presence of light or at 4 °C and in the absence and presence of light. Stability was assessed based on both UV and mass trace.

Stability Towards Glutathione

1.5 mL 10 µM dye solutions in 50 mM PBS (pH = 7.45) were prepared and analyzed on a UHPLC system equipped with a PDA detector and a Hamilton PRP-1 (100 x 4.1 mm) column (Knauer, Berlin, Germany). Runs were conducted with a gradient of 15 - 95% 10 mM ammonium bicarbonate (pH = 7.4) /MeCN (15 min), at a flow rate of 1 mL/min. 7.5 µL of a 200 mM glutathione solution in de-ionized water was added to each dye solution to afford a 1 mM final glutathione concentration. Subsequently, the samples were analyzed every 30 min, and the integrated peak areas of absorption at 770 nm were plotted versus time. To confirm the formation of the glutathione adduct, a 100 µM solution in PBS was incubated with glutathione (1 mM) for 7 h and analyzed using **LC-MS system (3)**.

Proteome Reactivity

4T1 cells (murine breast tumor cell line) were harvested by washing cells with ice-cold PBS and subsequent trypsinization. The cell suspension was transferred in a falcon tube, centrifuged (1500 rpm, 3 min, 4 °C), and cells were washed 3x with ice-cold PBS to form a cell pellet. Cells were counted using the Invitrogen cell counter using trypan blue ($5*10^6$ cells). For lysis, cells were resuspended in RIPA buffer (1 mL/10^7 cells) containing protease inhibitor cocktail, incubated on ice for 30 min, and then sonicated using a Q125-220 Sonicator (Qsonica, Newton, USA), applying the following specifications: 3x 1 s pulse, amplitude 50%, 50 s resting on ice between pulses. Lysate was transferred into a 2 mL Eppendorf vial and pelleted by centrifugation (12000 rpm, 20 min, 4 °C). The protein content (1500 µg/mL) of the supernatant was determined using a BCA assay (Thermo Fisher Scientific, Waltham, USA). For gel-based analysis of cyanine reactivity, 20 µL lysate (~30 µg protein) was treated with 20 µL of a 20 µM dye solution in PBS. The mixtures were either incubated for 5 min or 24 h at rt, treated with 14 µL of Laemmli Sample Buffer (x4) (Bio-Rad, Hercules, USA), incubated for 5 min at 95 °C and then loaded onto a 4-15% mini protean tgx precast gel (Bio-Rad, Hercules, USA), and electrophoretically separated (Tris/glycine/SDS running buffer, 220 V, 30 min). The gel was imaged using custom-built setup #2 (1.7 mW/cm^2). Protein loading was confirmed by Coomassie stain (1 h incubation PageBlue Protein Staining Solution, rinsing overnight in water with tissue paper).

Culture of LNCaP cells

Human LNCaP cells (ATCC: CRL-1740, CLS Cell Lines Service, Eppelheim, Germany) were cultured as monolayers in RPMI medium (Thermo Fisher Scientific, Waltham, MS, USA) supplemented with 10 % fetal bovine serum (Biochrom AG, Berlin, Germany), and maintained in a humidified atmosphere containing 5 % CO2 (v/v) and 95 % (v/v) air at 37°C. Once the cells reached confluence, they were detached with phosphate-buffered saline containing 0.05 % (w/v) and 0.02 % EDTA (w/v) followed by subcultivation or experiment-specific preparations.

Culture of MDA-MB-468 cells

Human breast cancer cell line MDA-MB-468 (HTB-132), overexpressing epidermal growth factor (EGFR), were purchased from the American Type Culture Collection (ATCC). The cells were cultivated in Leibovitz's L15 medium supplemented with 10% heat-inactivated FBS, 100 units per ml penicillin and 100 μg ml−1 streptomycin. The cells were grown at 37 °C and were passaged following trypsinization with 0.25% Trypsin-EDTA in PBS.

Culture of IOMM-Lee cells

IOMM-Lee cells (ATCC, CRL-3370™) were grown in DMEM (Dulbecco's Modified Eagle's Medium, high glucose, Gibco; 10566016) media supplemented with 10% fetal bovine serum at 37 °C under 95% air and 5% CO_2. 100 U/mL penicillin and 100 μg/mL streptomycin were added to the medium to prevent contamination. The cell line was genetically characterized by STR-Profiling technology using 16 independent PCR systems (Thermo Fisher, AmpFlSTR® Identifiler® Plus PCR Amplification Kit) by Multiplexion (Friedrichshafen, Germany) (Fig. S12). In parallel, positive and negative controls were carried out, yielding correct results.

Transduction of IOMM-Lee cells

To achieve overexpression of SSTR2 in IOMM-Lee cells, a lentiviral vector (LeGO-iPuro2-hSSTR2) was used for stable transduction of the cells. The third generation, self-inactivating, HIV-1 derived lentiviral vector LeGO-iPuro2 was used, containing an SFFV promoter for the expression of the transgene and an internal ribosome entry site to express the puromycin resistance PAC from the same bicistronic mRNA. The 1.1 kb cDNA sequence of human SSTR2 (NM_001050.3), including a Kozak sequence, was codon optimized and synthesized (Eurofins, Ebersberg, Germany) as a BamHI/EcoRI fragment. After cloning into the multiple cloning site of LeGO-iPuro2, resulting in LeGO-iPuro2-hSSTR2, the sequence

was verified by Sanger sequencing. Packaging of the lentiviral particles was performed as described.[47] In short, HEK-293T cells were transfected with the four plasmids LeGO-iPuro2-hSSTR2, pMDLg/pRRE, pRSV-Rev, and phCMV-VSV-G using the calcium phosphate method. After 24 h, the supernatant containing VSV-G pseudotyped lentiviral particles was harvested, filtered through a 0.45 µm syringe filter, and frozen at -80 °C. The titration was done on HEK-293T cells and analyzed by flow cytometry after staining for hSSTR2 (Fig. S13), with and without puromycin selection (1 µg/mL). Antibody staining for flow cytometry was performed with 200,000 cells in 100 µL PBS with 1 µL antibody solution (R&D Systems R2/SSTR2 AlexaFluor405, Mouse IgG2A Clone # 402038, Cat. No. IC4224V at 0.2 µg/µL).

Transduction of IOMM-Lee^{WT} cells was done in a 24-well plate by the addition of 3 µL viral particle containing supernatant to 50,000 cells in 500 µL medium resulting in 40% SSTR2 positive cells, as determined by flow cytometry three days after transduction and after staining for SSTR2. Next, the puromycin selection was started at a concentration of 1 µg/mL for 11 days to select the transduced cells and to expand the cells at the same time. Non-transduced control cells were already dead after three days of puromycin treatment. After the selection and expansion, IOMM-Lee^{SSTR2} cells were analyzed by flow cytometry again (Fig. S13) and frozen in liquid nitrogen.

SSTR2 Immunohistochemistry

Specimens were fixed in 4% (w/v) neutrally buffered formalin and embedded in paraffin. 3 µm tissue sections were stained on a Discovery Ultra automated stainer (Ventana Medical Systems, Tucson, USA) with rabbit anti-Somatostatin Receptor 2 antibody (1:50; ab 134152, abcam, Cambridge, UK) and a biotinylated goat-anti-rabbit secondary antibody (1:750, BA-1000, Vector Laboratories Inc, Burlingame, USA). The signal detection was conducted using the Discovery® DAB Map Kit (Ventana Medical Systems, Tucson, USA), and tissue sections were scanned with an AxioScan 7 digital slide scanner (Zeiss, Jena, Germany) equipped with a 20x magnification objective.

1.2.4 *In Vivo* Experiments

Animal procedures

All animal ethics and protocols were approved by the governments of Upper Bavaria and Saxony and were in agreement with their regulations.

For studies involving healthy and meningioma and breast adenocarcinoma xenografted mice, female athymic nude mice (Crl:NU(NCr)-*Foxn1*^{nu}), 6-12 weeks old, were purchased from Charles River Laboratories (Wilmington, DE, USA). Before surgery, animals were anesthetized with ketamine (65-100 mg/kg) and xylazine (10 mg/kg) administered intraperitoneally. Local anesthesia with 50 µL lidocaine (1%) was applied before the skin incision. During surgery, vital parameters and temperature were monitored, and mice were warmed with a heating pad equipped with a feedback system. At the end of surgery and during the first three postoperative days, mice received meloxicam (1 mg/kg) subcutaneously to control pain. To minimize autofluorescence from stomach contents, mice were fed low-fluorescence food and were fasted for 3 h prior to imaging. Before imaging, mice were anesthetized for 3-4 minutes with 3% isoflurane in air that passed through a 0.2 µm filter (flow rate: 1 L/min). During imaging, the percentage of isoflurane was reduced to 2%, and the carrier gas was changed to oxygen. At the completion of all studies, mice were euthanized by cervical dislocation.

For studies involving pheochromocytoma allografted, female athymic nude mice (Rj:NMRI-*Foxn1*$^{nu/nu}$), 8-12 weeks old, were purchased from Janvier Labs (Le Genest-Saint-Isle, France). Animals were anesthetized through inhalation of 10% (v/v) desflurane in 30/70% (v/v) oxygen/air.

For studies involving prostate cancer xenografted mice, 8−12-week-old male nude mice (Rj:NMRI-*Foxn1*$^{nu/nu}$) were purchased from Janvier Labs (Le Genest-Saint-Isle, France). Anesthesia was induced and maintained with inhalation of 3−5% (v/v) sevoflurane in 50/50% (v/v) oxygen/air. During anesthesia, animals were continuously warmed at 37 °C.

Prostate cancer, meningioma, and breast adenocarcinoma xenografts

The ectopic prostate cancer xenograft model was generated via subcutaneous injection of 5×10^6 LNCaP cells into the right shoulder of 8−12-week-old male nude mice. *In vivo* studies were initiated 6-12 weeks after cell injection, when tumors reached a diameter > 6 mm.

For the single meningioma xenograft model, IOMM-Lee^{SSTR2} cells (1×10^5) were diluted in 50 µL PBS and 50 µL Matrigel, then implanted subcutaneously into the lower flank using a 27G needle. In vivo studies were initiated 2-3 weeks after tumor cell implantation.

For the orthotopic breast adenocarcinoma xenograft model, MDA-MB-468 cells (5×10^6) were diluted in 100 µl of HBSS, then implanted into the mammary fat pad of the mice. Tumors were monitored every 2 days until they reached 5–6 mm in the longest diameter. *In vivo* studies were initiated 30 days after cell injection of the mice.

Clearance and biodistribution of near-infrared fluorescent somatostatin analogs in healthy mice

To assess tissue clearance kinetics, anesthetized mice received 4 nmol of TATE-sNIR or TATE-IRDye800 as an intravenous injection (bolus into a tail vein) while being continuously imaged for up to one hour using custom setup #1. The laser (50 mW/cm^2) was turned on every 20 seconds for 500 ms by camera triggering to reduce photobleaching and avoid overheating of mice. Mice were additionally anesthetized and imaged at 75 min, 3 h, 6 h (and in some cases up to 48 h) post-injection using custom setup #1 (110 mW/cm^2). Mean counts of fluorescence in a region of interest on the left upper limb were measured to assess tissue clearance kinetics. For biodistribution studies, tumor mice were intravenously injected with 38 nmol/kg TATE-sNIR or TATE-IRDye800. For dose-escalation studies, mice were intravenously injected with TATE-sNIR (eight different doses from 0.03 nmol to 19 nmol).

2 Supplemental Data

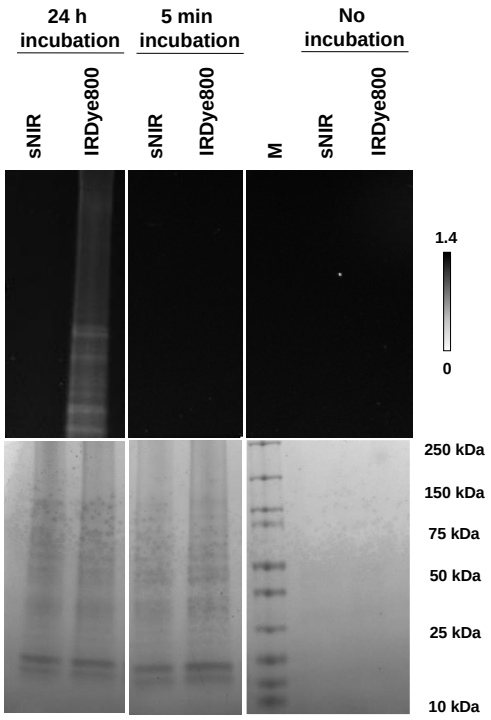

Fig. S1. Proteome-reactivity of sNIR and IRDye800 *in vitro*. 10 µM dye solutions were incubated with 4T1 cell lysate for 24 h or 5 min. Unincubated dye solutions were used as controls. Solutions were run on an SDS-PAGE gel, which was imaged using custom-built setup #2 (1.7 mW/cm^2) and Coomassie-stained to confirm protein loading. Scale bar of fluorescence intensity, counts/ms.

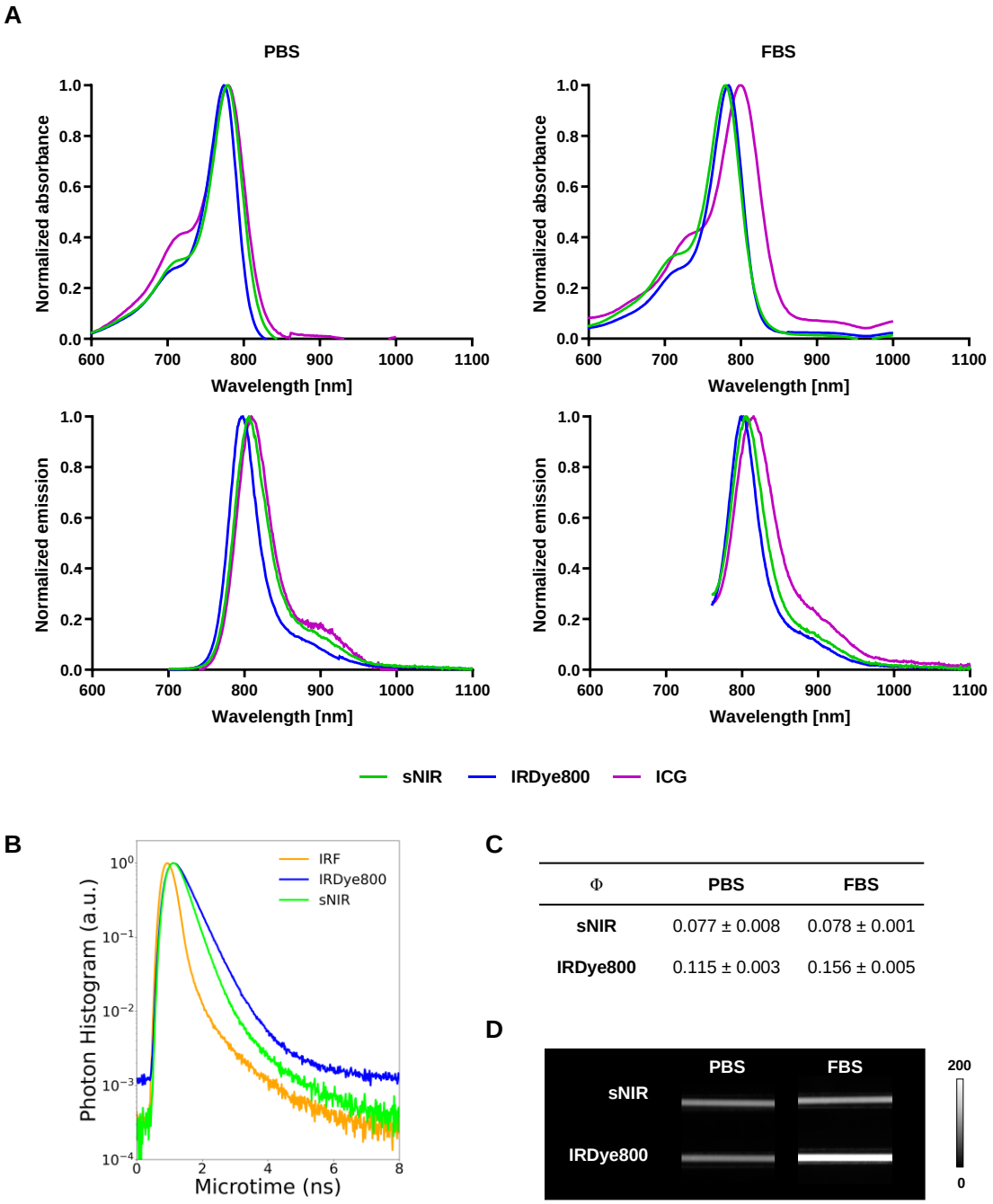

Fig. S2. Photophysical properties. (**A**) Normalized absorption and emission spectra of sNIR, IRDye800 and ICG in PBS and FBS (**B**) Fluorescence lifetime decay profiles of sNIR and IRDye800 in PBS. (C) Fluorescence quantum yields of sNIR and IRDye800 in PBS and FBS. (D) Non-specific serum interactions. 2.5 µM dye solutions in PBS and FBS were filled in capillaries and imaged using custom-built setup #1 (110 mW/cm^2). Scale bar of fluorescence intensity, counts/ms. Fluorescence brightening indicating non-specific interaction was observed only for IRDye800.

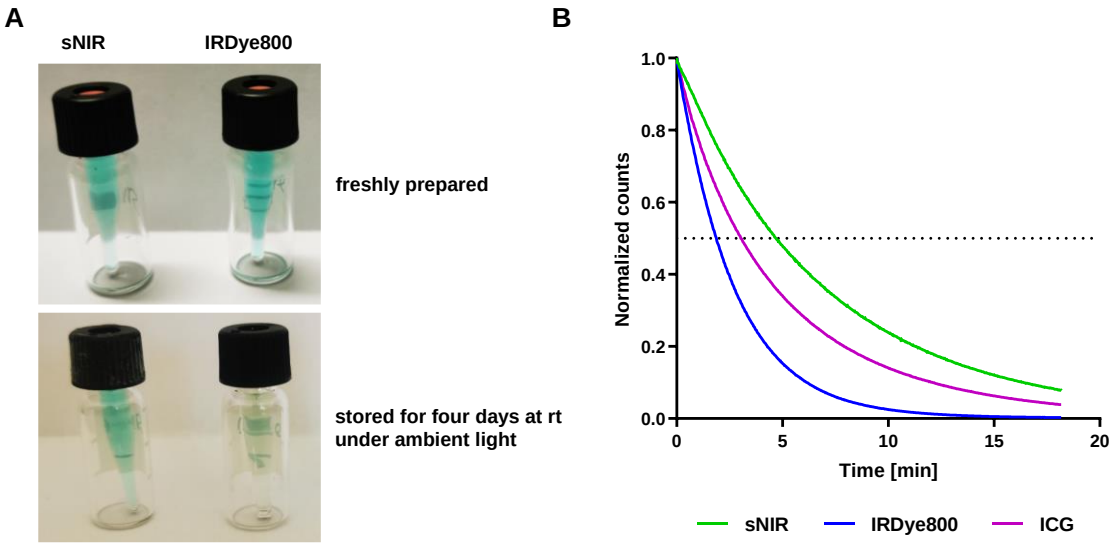

Fig. S3. Photostability of sNIR and IRDye800. (**A**) Photostability under ambient light. 50 µM dye solutions in PBS were freshly prepared (upper picture) and stored for four days at rt under ambient light (lower picture). Decomposition of IRDye800 was detected via HPLC after 24 h and could be visually traced by discoloration of the initially green solution. sNIR remained stable for the tested period. (**B**) Photostability under laser exposure. Capillaries containing 2.5 µM dye solutions in FBS were continuously irradiated using a 785 nm laser (110 mW/cm^2). Bleaching was detected using custom-built setup #1. ICG was included as a reference. The horizontal dashed line at 0.5 was used to estimate the half-lives.

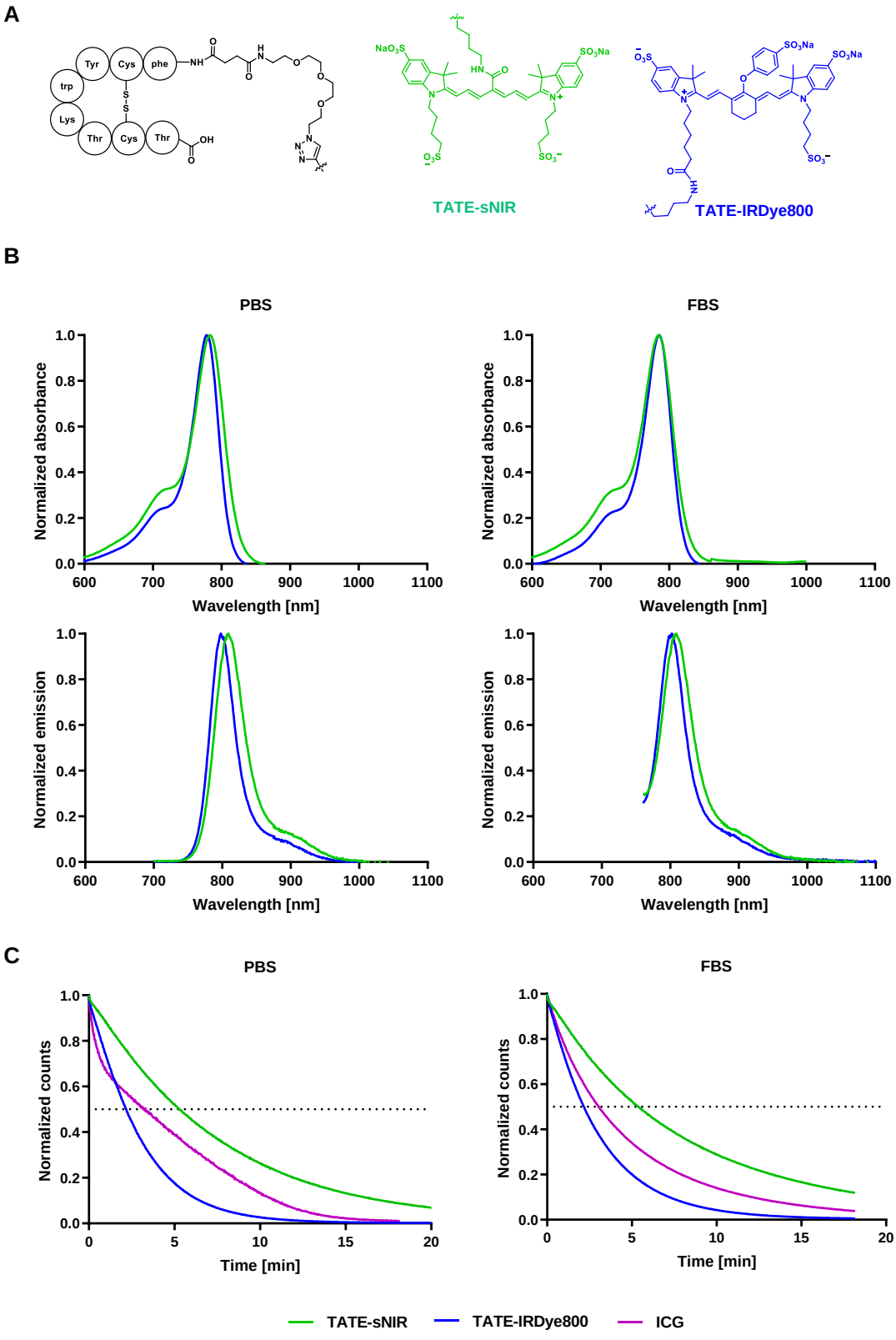

Fig. S4. Schematic design, spectra and photostability of TATE-sNIR and TATE-IRDye800. (A) Schematic design. (**B**) Normalized absorption and emission spectra in PBS and FBS. (**C**) Photostability under laser exposure. Capillaries containing 2.5 µM dye solutions in PBS or serum were continuously irradiated using a 785 nm laser (110 mW/cm^2). Bleaching was detected using custom-built setup #1. ICG was included as a reference. The horizontal dashed line at 0.5 was used to estimate the half-lives. In both solvents, TATE sNIR was more than twice as stable as TATE-IRDye800 and 60% more stable than ICG.

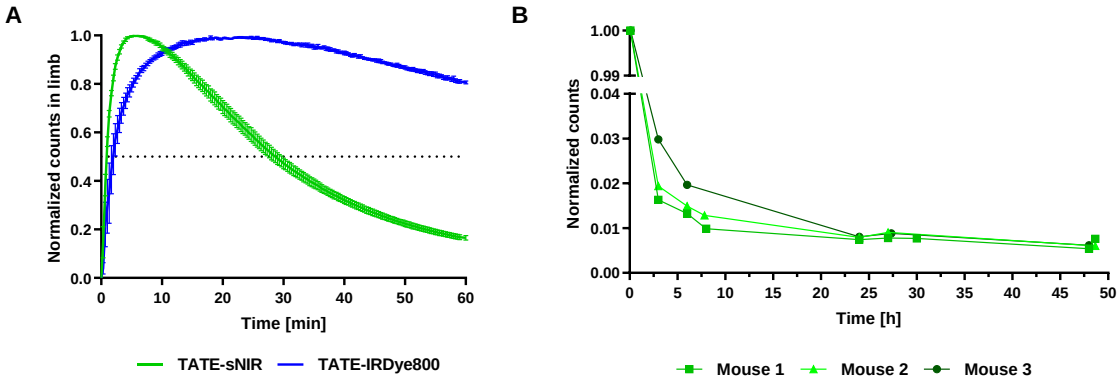

Fig. S5. Tissue clearance from healthy mice. (**A**) Short-term tissue clearance of TATE-sNIR and TATE-IRDYe800. Anesthetized animals in supine position were injected intravenously with 4 nmol probe, and near-infrared fluorescence was detected using custom-built setup #1 (for details, see Supplementary Materials 1.2.2). The laser (50 mW/cm2) was triggered every 20 s for 500 ms to avoid photobleaching. The decrease in signal intensity from an off-target tissue not expressing SSTR2 was extracted by analyzing the normalized mean counts in a region of interest on the left upper limb over time. Results are presented as mean ± standard error of the mean (SEM) (n = 3/probe). The horizontal dashed line at 0.5 was used to estimate the half-life of TATE-sNIR (28 ± 1 min), while the half-life of TATE-IRDye800 (ca. 140 min) was estimated via interpolation between the acquired data and the 3 h time point. (**B**) Long-term tissue clearance of TATE-sNIR. Healthy mice were injected intravenously with 4 nmol TATE-sNIR and imaged at different time points up to 48 h post-injection using custom-built setup #1 (110 mW/cm^2). Tissue clearance was extracted by analyzing the mean counts in a region of interest on the left upper limb. Autofluorescence before injection corresponds to 0.0012 normalized counts.

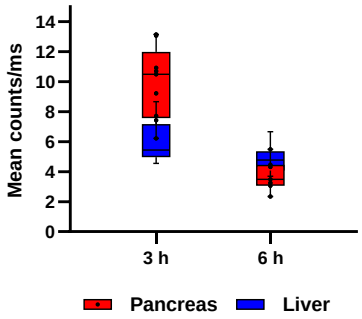

Fig. S6. Validating the imaging time point for TATE-sNIR. Mice were intravenously injected with 4 nmol of TATE-sNIR, and necropsies were performed at 3 h and 6 h. The pancreas, an SSTR2-expressing tissue (SSTR2+) with minimal autofluorescence, and the non-SSTR2-expressing (SSTR2-) liver were imaged *ex vivo* using custom-built setup #1 (110 mW/cm^2). Regions of interest were drawn on the organs, and the mean fluorescence intensity was measured. Data are mean ± SEM for 9 animals in the case of the 3 h time point or 7 animals in the case of the 6 h time point.

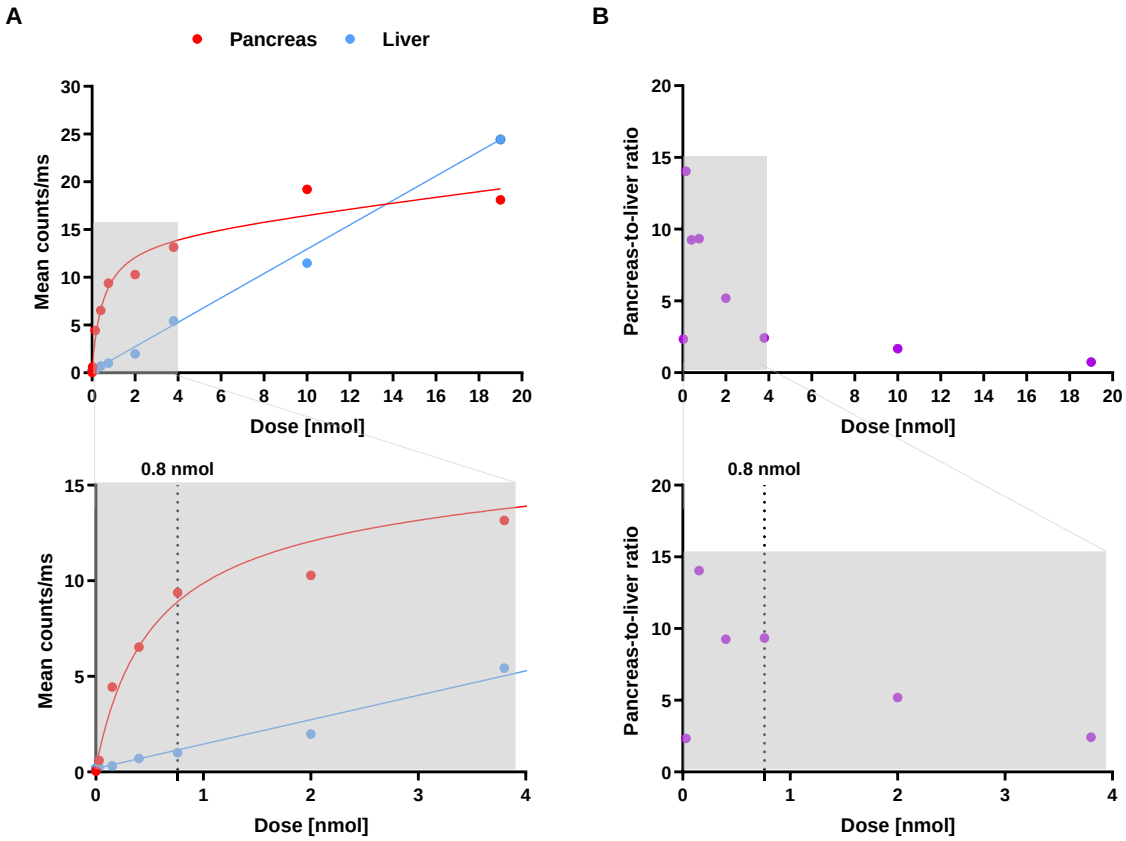

Fig. S7. Dose-depended enrichment of TATE-sNIR in the pancreas (SSTR2+) and liver (SSTR2-). Mice were intravenously injected with TATE-sNIR in dose escalation, necropsies were performed at 3 h post-injection, and organs were imaged *ex vivo* using custom-built setup #1 (110 mW/cm^2). Regions of interest were drawn on the organs, and the mean fluorescence intensity was measured. For the liver, only one lobe was imaged. (**A**) While the counts for the liver increase linearly with the injected dose, saturation can be observed for the pancreas. (**B**) The resulting pancreas-to-liver ratios suggest a low dose for high contrast. The dose of 0.8 nmol (corresponding to approximately 38 nmol/kg or 89 µg/kg) was considered the ideal dose, as the contrast between the pancreas (SSTR2+) and liver (SSTR2-) is high, while absolute counts are significantly higher than autofluorescence. The contrast ratios were confirmed in further experiments with a dose of 0.8 nmol (pancreas-to-liver 15 ± 5, n = 3).

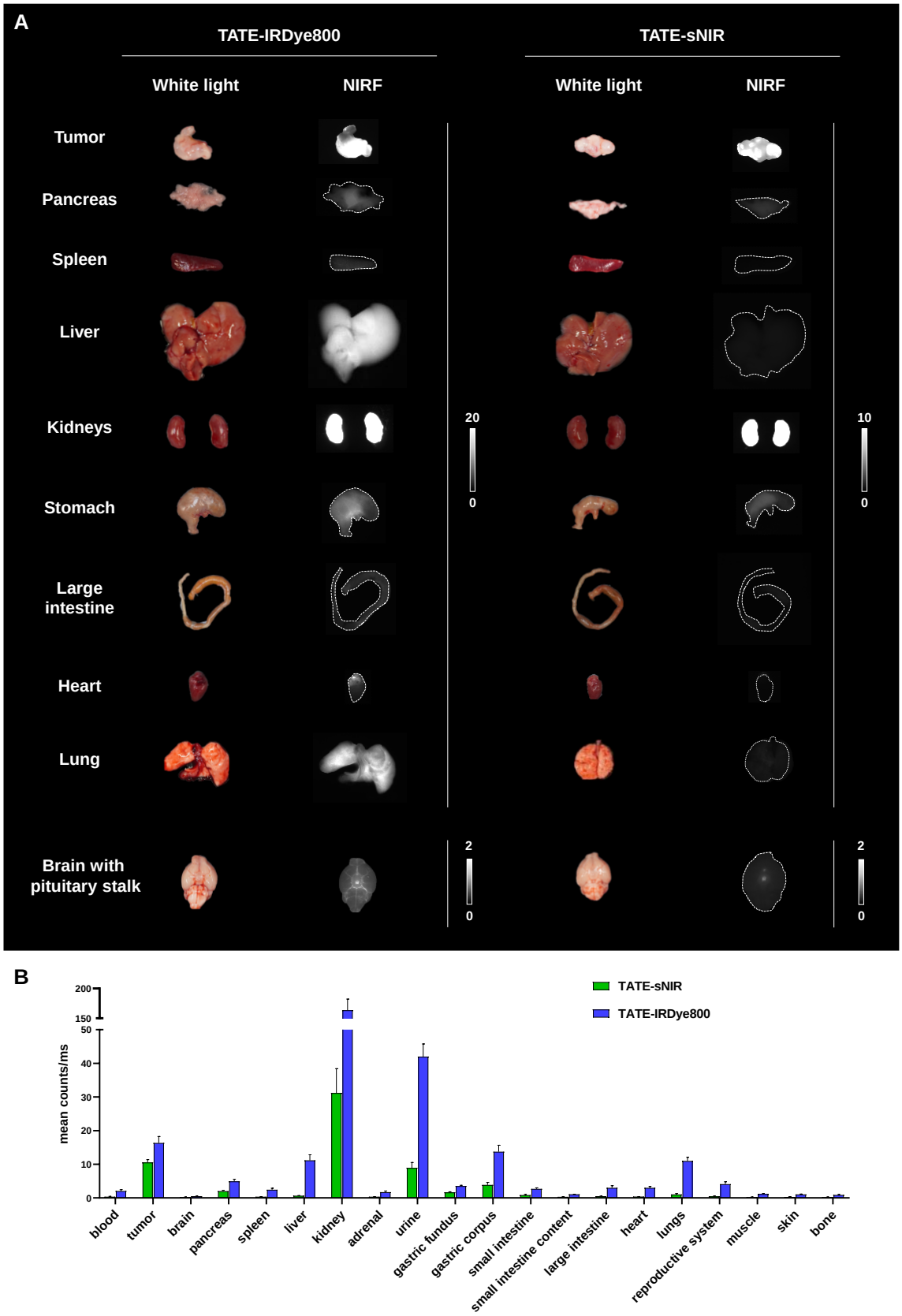

Fig. S8. Biodistribution of TATE-sNIR and TATE-IRDye800 in healthy mice at 3 h post-injection. Healthy mice were intravenously injected with probe (38 nmol/kg), necropsy was performed at 3 h post-injection, and organs were imaged *ex vivo* using custom-built setup #1 (110 mW/cm^2). (**A**) White light and NIRF images. Scale bar of fluorescence intensity, counts/ms. (**B**) Mean fluorescence intensities measured in organ preparations. Results are presented as mean ± SEM (n = 4/group).

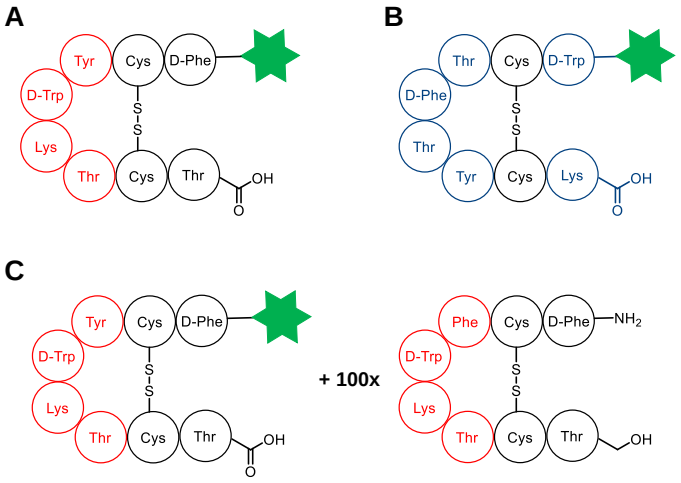

Fig. S9. Validation approaches. Besides the targeting probe TATE-sNIR (**A**, red amino acids form the SSTR2-targeting pharmacophore), two controls were used for validation: The negative control scTATE-sNIR (**B**) was generated by scrambling the amino acids marked in blue and does not bear the targeting pharmacophore. To demonstrate specificity, binding of TATE-sNIR to SSTR2 was competed by coinjection of a hundred 100-fold excess of SSTR2-targeting drug Octreotide (**C**). Each circle stands for one amino acid, while the green star represents sNIR.

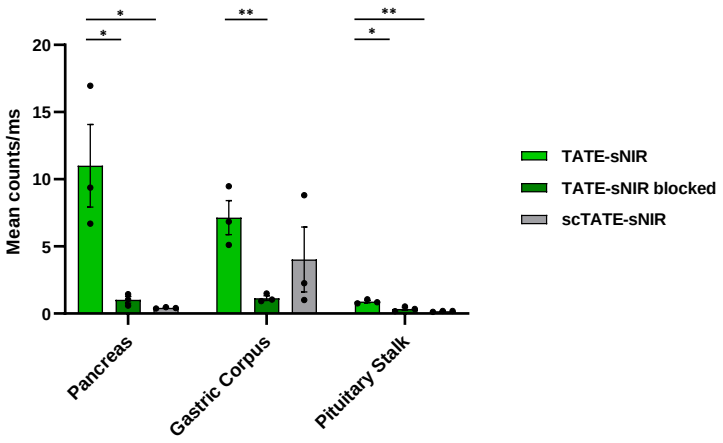

Fig. S10. Uptake of TATE-sNIR in physiologically SSTR2-expressing mouse tissues. Healthy mice were injected intravenously with 0.8 nmol of TATE sNIR alone or mixed with a 100-fold excess of SSTR2-binding octreotide, or with 0.8 nmol scTATE sNIR. Necropsy was performed at 3 h post-injection, and organs were imaged *ex vivo* using custom-built setup #1 (110 mW/cm^2). Regions of interest were drawn on the organs, and the mean fluorescence intensity was measured. We observed varying fluorescence intensities for the gastric corpus due to autofluorescent stomach contents. Although we changed the diet of our mice to low-fluorescence food and after injection of the probe, the mice fasted for three hours until they underwent the final imaging, we were not able to effectively reduce the fluorescent food signal in the stomach to a reliable, steady amount. This could be caused by different stomach passage times and eating behaviors, as some mice tended to eat cage enrichment material consisting of paper or cotton, both highly autofluorescent. Results are presented as mean ± SEM (n = 3/group).**P ≤ 0.01, *P ≤ 0.05.

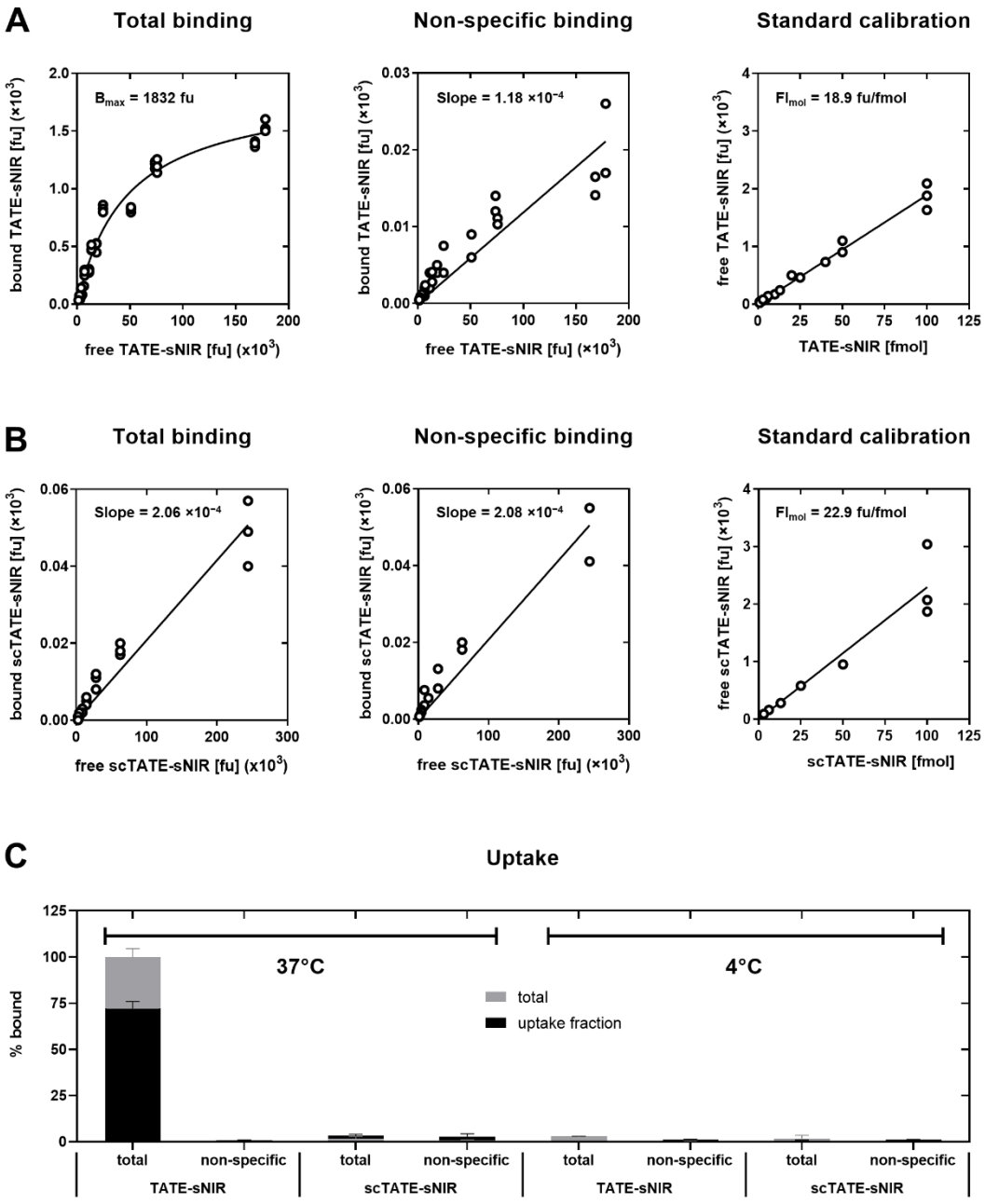

Fig. S11. Binding and uptake of fluorescent somatostatin analogs in mouse pheochromocytoma cell monolayers. (**A**) TATE-sNIR showing saturation of specific binding sites at increasing concentrations. (**B**) scTATE-sNIR showing a linear increase in binding corresponding to the slope in non-specific binding. (**C**) Uptake at different conditions showing highest total binding and uptake (acid wash-resistant fraction) of TATE-sNIR at 37 °C compared to scTATE-sNIR (negative control). Non-specific binding was assessed in the presence of 1 µM SSTR2-binding acetyl-TATE. [fu] fluorescence intensity units; data obtained from one experiment performed in sextuplicate; mean values with standard error.

Information from Customer			Results																Summary
Sample ID	Sample Name	Sample identifier	D8S1179	D21S11	D7S820	CSF1PO	D3S1358	TH01	D13S317	D16S539	D2S1338	D19S433	vWA	TPOX	D18S51	AMEL	D5S818	FGA	Data base hit
187	IOMM Lee p.12 (ATCC)	CL00003234	11,13	29,29	11,12	9,10	15,20	6,7	8,9	12,13	19,25	14,14	17,18	8,11	15,17	X,X	11,13	23,24	IOMM-Lee

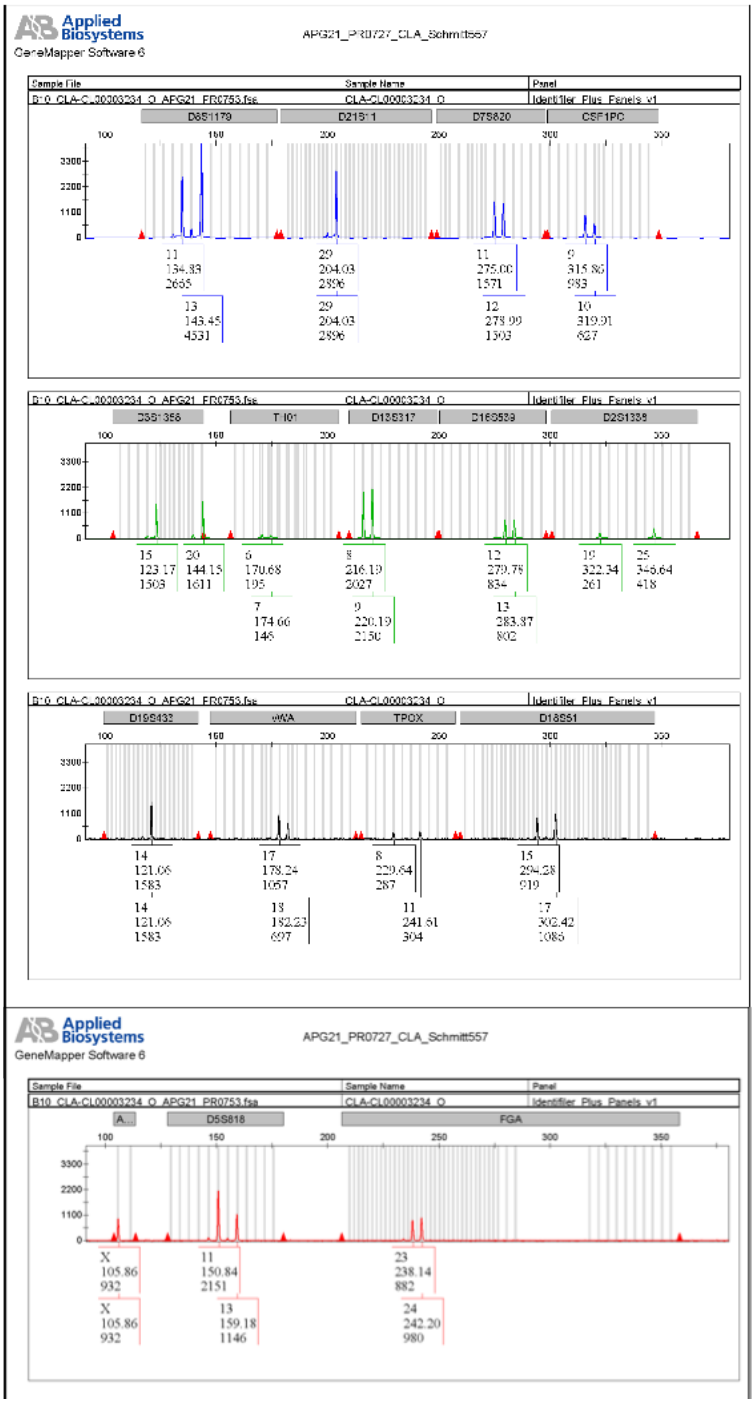

Fig. S12. Results of genetic characterization of IOMM-Lee^{WT} cells.

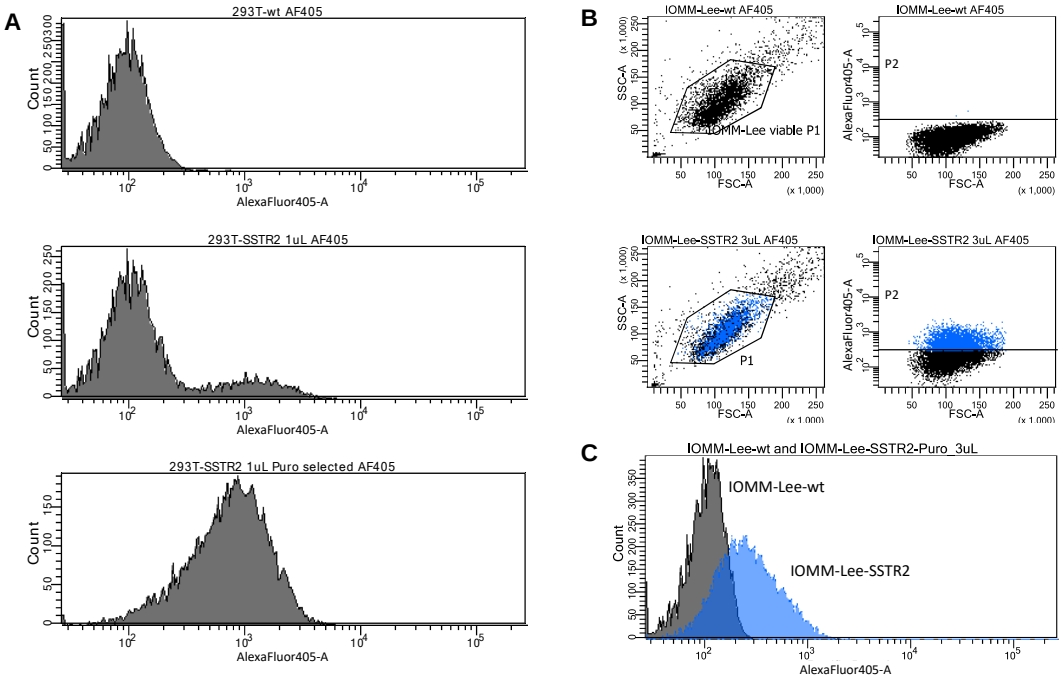

Fig. S13. Flow cytometric analysis of lentiviral overexpression of human SSTR2 in HEK-293T and IOMM-Lee cells. Cells were stained with a monoclonal antibody against human SSTR2 conjugated with AlexaFluor405. (**A**) Shown are non-modified HEK-293T cells^{WT} (top) and HEK-293T^{SSTR2} cells after transduction with 1 µL of lentiviral vector expressing SSTR2 without selection (middle) and after selection with 1 µg/mL puromycin (bottom). (**B**) IOMM-Lee cells transduced with the same lentiviral vector show a much weaker expression of SSTR2. Shown are non-modified IOMM-Lee^{WT} cells (top) and IOMM-Lee^{SSTR2} cells after transduction with 3 µL of lentiviral vector expressing SSTR2 and 11 days of selection with 1 µg/mL puromycin (bottom). (**C**) In the histogram overlay consisting of the cells shown in B, a shift of the whole SSTR2-positive population (blue) is visible, indicating that all cells are SSTR2-positive after selection. Stainings were done with 200,000 cells dissolved in 100 µL of PBS with 1 µL antibody (0.2 µg/µL, R&D systems IC4224V). SSC-A, side scatter area signal; FSC-A, forward scatter area signal; AF405, AlexaFluor405 dye; WT, wild type.

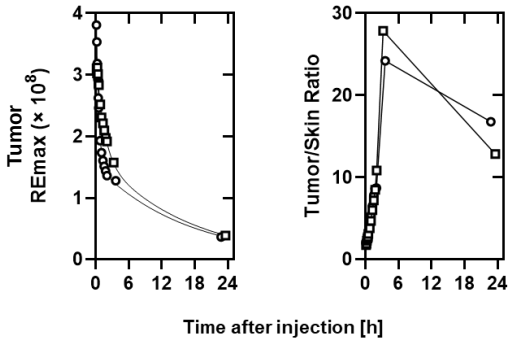

Fig. S14. Fluorescence of TATE-sNIR in pheochromocytoma allografted mice over 24 h. 2 MPC tumor-bearing animals were injected with 0.8 nmol of TATE-sNIR. The fluorescence intensities were measured for tumors (left panel) and skin over a time course of 24 h, and the tumor-to-skin ratio (right panel) was calculated. REmax; maximum pixel value of the radiant efficiency within the tumor region of interest. Connecting curves represent the time course of average values for each time point.

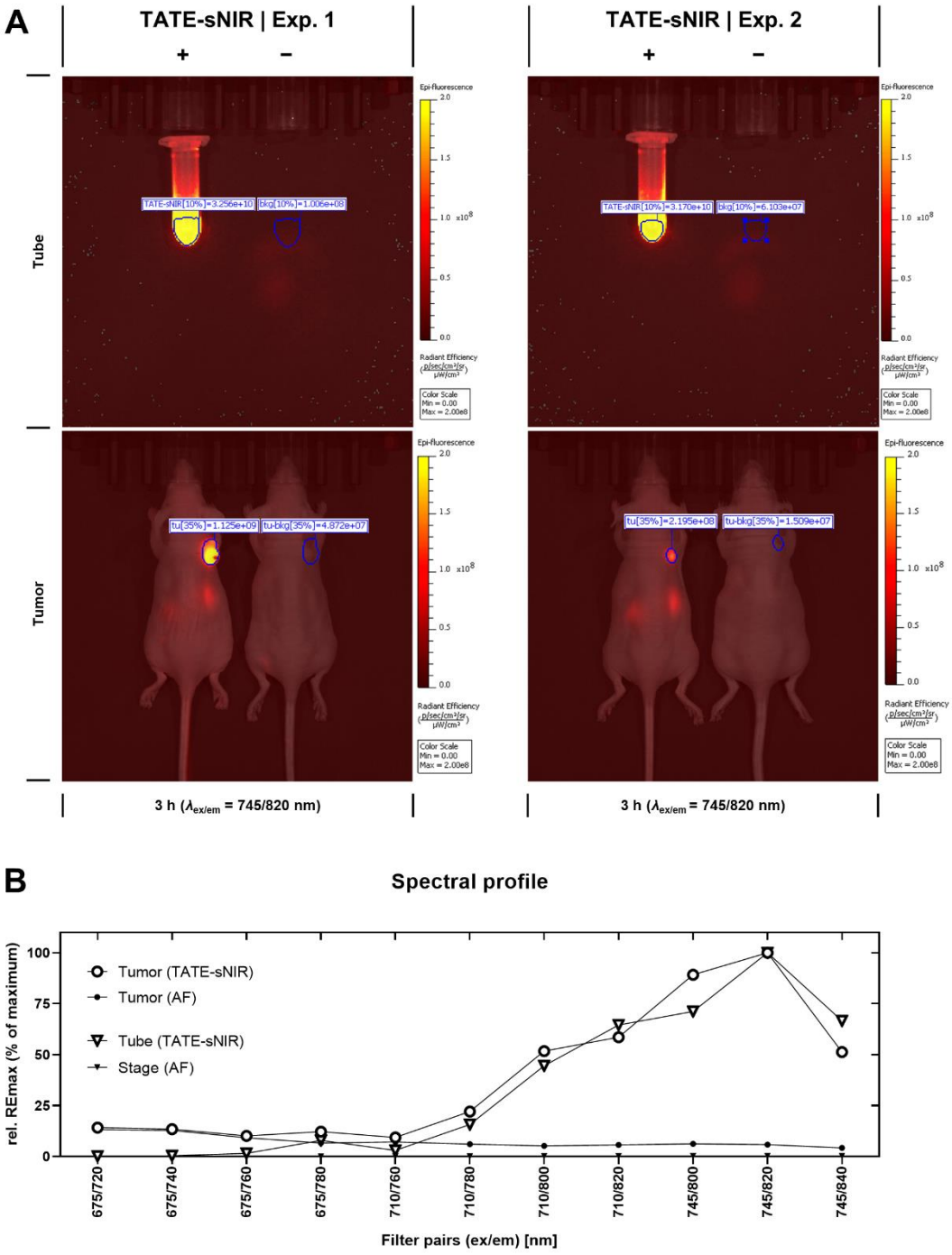

Fig. S15. Imaging and spectral profile of TATE-sNIR in fluorescence imaging of microtubes and pheochromocytoma allografted mice. (**A**) Positions and geometry of regions of interest for the analysis of fluorescence intensities detectable in microtubes and animals. %-Values in brackets represent the thresholds applied for intensity-based delineation. (**B**) Fluorescence intensities in microtubes and animals were measured using the automatic exposure time setting in 8×8 binning mode with the following combinations of bandpass filters for excitation/emission: 675 nm/(720, 740, 760, 780 nm), 710 nm/(760, 780, 800, 820 nm), 745 nm/(800, 820, 840 nm). For each spectral series, the corresponding reflectance image was captured and used for anatomical referencing. Data are mean ± SEM from two experiments. AF, autofluorescence; bkg, background; REmax, maximum pixel value of radiant efficiency within a specific region of interest; tu, tumor.

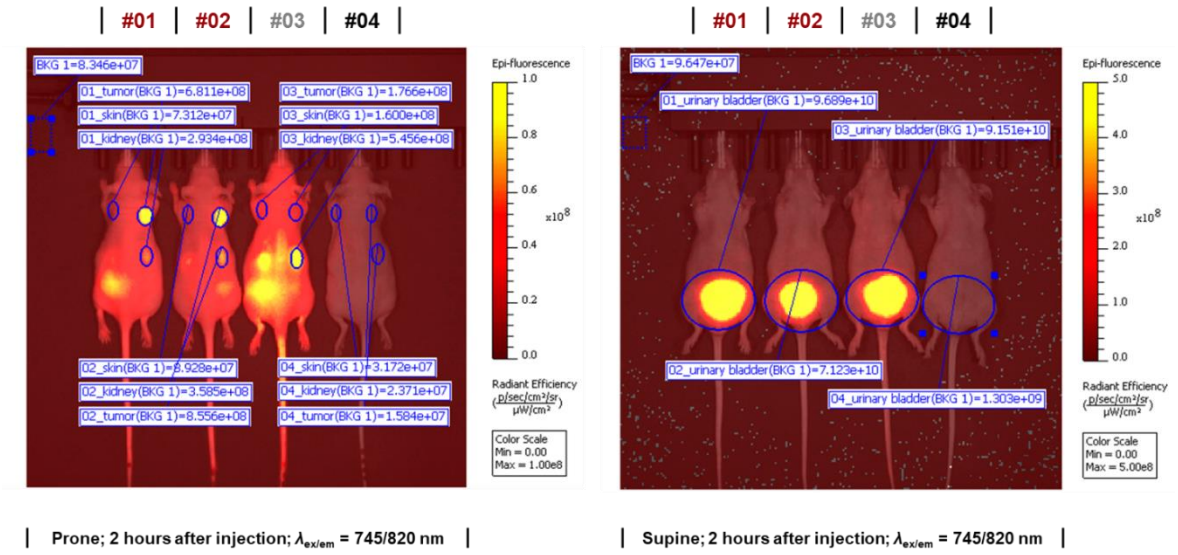

Fig. S16. Positions of regions of interest for analysis of fluorescence images of pheochromocytoma allografted mice. Animals received 0.8 nmol TATE-sNIR at positions #01 and #02, 0.8 nmol scTATE-sNIR at position #03, and no fluorescent probe at position #04. Fluorescence images were recorded using an IVIS SpectrumCT In Vivo Imaging System with the 745/820 nm excitation/emission filter combination. Fluorescence intensities of tumors, kidneys, and skin were measured in images captured in the prone position. The urinary bladder was measured in images captured in the supine position. Images were acquired according to the following body orientation and time series: prone (5−30 min, 8 min-intervals), supine (40 min), prone (45−120 min, 15 min-intervals), supine (125 min), prone followed by supine (3 and 24 h). Background (BKG 1) from the imaging stage was assessed and subtracted from the pixel intensities within each animal-region of interest. Fluorescence intensities measured at position #04 were reported as specific tissue background (Tissue BKG).

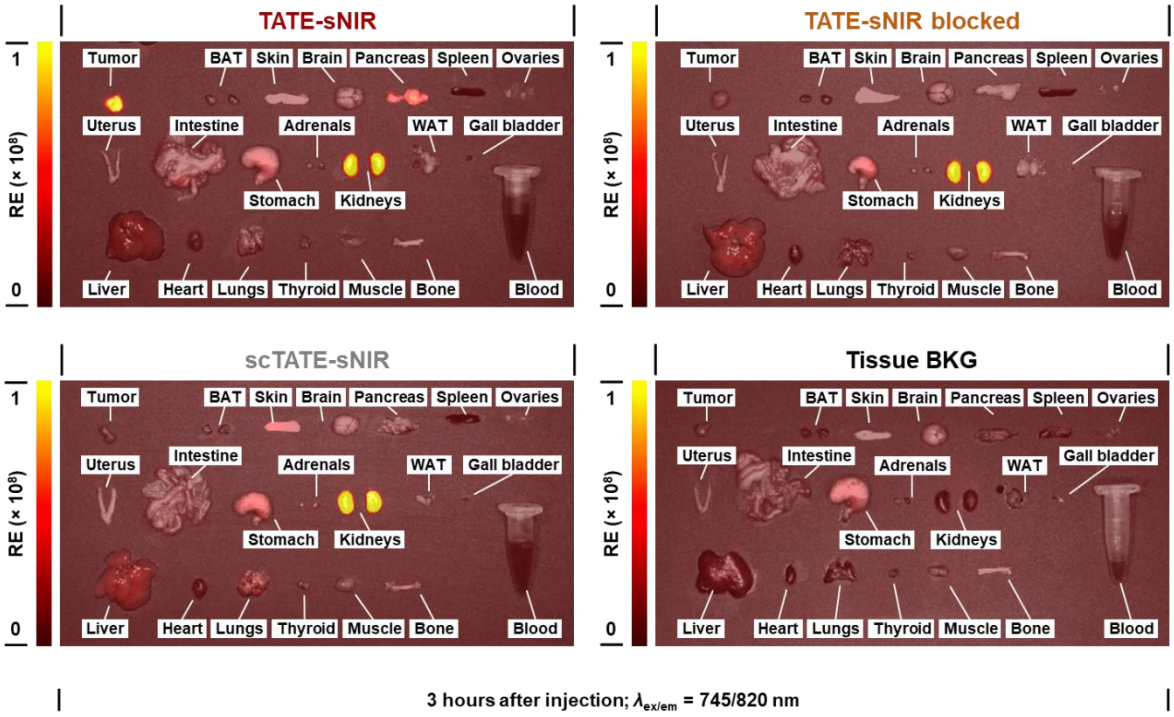

Fig. S17. Imaging of TATE-sNIR and scTATE-sNIR in organ preparations from pheochromocytoma allografted mice. Animals bearing subcutaneous tumors were injected intravenously with 0.8 nmol of TATE-sNIR alone or mixed with a 63-fold excess of SSTR2-binding acetyl-TATE, or with 0.8 nmol scTATE-sNIR. At 3 h post-injection, animals were euthanized, and organs were imaged *ex vivo* using the IVIS SpectrumCT In Vivo Imaging System with the 745/820 nm excitation/emission filter combination. Tissue background (BKG) from an animal without injection of a fluorescent probe. RE, pixel value of the radiant efficiency.

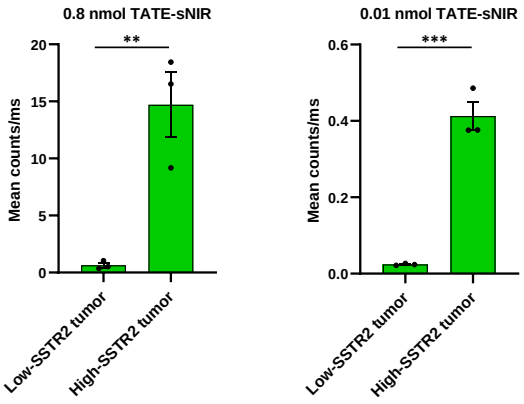

Fig. S18. TATE-sNIR-mediated tumor-uptake in dual implant (SSTR2±) ectopic meningioma mice. Two weeks after subcutaneous implantation of IOMM-Lee^{WT} and IOMM-Lee^{SSTR2} cells in the left and right flanks of the same mouse, tumor-bearing animals were injected intravenously with 0.8 nmol or 0.01 nmol of TATE sNIR. Necropsy was performed 3 h post-injection, tumors were imaged *ex vivo* using custom-built setup #1 (110 mW/cm^2), and the mean fluorescence intensities were measured. Data are presented as mean ± SEM for 3 animals per dose. $^{**}P \leq 0.01$, $^{\#}P \leq 0.001$.

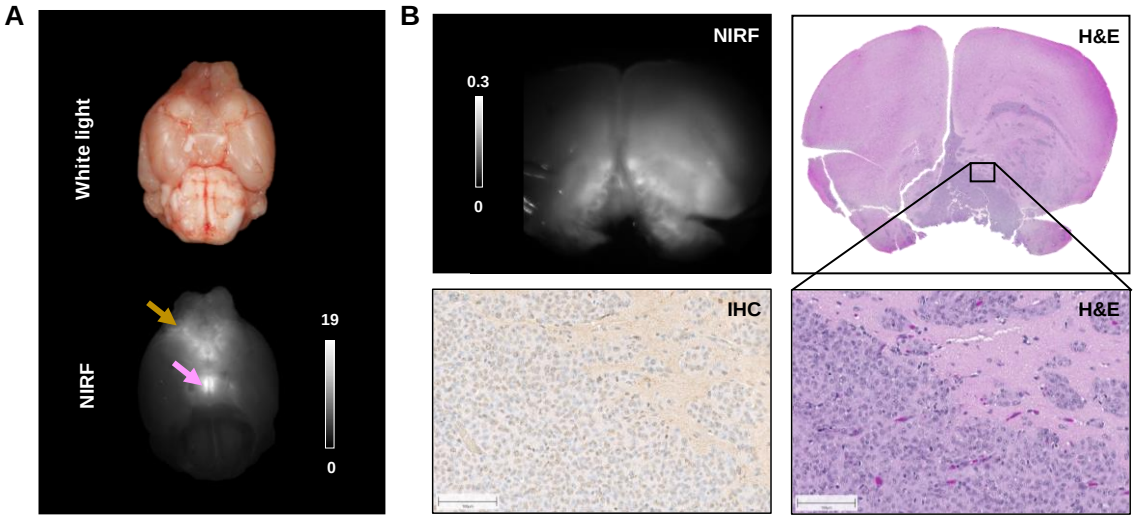

Fig. S19. TATE-sNIR-mediated imaging of an orthotopic meningioma with infiltrative growth. (**A**) Two weeks after intracranial implantation of IOMM-Lee^{WT} cells, the tumor-bearing animal was injected intravenously with 4.0 nmol of TATE-sNIR. Necropsy was performed 3 h post-injection, and the tumor-bearing brain was imaged *ex vivo* at 3 h post-injection, under white light, and using custom-built setup #1 (110 mW/cm^2). In the near-infrared fluorescence (NIRF) image, the brown and pink arrows indicate the tumor and pituitary stalk, respectively. (**B**) Analysis of tumor-bearing brain sections based on hematoxylin-eosin staining (H&E, scale bar 100 µm), immunohistochemical staining against SSTR2 (IHC, scale bar 100 µm), and fluorescence imaging using custom-built setup #1 (110 mW/cm^2). The infiltrative growth pattern visible in H&E corresponded to NIRF. IHC indicated low to intermediate SSTR2. Scale bar of fluorescence intensity, counts/ms.

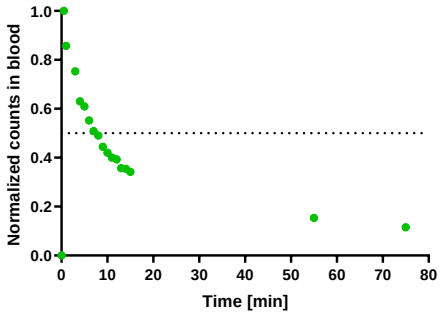

Fig. S20. Blood clearance of TATE-sNIR from a healthy pig. An anesthetized healthy pig was injected intravenously with TATE-sNIR at a dose of 30 nmol/kg. At the indicated time points, blood samples were collected in heparin tubes. The whole blood samples were filled into capillaries and imaged using custom setup #3 (68 mW/cm^2). The horizontal dashed line at 0.5 was used to estimate the half-life of TATE-sNIR (7 min).

Table S1. Comparative analysis between our dataset for TATE-sNIR and the data published for the fluorescent somatostatin analogs 800CW-TATE, MMC(FNIR-Tag)-TOC, and eTFC-01. TATE-sNIR exhibited a 6-, 4.5-, and 7.3-fold higher tumor-to-muscle ratio than 800CW-TATE, MMC(FNIR-Tag)-TOC, and eTFC-01, respectively. The tumor-to-liver ratio of TATE-sNIR was found to be more than 10-fold higher than that of the previously described probes. TATE-sNIR's tumor-to-brain ratio is comparable to the one reported for 800CW-TATE. However, Dijkstra *et al.* generated their tumor model by subcutaneous implantation of H69 cells (small cell lung cancer) between the scapulae, while we implanted IOMM-Lee cells (meningioma) intracranially. Moreover, their 1500-fold block using DOTA-TATE resulted in 58% reduction of 800CW-TATE uptake, while we were able to reduce the uptake of TATE-sNIR by 89% with a 100-fold excess of octreotide. Similar to Hernández Vargas *et al.*, we generated a dual implant (SSTR2±) ectopic mouse model. The SSTR2+ tumor-to-SSTR2- tumor ratio obtained using TATE-sNIR was 15-fold higher than the published ratio for MMC(FNIR-Tag)-TOC. However, as the tumors might vary in their degree of SSTR2 expression, those comparisons should be treated with caution. Therefore, we additionally compared pancreas-to-liver ratios, with the pancreas being a more suitable SSTR2+ reference due to its physiological SSTR2 expression and the liver being an SSTR2- organ frequently affected by non-specific retention. A 50-fold higher pancreas-to-liver ratio was observed for TATE-sNIR than for both 800CW-TATE and MMC(FNIR-Tag) TOC. These findings highlight the minimal non-specific binding of TATE-sNIR to non-target tissues, which we attribute to the absence of IRDye800 and DBCO and the presence of our newly developed dye sNIR.[39-41] NA, not applicable; ND, not determined.

Probe	**TATE-sNIR**	800CW-TATE	MMC(FNIR-Tag)-TOC	eTFC-01
mono-/bimodal	**mono**	mono	bi	bi
group, year	**this work, 2025**	Dijkstra *et al.,* 2021	Hernández Vargas *et al.,* 2022	Chapeau *et al.*, 2024
dose, imaging time	**0.8 nmol, 3 h**	1.4 nmol, 4 h	2 nmol, 3 h	2 nmol, 4 h
tumor-to-muscle ratio	**67**	11	15	7.3
tumor-to-liver ratio	**17**	1.05	1.5	0.65
tumor-to-brain ratio	**29**	21	ND	ND
SSTR2+ tumor-to-SSTR2- tumor ratio	**30**	NA	2	NA
pancreas-to-liver ratio	**15**	0.3	0.2	0.17